DISSERTATION

SIMULATING CANOPY DYNAMICS, PRODUCTIVITY AND WATER BALANCE OF ANNUAL CROPS FROM FIELD TO REGIONAL SCALES

Submitted by

Yao Zhang

Department of Soil and Crop Sciences

In partial fulfillment of the requirements

For the Degree of Doctor of Philosophy

Colorado State University

Fort Collins, Colorado

Summer 2016

Doctoral Committee:

Advisor: Keith Paustian

Mazdak Arabi
William Parton
Meagan Schipanski

ABSTRACT

SIMULATING CANOPY DYNAMICS, PRODUCTIVITY AND WATER BALANCE OF ANNUAL CROPS FROM FIELD TO REGIONAL SCALES

To provide better understanding of natural processes and predictions for decision support, dynamic models have been used to assess impact of climate, soils and management on crop production, water use, and other responses from field to regional scales.

It is important to continue to improve the prediction accuracy and increase the reliability. In this work, we first improved the DayCent ecosystem model by developing a new empirical method for simulating green leaf area index (GLAI) of annual crops. Its performance has been validated using experimental observations from different experimental field locations as well as more aggregate NASS yield data spanning the country. Additionally, sensitivity and uncertainty of important parts of the crop growth model have been quantified.

Our results showed the new model provided reliable predictions on crop GLAI, biomass, grain yield, evapotranspiration (ET), and soil water content (SWC) at field scale at various locations. At national scale, the predictions of grain yields were generally accurate with the model capable of representing the geographically-distributed differences in crop yields due to climate, soil, and management. The results indicated that the model is capable of providing insightful predictions for use in management and policy decision making. Although there are challenges to be addressed, our results indicate that the DayCent model can be a valuable tool to assess crop yield changes and other agroecosystem processes under scenarios of climate change in the future.

ACKNOWLEDGEMENTS

During this PhD study, the most important thing I learned is the importance of collaboration. Without collaborating with others, this work would not be possible. I would like to acknowledge people who have provided valuable insight, measurement data, technical support, manuscript reviewing, and other help.

I give special thanks to my advisor Dr. Keith Paustian, who has always been encouraging, enlightening, and supportive. He did not ask me to follow his agenda in a strict way; rather, he gave me freedom to explore science within my studies and provided insight to lead me in the process. As a humble leader, respectful friend and world famous scientist, Dr. Paustian may not have taught me basic knowledge in crop and soil sciences, but his knowledge in scientific thinking, problem solving, innovation, leadership and life attitude has benefitted me enormously.

I would like to thank Dr. Bill Parton, Dr. Mazdak Arabi, and Dr. Meagan Schipanski for serving in my graduate committee. They have supported me substantially in critical discussions, gaining knowledge, manuscript editing, measurement data supply, connection building with collaborators, and more. Thanks are also due to my coworkers Andre Dozier, Ernie Marx, Ram Gurung, Stephen Williams, Mark Easter. It has been a great pleasure to work with each of them. I appreciate Dr. Andrew Suyker, Dr. Neil Hansen, Dr. Tom Trout, and Dr. David Nielson for providing me valuable experimental measurement data.

Finally, I give thanks to my parents and friends who have encouraged and inspired me in all situations. Research is sometimes boring, but love and friendship from family and friends have added spice to my life and made it wonderful. I am excited to open a new page in my life with all of them!

TABLE OF CONTENTS

CHAPTER 1. SUMMARY

I remember, in the first meeting with my advisor Dr. Paustian after I started my PhD program, he pointed out some critical problems found in previous simulations using the DayCent ecosystem model. He asked me if I was interested in solving some of them. I answered yes. So DayCent improvement became one of the goals of my PhD study.

One of the biggest challenges we were facing was modeling the soil water balance. Water is the most limiting factor for plant growth besides temperature. As we know, precipitation is the main source of fresh water. The amount of precipitation in a year ranges from more than 300 cm in some tropical forests to a few cm in arid deserts. When precipitation cannot supply the demand of plants, this drought stress retards their growth and may even kill them. So it is important to accurately estimate the amount of water available for plants.

Not all precipitation that falls on the ground can be utilized by plants. Most precipitation infiltrates into the soil while some run offs the soil surface into surface waters. Part of the infiltrated water gets retained in the top soil layers where roots can reach. The rest goes deeper into groundwater. Water in the root zone can be taken up by plants and used in transpiration. It is the major way of returning soil water back to the atmosphere. Soil surface without canopy cover may also return some water through evaporation. These movements of water compose the soil water balance.

The DayCent model soil water submodel is a one-dimensional model which simulates the components of the mass balance of water including the infiltration of precipitation and irrigation, surface runoff, saturated and unsaturated flow in the root zone, percolation to the groundwater, evapotranspiration (ET; evaporation plus transpiration), and capillary rise of groundwater. It simulates the movement of water within the soil with the field capacity concept of the tipping-bucket approach and applies Richards' equation for water re-distribution after the drainage from saturation to field capacity (Parton et al., 1998). Similar to many other models, DayCent calculates reference ET using weather data and applies

coefficients to derive the potential ET for a specific plant (the amount of ET under no water limitation in soil).

The splitting of potential ET into evaporation and transpiration is based on the percentage of ground covered by the canopy. The first problem we found out was that DayCent model did not simulate the canopy coverage of crops well. No gradual senescence of leaves of annual crops was simulated in the DayCent model. By not capturing the gradual senescence after peak biomass is reached, the model over-predicted soil water loss via transpiration in late growing season. In addition, the model assumed the attainment of a full canopy during the middle and late growing season, but in the case of severe stresses (drought or nutrient deficit), canopy development can be affected; thus the assumption was not valid.

So finding a better way of simulating canopy development became the goal of the first part of my research (in Chapter 1). Initially, we first created a very simple triangle function to simulate the decrease of green leaf area index (GLAI; a representation of the green canopy) to account for the loss of green canopy in the late growing season. As expected, there was significant improvement in the simulated ET and soil water content (SWC) in comparison with the daily measurements of three irrigation×rotation treatments over 11 years in eastern Nebraska. However, there were limitations with this method. When crops are grown in drier area like eastern Colorado, they likely do not develop a full canopy in the middle of growing season, while our simple triangle method assumed a fully canopy. So we tried to adopt methods from some other crop models. After spending months on reading and testing the existing methods, we found some of them are too complicated for implementation in DayCent while some are not very accurate in a stressed environment or do not fit the current structure of the DayCent model. Eventually, we decided to create a new method for the use in DayCent. After analyzing a lot field data, the change of green leaf weight ratio (GLWR) of various grain crops caught our attention. The ratio of green leaf weight to total aboveground weight was initially high at the beginning of growth and gradually decreased to zero at the end of growing season. The change along the growing season could be described by three linear relationships as a function of growing degree units (GDD; a measurement of phenological development). As leaf weight is proportional to leaf area, LAI can be calculated.

We implemented this new method in DayCent model and tested with measured data of corn, soybean, and winter wheat which are the three major crops in the United States. The method worked well for all three crops grown in different conditions, with the temporal dynamics of canopy development being well represented, especially the canopy senescence. As the simulated canopy coverage is also used to estimate the amount of light intercepted for photosynthesis of leaves, the simulated daily biomass production was also improved. As a result, we also saw better results for predictions of daily ET and SWC, especially in late growing season period.

To further validate the model under stressed condition, we choose three limited irrigation experiments of corn conducted in semiarid northeastern Colorado (in Chapter 2). In this region, the average annual precipitation is only 30-60 cm and lack of sufficient water is the main cause of the lower yields of dryland fields. Irrigation has been applied in this region for over a century to achieve higher crop production; however, as the demand of fresh water from municipal and industrial sections grows, water is being increasingly diverted from agricultural use. Hence limited irrigation practices, which supply less water than maximum crop demand, are seen as promising alternative. The original DayCent model did not reflect well the relationships between irrigation amount, canopy dynamics and crop production. With the improvement in canopy simulation and other improvements in the soil water submodel, we expected better estimates of crop water use and yield. Our results showed that the modified model accurately simulated the drought stress effect on GLAI, biomass production and grain yield of corn across irrigation treatments. The accuracy is better or similar to those reported of other dedicated crop models, which is a significant achievement in that DayCent is a more general ecosystem model that can simulate all types of terrestrial ecosystems.

After model improvement, a new version should be analyzed for parameter sensitivity and uncertainty. This is the research goal of Chapter 3, in which a global sensitivity analysis has been conducted and uncertainty has been quantified. First, 24 parameters that were closely related to crop growth, production and water stress effect were identified. Then, the ‘sobol’ global sensitivity method (Sobol, 1993) was used to identify the most sensitive parameters under both rainfed and irrigated

conditions. We found the growth/production related parameters in DayCent have relative more impact on grain yield, GLAI, and biomass than ET and soil water related parameters. We selected the 12 most sensitive parameters for uncertainty analysis using a formal Bayesian method called DREAM (Vrugt et al., 2008; Vrugt et al., 2009). As the inclusion rate (the percentage of observed data points within the 95% confidence interval of predictions) of the predictive uncertainty was low, we adjusted the estimated σ variable in the likelihood equation to increase it. Using 440% of the original estimated σ, the inclusion rate of the calibration and validation datasets reached 0.95 and 0.96, respectively. Some limited irrigation scenarios were created to analyze yield response to irrigation. It was interesting to find that for all irrigation levels, CV (coefficient of variation) of predicted yields was relative stable. This implies that the uncertainty of a water production function could be easily estimated using CV, which could be directly applied to simulations of similar conditions without running the complicated time-consuming uncertainty analysis.

The sensitivity and uncertainty analysis provided us a better understanding of the model. We decided to use it for broader application. Previously, many projects have used DayCent model for large regional analysis on crop yields, soil carbon and nitrogen, soil water, and trace gas emissions. Thus there is a need to continually improve the model to increase the accuracy of model predictions of these variables. So in Chapter 4, we parameterized the modified version of DayCent and used it to predict corn and soybean yields for the continental U.S. at county-scale. In this study, the National Resources Inventory survey (NRI) data, high resolution weather data (PRISM) and SSURGO soil data were used to derive inputs for the simulations. As different varieties of crops are grown in climatically different regions, in our simulation, corn and soybean were divided to several variety groups based on their length of maturity. To validate model performance, our predictions were compared with 15-year USDA NASS (National Agricultural Statistics Service) county level yields. The results across the major production areas, the model predictions were generally accurate, and substantially improved over the previous version. The model was able to catch the variation of crop yields due to differences in climate, soil, and management. Additionally, in regions with high variation in year-to-year yields, the interannual variability was well

simulated for both crops. These results provided us greater confidence in performing regional simulations for other ecosystem variables such soil carbon dynamics because crop production substantially impacts soil carbon input, crop water use, soil nitrogen concentration, and other essential variables.

In our simulations, we found there are many areas that we still can improve on. First, there is need for a better phenology submodel. The current method used is the simple growing degree day method (also called heat unit). It is generally accurate for crops like corn that are not affected by photoperiod (day length or night length). For photoperiod sensitive crops (soybean, wheat, etc.), phenology stages are not well represented and it causes the inaccuracy in simulated GLAI, water balance and biomass accumulation. Second, the simulated GLAI and biomass at early development stages are very sensitive to the input parameter BMINI (initial biomass at emergence). This is a cultivar specific parameter which is hard to estimate. What's more, for the same cultivar, its value is not a constant in the real world and is affected by soil temperature and moisture in the period between planting and emergence. So seed germination and seedling emergence should be considered when parameterizing. Third, irrigation types are not explicitly modeled in DayCent. Irrigation is assumed as sprinkler type and simulated as the same as rainfall. As more efficient technology such as dripping irrigation becomes more popular, it is necessary to add more options in the model to better represent the real practices on farms. Fourth, the soil hydraulic parameters are fixed for each soil layer for a site in the entire simulation. These parameters are actually impacted by management practices like tillage, application of organic amendments, etc. These changes affect soil water movement significantly. The good news is that building a dynamic process of soil parameters is currently in the improvement plan.

To summarize, the work described in the four chapters of this dissertation was all closely linked together. This work has provided an improved version of DayCent model and a systematic analysis of the model. Its performance has been validated using experimental observations from different experimental field locations as well as more aggregate NASS yield data spanning the country. Additionally, sensitivity and uncertainty of important parts of the crop growth model have been quantified. Our results showed that the model is capable of providing insightful predictions for use in management and policy decision

making. Although there are challenges to be addressed, our results indicate that the DayCent model can be a valuable tool to assess crop yield changes and other agroecosystem processes under scenarios of climate change in the future.

Using the calibrated model, we are able to explore scenarios and provide decision support for various needs. There are a few studies that are either currently undergoing or may be conducted in the future. In collaboration with experts in hydrology in CSU, we implemented the modified version of DayCent model into the eRAMS platform which was designed for building accessible and scalable analytical tools and simulation models that can be accessed via desktop or mobile devices (https://erams.com/). Using this powerful platform, we are able to get input information from the embedded databases and run simulations. We have simulated crop water use and yield response for South Platte River Basin (SPRB) for 17 crops under various level of irrigation and tillage types. Optimized water allocation scenarios were selected and the results are being processed by an economic model for policy making support. Simulations using predicted future weather data will be conducted to access climate change effect on cropping system water demand and crop yields in SPRB. We will also be deploying the new DayCent version in the COMET-Farm decision support platform, which is being used by USDA, carbon offset developers and agricultural companies to estimate the carbon and water footprints of alternative agricultural management systems. Another project is to investigate the crop yields change and land use change of the continental U.S. for the near future (2010 – 2060) using projected weather data. Crop growth response to elevated CO_2 has been parameterized for crops in the new DayCent model version. The results will also be used with an economic model to optimize the economic return while considering environmental impacts. A third study is in collaboration with some researchers in Italy to investigate soil water movement and nitrogen cycling. An updated DayCent-Hydrus model (Dozier et al., 2016; Yuan et al., 2011) is used to simulate water table changes. In this version, the soil water submodel of DAYCENT was replaced by the Hydrus module (Simunek et al., 2008) which uses Richard's equation for water flow instead of original tipping bucket method.

This work is done because of the foundation of numerous previous studies and collaboration with field experimental researchers and fellow modelers. In the past 50 years, dynamic modeling has gone through a journey from an idea to a relatively mature tool for decision making and knowledge testing. Although, modeling, as a manifestation of the scientific process, is never done and is always being questioned, renewed and improved, through the effect of generations of scientists and researchers, it will play a more and more important role in the future to provide better understanding of underlining processes, regional assessment for decision making, and provide forecasting services for agricultural communities.

REFERENCES

Dozier A, David O, Arabi M, Lloyd W, Zhang Y. (2016) A minimally invasive model data passing interface for integrating legacy environmental system models. Environmental Modelling & Software 80: 265-280.

Parton WJ, Hartman M, Ojima D, Schimel D. (1998) DAYCENT and its land surface submodel: description and testing. Global and Planetary Change 19: 35-48.

Simunek J, van Genuchten MT, Sejna M. (2008) Development and applications of the HYDRUS and STANMOD software packages and related codes. Vadose Zone Journal 7: 587-600.

Sobol IM. (1993) Sensitivity estimates for nonlinear mathematical models. Mathematical Modelling and Computational Experiments 1: 407-414.

Vrugt JA, ter Braak CJF, Clark MP, Hyman JM, Robinson BA. (2008) Treatment of input uncertainty in hydrologic modeling: Doing hydrology backward with Markov chain Monte Carlo simulation. Water Resources Research 44.

Vrugt JA, ter Braak CJF, Diks CGH, Robinson BA, Hyman JM, Higdon D. (2009) Accelerating Markov Chain Monte Carlo Simulation by Differential Evolution with Self-Adaptive Randomized Subspace Sampling. International Journal of Nonlinear Sciences and Numerical Simulation 10: 273-290.

Yuan FM, Meixner T, Fenn ME, Simunek J. (2011) Impact of transient soil water simulation to estimated nitrogen leaching and emission at high- and low-deposition forest sites in Southern California. Journal of Geophysical Research-Biogeosciences 116: 15.

CHAPTER 2. IMPROVED CROP CANOPY AND WATER BALANCE DYNAMICS FOR AGROECOSYSTEM MODELING USING DAYCENT

2.1. SUMMARY

Field experimental data of maize and soybean from two locations in the US Corn Belt and winter wheat in northern Oklahoma were used to develop a new empirical method for simulating green leaf area index (GLAI) in the DayCent model. The method is based on the change of green leaf weight ratio as a function of phasic development in grain crops and required minimal changes to other parts of the model. The simulated results from the modified DayCent model compared well with field measurement of GLAI and aboveground biomass for all three crops. The improvement in GLAI resulted in substantial improvement in simulated evapotranspiration and soil water content, especially in late growing season period, with the improved representation of canopy senescence. Simulation of biomass and grain yield by the modified model was also slightly improved (R^2 was 0.69 for grain yield of maize and 0.65 for soybean).

2.2. INTRODUCTION

The expansion and duration of green leaf area is one of the most important processes in crop growth development. Green leaf area determines the amount of light intercepted by the canopy and hence photosynthesis rates and biomass accumulation. Canopy dynamics are also directly linked to evapotranspiration processes and thus are a major determinant of the soil and ecosystem water balance. For crop models, in order to accurately predict crop production and water use, accurate simulation of green leaf area is one of the essential components.

Several approaches have been used to predict green leaf area in crop simulation models. Generally, these approaches can be divided into two categories, depending on whether or not the leaf expansion is explicitly dependent on modeled biomass production. Approaches in the first category simulate the potential increase in leaf area independent of simulated increase in biomass. These methods can be simple

as those in the APEX model (Williams et al., 2008) and AquaCrop model (Steduto et al., 2009) in which polynomials or other functions are fitted to describe the change of green leaf area index (GLAI) or canopy cover (CC) over part or all of the growing season, using daily or thermal unit time scales. Methods in this category can also be very complicated like the one proposed by Lizaso et al. (2003) which simulates the appearance, expansion and senescence of each individual leaf. Both leaf expansion and senescence are directly affected by abiotic stresses in most of the models in this first category.

The approaches in the second category relate the increase of leaf area to the increase in leaf biomass through the concept of specific leaf area (SLA; the ratio of leaf area to its biomass). The assumption is that SLA is relatively stable (or its change over time is well characterized) and thus leaf expansion is modeled as a function of the allocation of photosynthate to leaf biomass. Models in this category include the Cropsyst model (Stockle et al., 1994) and WOFOST model (Vandiepen et al., 1989). The SLA is usually a fixed input parameter or a simple function of solar radiation and temperature or crop growth (Soltani and Sinclair, 2012). The abiotic stress effects on leaf area are indirect via the stress effects on biomass production. In these models, leaf senescence is commonly modeled as a decrease of GLAI at a certain rate over a growth stage or that leaves have a fixed longevity, followed by senescence.

A sound approach for simulating leaf area dynamics is fundamental for any crop modelling application. The DayCent model (Del Grosso et al., 2008; Del Grosso et al., 2006; Parton et al., 1998) is a generalized ecosystem model designed to simulation biogeochemical (C, N, P, S) and water dynamics for multiple ecosystem types (e.g., grassland, forest, savanna), including annual crops. The DayCent model has been widely used to simulate soil carbon dynamics and soil greenhouse gas (CO_2, N_2O, CH_4) emissions, especially for agricultural ecosystems (e.g. Del Grosso et al., 2008; Del Grosso et al., 2006; Jarecki et al., 2008; Zhang et al., 2013). The crop growth sub-model in DayCent is designed to model the productivity, nutrient uptake, and water use of the crop, which in turn have a large impact on the carbon and nutrient cycling processes of the agroecosystem. For example, after precipitation, crop water use is the single largest component of the soil water balance and the rate and timing of plant water uptake

strongly effects soil moisture contents and depth distribution, which are key controls on soil organic matter and nutrient dynamics (Parton et al., 1987).

Currently, the method used in DayCent to simulate leaf area dynamics is very simple. Similar to other models in the 'second category', described above, the GLAI during early vegetative growth is dependent on the aboveground biomass using a fixed leaf area ratio (LAR; the ratio of leaf area to total aboveground biomass). The simulated GLAI is not used after crop reaches full canopy (usually GLAI is above 3) and full canopy is assumed until harvest of crop. Despite its advantage of simplicity, there are a few flaws of this method. First, LAR should not be treated as a constant, as it has been observed to decrease along with the early vegetative growth in some crops (Miller et al., 1988; Wallace and Munger, 1965). Second, under some severe abiotic stresses, crops might not reach full canopy. So the assumption of full canopy is not always valid. Third, leaf senescence or loss of green leaf area is a gradual process. The method in DayCent over-predicts the canopy coverage in the late growing season. These flaws can result in poor prediction of biomass production and water use. Some studies have reported a weak correlation of simulated soil water content (SWC) by DayCent model and field observations (Jarecki et al., 2008; Smith et al., 2008), which may in part be due to the inaccuracy of simulated GLAI.

To improve the simulation of leaf area dynamics in DayCent model, we recognized several constraints relating to the structure and purpose of the model. First, any new method needs to be general. DayCent model is designed to simulate all kinds of terrestrial ecosystem types using general formations of key processes. It uses two general submodels for plant growth, grass/crop and tree, so the new method needed to be compatible with this general design and not entail major changes in the model structure. Thus generalized algorithms with only crop-specific parameters that reflect major differences of crop species and cultivars were needed. Secondly, the method should be simple and not substantially increase the input data requirements of the model. An important attribute of DayCent is that it can be run with ready available input data; the model is often used for regional, national and global applications that don't allow for local calibration of model parameters. Third, the new method should improve the accuracy of current method and be robust across a range of climatic and edaphic conditions.

In this paper, we describe the new methods used to model leaf area dynamics in DayCent and the derivation of model parameters for three major grain crops in the US: maize (*Zea mays* L.) soybean (*Glycine max* L.) and wheat (*Triticum aestivum* L.). We then test the new method against field measured leaf area data from three research sites in the US and evaluate and compare the model performance on other system variables, including evapotranspiration (ET), soil water content, crop biomass production and yield, that are affected by the crop canopy dynamics.

2.3. MATERIAL AND METHODS

2.3.1. Field Experiment

2.3.1.1. Mead, NE

This field experiment was conducted at the University of Nebraska Agricultural Research and Development Center near Mead, NE, on three large fields of about 49-65 ha, each of which are instrumented with an eddy covariance tower. The research site is part of the AmeriFlux site network and complete details of the experiment can be found in Suyker and Verma (2009). Each of the three fields represents a different management treatment: 1) irrigated continuous maize (ICM), irrigated by a center pivot system, 2) irrigated maize-soybean (IMS) was managed as a maize-soybean rotation from 2001 to 2008, but changed to continuous maize since 2009, and 3) a rainfed maize-soybean (RMS) rotation. Standard best management practices prescribed for production-scale maize-soybean systems have been employed which includes herbicide and pesticide applications, fertilization, irrigation, etc. The crop management details are summarized in Table 2.1. No-till practice was used after the start of the experiment for a few years. As a heavy litter layer became a problem for the continuous maize system, a reduced tillage operation was introduced in 2005 on ICM site and in 2010 on IMS site.

Soils at the site are deep silty clay loams with very little slope, lacking shallow groundwater (Table 2.2). Measurements at the site include eddy covariance towers for each treatment (to measure CO_2, H_2O and energy fluxes) and soil moisture sensors (Theta probe, Delta-T Devices, Cambridge, UK) were placed at 10, 25, 50, 100 cm depth. Detailed information on sensors used are given in Suyker and Verma (2009). As described in Grant et al. (2007), six 20 by 20 m intensive measurement zones (IMZ) were established

in each field. In each IMZ, leaf area and aboveground biomass were measured destructively on an average of 11-day basis at six different locations of each site. Before harvest, at least six samples per site were hand-harvested to estimate harvest index. Grain yield data were from combine harvest of each entire site. Crop phenology was observed frequently and the records included most vegetative and reproductive stages since 2003 while fewer growth stages were recorded in 2001 and 2002. Severe hail storms occurred in September of 2010 and damaged the crops and thus yields in 2010 were not included in our study.

2.3.1.2. Bondville, IL

We used field data for maize and soybeans from another site in the AmeriFlux network at Bondville, IL (Meyers and Hollinger, 2004). The site was established in 1996 and was managed as a maize and soybean rotation. We evaluated the model against measurement data from 2001 to 2005, during which time GLAI and biomass were frequently measured during the growing season and biomass of different aboveground organs was recorded. Maize was planted in 2001, 2003, and 2005 on DOY 108, 105, and 111 respectively. The planting density was 78,000 plants ha^{-1} for all three years. Soybean was planted at 360,000 plants ha^{-1} on DOY 152 in 2002 and 416,276 plants ha^{-1} on DOY 127 in 2004. Crop variety information was not available. The soil texture is silt loam with an average bulk density of 1.45 g cm^{-3}.

2.3.1.3. Ponca City, OK

The third Ameriflux network experiment used in our study was near Ponca City, OK (Hanan et al., 2002). The site was a 65 ha field planted with winter wheat continuously from 1996 to 2000. Planting was in mid-autumn and harvest was conducted at mid-summer. Details about crop varieties were not available from published reports. Aboveground biomass and LAI were measured using destructive method roughly at bi-weekly intervals throughout each growing season. The soil is silty clay loam (Typic and Pachic Argiustolls of Poncreek and Kirkland complexes) in the upper 0.6 m and underlain by a thick clay horizon. Weather data were available from the on-site eddy-covariance tower. However, air temperature measurements were not fully reliable and so data from the nearby weather station at Ponca City Regional

Airport were used and some missing data were filled from observations from the Blackwell station of the Oklahoma Mesonet meteorological network which is about 16 km distant.

2.3.2 Model description and parameterization

2.3.2.1. Water flow sub-model

In a review of existing water flow models, Ranatunga et al.(2008) defined two broad categories: simple models, using a 'tipping-bucket' approach, and complex models which solve the Richards equation. The tipping-bucket approach is charaterized as a high efficiency method and is often used for regional or global scale simulation. It assumes that free drainage of soil water ceases at field capacity (and below) and it uses empirical methods to calculate drainage rate and plant water uptake rate. The dynamic models employing Richards' equation (Richards, 1931), represent a more physically-based mechanistic approach. These models are capable of greater accuracy but require more input data which might be not readily available in many cases. Also the computing power needed for numerial solutions of models employing the Richards-equation is much greater than for models employing a tipping-bucket approach (Yuan et al., 2011). The DayCent ecosystem model adopted advantages from both approaches. It simulates water flow with the field capacity concept of the tipping-bucket approach and applies Richards' equation for water re-distribution after the dainage from saturation to field capacity (Parton et al., 1998). The water flow sub-model of DayCent model predicts the components of the mass balance of water which mainly includes the infiltration of precipitation and irrigation, surface runoff, percolation to the groundwater, evapotranspiration (ET), and capillary rise of groundwater. The relationship of the components is described by the equation of the water balance (daily):

$$\Delta S_i = P + I_{net} - ET_c - RO - DP + GW \quad (2.1)$$

where, ΔS_i is the net change in soil water at the end of day i and i-1. In this equation, *P*, *RO*, and *DP* are precipitation, runoff, and deep percolation on day i, respectively. I_{net} is the net irrigation on day i. *GW* is the ground water contribution if a shallow water table is present. *ETc* is the actual evapotranspiration on day i. All units are in cm day^{-1}.

2.3.2.2. Evapotranspiration

In the water balance of cropping systems, evapotranspiration comprises the largest part of water loss. Models using meteorological data has been developed and applied to estimate ET (Farahani et al., 2007). Like many other crop models, the standardized Penman-Monteith model is an option in DayCent model for potential ET estimation. The standardized Penman-Monteith model has been shown to have high accuracy and has been promoted world-widely by the Food and Agriculture Organization of the United Nations (FAO) (Allen et al., 1998).

Potential ET is usually partitioned into potential evaporation and potential transpiration as a function of the green canopy coverage. Actual transpiration is affected by the available water in the root zone; a method similar to the non-linear equation for the response of transpiration to SWC in the review by Sadras and Milroy (1996) is adopted in DayCent. Regarding potential soil evaporation, it can be reduced by the amount of standing dead biomass and litter on the soil surface. In DayCent, actual evaporation is also limited by the low soil water potential of the top soil layer and the upward fluxes from underlying layers (Parton et al., 1998).

The partition of potential ET is usually estimated by Beer's law equation or modified Beer's law equations in models (Monsi and Saeki, 1953; Sellers, 1985), to calculate the green canopy coverage (CC), which represents the fraction of intercepted light. In the DayCent model, a standard Beer's law equation is used, i.e.

$$CC = 1 - exp(-k \times GLAI) \quad (2.2)$$

where *k* (dimensionless) is the light extinction coefficient of the vegetation, and *GLAI* is green leaf area index (m m^{-1}).

2.3.2.3. Plant production

Green CC is also widely used for modeling carbon assimilation by the crop. In DayCent, daily potential plant production (PP; g biomass m^{-2}) is a function of the intercepted light; similar to many other models (Soltani and Sinclair, 2012), where solar energy is converted to biomass (aboveground and belowground) via radiation use efficiency (RUE_{TB}; g biomass m^{-2} $langley^{-1}$ PAR).

$$PP_i = CC_i \times PAR_i \times RUE_{TB} \quad (2.3)$$

PAR_i is the photosynthetic radiation (langley) on day i. Actual production (AP; g biomass m^{-2}) is the amount PP adjusted for temperature and water stress and it is also limited by nutrients availability.

$$AP_i = min(PP_i \times T_e \times W_e , PP_{nutrient}) \quad (2.4)$$

where T_e and W_e are temperature and water effect (unitless); $PP_{nutrient}$ is the maximum production that can be supported by available nutrients. The actual daily biomass production is then allocated to belowground and aboveground biomass using time-dependent empirical partitioning factors. DayCent does not explicitly model stem, leaf, and grain pools of aboveground biomass for crops. Grain mass is calculated as a fraction of total aboveground biomass at harvest using the concept of harvest index (HI).

Relative soil water content (RSWC) of the wettest soil layer in the root zone is used to estimate the level of drought stress on production.

$$RSWC_i = (WC_i - WP_i)/(FC_i - WP_i) \quad (2.5)$$

$$RSWC_{wet} = max(RSWC_i) \quad (2.6)$$

where *WC*, *FC*, and *WP* are the water content, field capacity, and wilting point (cm/cm) of soil layer i and $RSWC_{wet}$ is the RSWC of the wettest soil layer in the root zone. W_e (in Equation 2.4) is a logistic function of daily $RSWC_{wet}$ (lower W_e at lower $RSWC_{wet}$) with parameters adjusted for crop types.

2.3.2.4. Original GLAI method in DayCent

In order to predict green CC, a model for GLAI is needed (Equation 2.2). The DayCent model uses the second approach as described earlier, however the previous version of the model did not explicitly use the concept of specific leaf area. To estimate LAI, the DayCent model assumed a linear relationship between GLAI and the cumulative total aboveground live biomass (g m^{-2}):

$$GLAI = Biomass_{aboveground} \times LAR \quad (2.7)$$

where *LAR* is leaf area ratio (unitless) which is assumed constant. This approach is also found in the AZODYN model (Jeuffroy and Recous, 1999). Equation 2.7 can be seen as a simplification of the equation below:

$$GLAI = Biomass_{aboveground} \times GLWR \times SLA \quad (2.8)$$

where *GLWR* is the green leaf weight ratio (percentage of leaf biomass relative to aboveground biomass) and *SLA* is the specific leaf area. Equation 2.8 is equivalent to Equation 2.7 when GLWR and SLA are approximated as constants. Leaf area ratio or the product of GLWR and SLA is close to a constant only in vegetative grow stages before crops reach full canopy (Aase, 1978; Ashley et al., 1965). After the crop reaches full canopy (CC is close to 1.0), full green CC was assumed up until the time of harvest. DayCent did not model pre-harvest leaf senescence for annual crops.

In reality, green CC decreases during late growing season due to ongoing leaf senescence. In the previous version of DayCent, the lack of leaf senescence led to an over-prediction of ET in the late growing season as senescent leaves do not actively transpire water and they also block radiation from reaching the bare soil, thus reducing evaporation. Plant production was often over- predicted at late growing season stages for the same reason. Additionally, in the case of dryland agriculture, as a result of drought effect, crops are not able to develop full canopy in semi-arid regions; thus, the assumption of full canopy is not appropriate for dryland conditions. To address these problems, we developed a new simple method for modeling GLAI in DayCent.

2.3.2.5. New GLAI method

In order to minimize changes to the original model structure, Equation 2.8 is still used in the new method and we assume SLA to be a constant. Specific leaf area has been found to be relatively stable for a given crop type and has been simplified as a constant input parameter in models like CropSyst (Stockle et al., 1994). Although some studies have shown SLA changes during crop development and can be affected by light intensity, drought stress, nitrogen availability, planting density, and atmospheric CO_2 concentration (Amanullah et al., 2007; Lafarge and Hammer, 2002; Sionit et al., 1982; Tardieu et al., 1999), simulation with constant SLA has been shown to give good accuracy in simulating GLAI for general purpose crop models (Maas, 1993; Todorovic et al., 2009). Measured SLA of maize and soybean of Mead, NE experiment is plotted (Fig. 2.1) against heat unit index (HUI, 0 at planting and 1 at physiological maturity). There is a trend of decrease of SLA of maize in the vegetative growth period

starting at an average of 0.025 $m^2 g^{-1}$ and maintained at about 0.016 $m^2 g^{-1}$ afterward. No clear trend of SLA for soybean is observed. Also, no clear difference between irrigated and rainfed treatments for both crops is observed. For simplicity, in our model, SLA is set as a constant for the entire growing season.

The other component in Equation 2.8 GLWR, is made as a function of crop development in the new method. It has been long observed that annual crops partition the majority of photosynthate to leaves for several days following emergence. As the crop develops, more is allocated to support root and stem biomass and the relative allocation to leaf growth is reduced. For determinate crops, leaf growth stops at flowering stage while indeterminate crop overlap in their leaf growth and reproductive growth periods. Fig. 2.2 and Fig. 2.3 show changes of measured LWR of determinate crop maize and indeterminate varieties of soybean in Mead, NE and Bondville, IL. Linear relationships can be drawn for both the period of growth before maximum GLAI and after maximum GLAI, with different slopes. The growth stages of peak GLAI of maize and soybean were found to be stable in Mead, NE field experiment and also other studies (Dale et al., 1980; Kumudini et al., 2001) which occurred at silking (R1) and beginning seed/full seed (R5/R6), respectively. As a determinate crop, the peak of GLAI of winter wheat is at the beginning of anthesis. Similar linear relationships or two-stage linear relationships (plateau and linear decrease) for the period before maximum GLAI can be found in many studies of different crops including maize (Bullock et al., 1988; Voldeng and Blackman, 1973), indeterminate and determinate varieties of soybean (Heinemann et al., 2006; Koller et al., 1970; Scott and Batchelor, 1979; Unsworth et al., 1984), dry beans (Wallace and Munger, 1965), sorghum (Lafarge and Hammer, 2002), wheat (Morgan, 1988; Oleary et al., 1985; Assuming SLA is constant.), barley (Mallott and Davy, 1978), rice (Abe and Suge, 1993) and cotton (Miller et al., 1988). For the period after maximum GLAI, although only a few published studies are available (Bullock et al., 1988; Miller et al., 1988; Morgan, 1988), together with our measurements from Mead, NE and Bondville, IL (Fig. 2.3), they show a high linear correlation between GLWR and HUI after maximum GLAI, which represents the gradual senescence of green leaves when approaching maturity.

Based on these findings, we developed a simple method for modeling GLWR (Fig. 2.4), by dividing the growth period into three stages. In the first stage, we assume GLWR is a constant; then followed by a linear equation that represents the decrease in GLWR before maximum GLAI; in the final stage, extending to physiological maturity, another linear equation with different slope and intercept is used. The added input parameters are the ceiling GLWR at early development stage, the intercept of the second-stage linear equation at emergence, the GLWR at maximum GLAI, and the GLWR at physiological maturity. Observed GLWR at physiological maturity is not necessarily zero because the 'stay green' trait (leaves remaining green at physiological maturity) has been found in some varieties of maize, sorghum, sunflower and other crops (Borrell et al., 2001; de la Vega et al., 2011; Subedi and Ma, 2005).

In order to simulate the initial growth at emergence, we added a parameter to present the initial aboveground biomass at emergence. This approach is similar to some other crop models (e.g. WOFOST). This parameter should be variety-specific and reflect the difference of planting population.

2.3.2.6. Other modifications to the DayCent crop submodel

The original plant production function in DayCent used a coefficient (PRDX) for calculating potential aboveground monthly production as a function of solar radiation outside the atmosphere to implicitly represent RUE_{TB}. We modified it to use RUE_{TB} explicitly with unit of g biomass m^{-2} $langley^{-1}$ PAR at the top of the canopy, using measured short-wave solar radiation instead of estimated values in original DayCent. Half of the measured short-wave solar radiation is assumed as PAR (Soltani and Sinclair, 2012).

We also modified the calculation of water stress index. Studies (e.g. Sudar et al., 1981) have demonstrated that AT/PT is a good indicator for water stress effect on production and is used in models like WOFOST (where AT is actual transpiration and PT is potential transpiration). We replaced the original logistic function of water stress effects on daily plant production (where the stress factor was a function of SWC of the wettest soil layer) with the AT/TP relationship in which the water stress effect (0-1 multiplier) on total biomass production is directly proportional to AT/PT.

2.3.2.7. Model parameterization

The manually calibrated parameters for the new GLAI method are shown in Table 2.3. Parameter values for the original and modified model were then calibrated with biomass measurements at Mead, NE for the Pioneer maize cultivar using data of 2002 and 2003 at the site ICM and for the DeKalb cultivar using data of 2005 at ICM. Soybean was calibrated using biomass data of 2006 (relative maturity group 3.5) at IMS. Soybean of 2002 (relative maturity group 2.7) and 2004 (relative maturity group 3.1) were adjusted for the cultivar difference by modifying the parameter of initial aboveground biomass at emergence. The harvest index (HI) of soybean has been found to be very stable within a cultivar but varies dramatically among cultivars (Spaeth et al., 1984). Since there were no readily available data for HI of the cultivars used in the experiment, we derived best estimates of potential HI parameters from measurement (0.48 for Pioneer 93B09 in 2004 and 0.4 for the rest). Phenology in DayCent is expressed using the growing degree days (GDDs) method. For the Mead NE experiment, observed GDDs for critical stages were used as input for each cultivar in each site in the simulation except in 2012. The cumulative GDDs at silking of 2012 has been replaced by the average of the GDDs of other years because the recorded silking date in 2012 is much earlier than those of maize in other years with similar planting date, which implies an error in recording.

For the experiment at Bondville, IL, calibration was done by using data of maize in 2005 and soybean in 2004. We assumed the same cultivars of maize and soybean have been grown every year and calibrated the required cumulative GDDs for critical stages accordingly. In the modified model, when different planting density was used in the field experiments, adjustment to the initial aboveground biomass at emergence was done by reducing the parameter value using the ratio of the two planting density ($Density_{rainfed}/Density_{irrigated}$).

At the site near Ponca City, OK, where no specific information was given about the cultivars grown, we used observed data in 1997 and 1998 seasons for calibration and assumed the same cultivar was used throughout the experiment period.

Potential ET in our simulations was calculated by the standardized Penman-Monteith equation described in FAO Paper 56 (Allen et al., 1998). The mid-season crop coefficient K_c of 1.03 and 0.98 for maize and soybean was previously fit with measured ET of the field experiment at Mead, NE using data from 2001 to 2005 by Suyker and Verma (2009). Thus, for simplicity K_c was set 1.0 for both maize and soybean in the simulations. The mid-season K_c of 1.15 is used for winter wheat according to Allen et al. (1998).

2.3.3. Statistical evaluation

Simulated results by both the original DayCent model and the modified model were compared with experimental observations. The statistical evaluation criteria used were root mean square error (RMSE) and coefficient of determination (R^2), i.e.,

$$\text{RMSE} = \sqrt{\frac{1}{n}\sum_{i=1}^{n}(O_i - P_i)^2} \quad (2.9)$$

$$R^2 = 1 - \frac{\sum_{i=1}^{n}(O_i - P_i)^2}{\sum_{i=1}^{n}(O_i - \bar{O})^2} \quad (2.10)$$

where O_i is the observed value, P_i is the predicted value, n is the total number of observations, and $\bar{O}$ is the average of the observed values.

2.4. RESULTS AND DISCUSSION

2.4.1. GLAI, CC, and Biomass

The measured field data showed a strong correlation between GLAI and total aboveground live biomass over the time period from emergence to full canopy (Fig. 2.5). Aase (1978) also found a correlation of $R^2 = 0.95$ in winter wheat and Ashley et al. (1965) found a similar correlation in cotton. However, in the two locations used in this study, the slopes of the regression (which equals the value for leaf area ratio (LAR) used in the original DayCent) were significantly different for maize (0.0106 at Mead, NE and 0.0054 at Bondville, IL), suggesting that LAR is site or cultivar specific. In the original DayCent model LAR is assumed to be a fixed parameter with a value of 0.011 $m^2\ g^{-1}$, and therefore cannot capture differences between cultivars. In contrast, the slopes and intercepts of the regressions of the new GLAI method as a function of normalized cumulative degree days (shown in Fig. 2.2 and Fig.

2.3) were similar for each crop across cultivars and sites, indicating that the new method is more robust than the original method. To simulate crop canopy development, we used a single set of GLWR input parameter values for each crop across all sites (Table 2.3). The simulated GLAI by the modified model gave generally good agreement with measured data (Figs. 6-8) for the three experimental locations; statistics on model fit are summarized in Table 2.4.

However, the new GLAI method is quite sensitive to the prediction of phenology, which can be seen in 2003 at the Bondville site, where peak GLAI was underpredicted by 23% (measured and simulated were 6.04 and 4.67 respectively). In this year the predicted date of peak GLAI based on thermal time calculated in DayCent occurred 10 days earlier than the measured date and hence simulated leaf growth stopped 10 days too early.

While crops at IL and OK recieved enough rainfall to support ET demands in most years, drought stress occurred in Mead, NE in the rainfed treatment. Our result indicates the model could adequately simulate the effect of drought stress on growth and canopy development at this site. However, more studies should be carried out on the simulation of more severe drought (e.g. experiments in semi-arid regions) to further test this method.

Nutrient stress is another factor that can have a large impact on crop growth. Although there were no treatments with varying nutrients supply to test the new method in this study, our method is potentially valid under nutrient stress, because GLWR can be very stable. One experiment showed that the GLWR of fertilized and un-fertilized spring wheat was not significantly different until close to maturity (Morgan, 1988), indicating the new method will potentially work under conditions of nutrient stress, although additional work is needed to fully test this assumption.

An example of simulated canopy coverage (CC) by the modified and original model is shown in Fig. 2.9. There was not a direct measurement of CC in the experiments so we estimated CC from measured LAI by applying Equation 2.2 with extinction coefficient of 0.6 for both maize and soybean (Ahuja et al., 2000). The accuracy of simulated CC in the late growing season has been dramatically improved

compared to the previous version of DayCent. The overall R^2 was improved from 0.66 to 0.93 for maize and 0.52 to 0.88 for soybean in the Mead, NE experiment.

As GLAI and CC play an important role in crop modeling, various methods have been used in predicting GLAI and CC and evaluations of these methods can be found in many studies. Although we used a simple empirical method on simulation of GLAI and CC, the accuracy of the modified DayCent model is comparable to those of models with a similar (or greater) number of parameters to model GLAI and CC using other approaches (Fraisse et al., 2001; Heng et al., 2009; Lizaso et al., 2003; Todorovic et al., 2009).

Both the original and new methods of GLAI modeling depend on the accuracy of predicting aboveground biomass. The predicted aboveground biomass was fairly accurate for maize ($R^2 = 0.83$) and soybean ($R^2 = 0.89$) at Mead, NE by the original DayCent model. The modified DayCent slightly improved the prediction by improving the overall R^2 to 0.88 and no increase for soybean ($R^2 = 0.89$) (Fig. 2.10). Note that both model versions significantly underestimated biomass of maize in 2003 and 2009 in the rainfed maize-soybean treatment and in 2012 in the irrigated maize-soybean. A possible reason is an underestimation of nitrogen fixation by soybean in the rotation (nitrogen stress was found in simulation but no observed in field).

The effect of changing the function for the water stress effect on plant production is illustrated by the 2012 growing season at Mead, NE, where only 22.2 cm of rain was observed (the driest year in the experimental period; Table 2.1). Both versions of the model provided a good estimation of water stress effect on production, but the new water stress effect method was slightly better, while requiring fewer crop-specific parameters (Fig. 2.10). However, our data was not sufficient to draw a firm conclusion on improved performance and further testing is needed. At Bondville, IL, similarly to the Mead, NE experiment, the overall R^2 of maize on biomass was improved from 0.82 to 0.89 and there was no improvement for soybean with same R^2 of 0.79 (Fig. 2.7). For winter wheat (Fig. 2.8), both models' predictions on biomass are similar with average R^2 of 0.90 and 0.92 for the original and modified models.

2.4.2. ET

The accurate simulation of CC contributed to improved simulation of evaporation and transpiration rates as shown in comparison to weekly cumulative ET measured at Mead, NE (Fig. 2.11). We choose weekly cumulative values because the standardized Penman-Monteith method is more accurate on predicting weekly cumulative ET than daily values since the crop coefficient value can vary significantly on a daily basis (Suyker and Verma, 2009). The analysis of ET at the Mead, NE sites is divided into three periods: non-growing season (harvest to planting of next year), early to middle (planting to DOY 210) and middle to late growing season (DOY 210 to harvest). During the non-growing seasons, the amount of surface residue has a major effect on evaporation. Surface residue blocks solar radiation and advective energy from reaching the soil surface and thus reduces evaporation (Steiner, 1989). Overall, the DayCent model could simulate the effect of surface residue cover on soil evaporation but tended to overestimate the effect in some years (Fig. 2.11). The weekly evaporation during the non-growing season was not well simulated by either model version but the new version had a slightly improved the R^2 of the rainfed site at Mead, NE from 0.30 to 0.34 (Table 2.5). The poor agreement of simulated ET with the measurement in non-growing season likely resulted from the difficulties in simulating the residue cover on the soil surface, effects on snow capture and melting, and the amount of rain intercepted by residue.

For ET during the early to middle growing season, both the original and modified model show relative accurate results. The overall weekly cumulative ET simulation in these periods of the modified model (average RMSE = 0.45 cm, R^2 = 0.81) was better than the original model (average RMSE = 0.56 cm, R^2 = 0.69) for both maize and soybean at the three sites at Mead, NE.

In the late growing season (from DOY 210 to harvest), our simulation shows that the original model substantially over-estimated ET (Fig. 2.11). For example, in 2005 at IMS site, the weekly ET was over-predicted by 35% while the modified model was within 3% of the measurement. The average RMSE of each year decreased from 0.78 cm to 0.42 cm and R^2 increased from 0.53 to 0.82 with the new version. Our modifications resulted in better simulation of green CC at the period of senescence (Fig. 2.9) and thus the allocation of potential soil evaporation and crop transpiration were more accurate.

2.4.3 SWC

Simulated soil water contents (SWC) were compared with the measurement at 10 cm, 25 cm, 50 cm and 100 cm at Mead, for measurements between DOY 90 and DOY 330 when the soil temperature was generally above 0 ^{0}C and water was in liquid phase (and thus measureable by the soil water probes). Both the original and modified model were relatively accurate and the average RMSE of daily SWC was less than 0.06 cm cm^{-1} at all four measurement depths. However, the modified model had a better correlation with measurements than the original model because of the improvement of ET simulation in the late growing season (Table 2.3). For both models, the R^2 was generally higher in the rainfed site than the two irrigated sites. For the modified model, the average R^2 of SWC at the rainfed site at 10 cm and 25 cm improved from 0.57 and 0.56 to 0.71 and 0.73, respectively, compared to the original DayCent version. The lower agreement of simulated SWC with measurements at the irrigated sites may be due to the unevenness of the irrigation application and spatial variation of soil. Fig. 2.12 shows simulated results of the three years which represent a dry year (2003), a normal year (2006) and an annual time series from the irrigation treatment (2005). In all three years, it is clear that the original model underestimated the SWC from DOY 250 to DOY 300, which corresponded to the overestimation of ET for the same period by the original model.

Although the simulation of SWC has been significantly improved by the new method, our analysis also showed some defects of the water flow submodel. As shown in Fig. 2.12, when SWC measurement was above field capacity (e.g., for surface layers in spring of 2003), the simulated values do not exceed field capacity because the default parameterization in DayCent is that water above field capacity is set to drain immediately to field capacity within the same day of infiltration in our simulation. A delayed drainage option was added to the DayCent model to allow the SWC to remain at saturation for 1 or 2 days following rainfall events (Smith et al., 2008). However, in several instances the model overestimated SWC following significant precipitation events and thus the delayed drainage option should be used with caution and needs further evaluation. Accurate simulation of the timing and duration of saturated

conditions is important for simulating N gas loss via denitrification process as pointed out by Yuan et al. (2011).

2.4.4 Crop grain yield

Both the original and modified model provide reasonably accurate simulation on grain yields. The observed yields range from 6.6 to 11.9 and 1.8 to 3.8 for maize and soybean, respectively (Fig. 2.13). Simulated grain yield of maize at Mead, NE and Bondville, IL by the modified model (R^2 = 0.69) was better than the original model (R^2 = 0.47) and the fit for soybean yield was also improved (R^2 of 0.65 vs 0.55). Both models captured the inter-annual variations due to management and climate. For maize simulation, both model versions tended to over-estimate grain yield when observed yield were high. In contrast, for soybean, the modified model underestimated yield when observations were high. The accuracy of prediction is generally similar to other studies using commonly used crop models (Donatelli et al., 1997; Kozak et al., 2006; Todorovic et al., 2009; Xie et al., 2001).

2.5. CONCLUSIONS

In summary, the new empirical method produced accurate estimates of green leaf area index (GLAI) for maize, soybean, and winter wheat. Along with the improvement in GLAI estimates, our modifications improved the model performance of the DayCent model for time series estimates of canopy coverage, evapotranspiration, and soil water content, especially in late growing season period. The modified model also provided slightly better results for biomass and grain yield in both irrigated and rainfed treatments. Although more tests are needed for these three crops and potentially other grain crops, the simplicity, robustness, and generality of the new GLAI method provides potential broader use for simulations of canopy dynamics which has been identified as critical in all kinds of biogeochemical and agricultural modeling.

Table 2.1. Crop management for the three sites at Mead, NE during 2001 to 2012. Data from 2001 is incomplete.

Site/ Year	Crop/cultivar	Plant population (plants ha^{-1})	Planting time (DOY)	Harvest time (DOY)	N application (Kg N ha^{-1} yr^{-1})	Irrigation and rainfall from planting to harvest (cm)
Irrigated continuous maize (ICM)						
2001	M/Pioneer 33P67	82,000	131	291	196	
2002	M/Pioneer 33P67	82,000	130	308	314	72.09
2003	M/Pioneer 33B51	77,000	135	300	235	62.89
2004	M/Pioneer 33B51	79,800	125	288	293	61.25
2005	M/DeKalb 63-75	70,800	125	285	247	64.89
2006	M/Pioneer 33B53	81,800	125	277	211	68.46
2007	M/Pioneer 31N30	78,600	121	309	226	84.73
2008	M/Pioneer 31N30	80,600	120	323	241	77.22
2009	M/Pioneer 32N73	81,500	110	313	243	58.6
2010	M/DeKalb 65-63 VT3	81,700	109	268	235	78.25
2011	M/Pioneer 32T88	85,000	137	299	240	62.73
2012	M/DeKalb 62-97	84,000	114	284	219	57.06
Irrigated maize-soybean rotation (IMS)						
2001	M/Pioneer 33P67	80,900	132	295	196	
2002	S/Asgrow 2703	333,100	140	280	0	57.41
2003	M/Pioneer 33B51	78,000	134	296	226	63.27
2004	S/Pioneer 93B09	296,100	154	287	0	47.06
2005	M/Pioneer 33B51	81,000	122	290	231	63.58
2006	S/Pioneer 93M11	370,600	132	276	0	54.47
2007	M/Pioneer 31N28	78,700	121	309	181	89.92
2008	S/Pioneer 93M11	369,500	135	283	0	72.7
2009	M/Pioneer 32N72	81,500	111	314	171	61.98
2010	M/DeKalb 65-63 VT3	82,500	110	259	246	72.7
2011	M/Pioneer 32T88	85,000	137	299	224	57.79

2012	M/DeKalb 62-97	84,000	115	283	225	60.96
Rainfed maize-soybean rotation (RMS)						
2001	M/Pioneer 33B51	52,600	134	302	128	
2002	S/Asgrow 2703	304,500	140	282	0	37.23
2003	M Pioneer 33B51	57,600	133	286	90	29.15
2004	S/Pioneer 93B09	264,700	154	280	0	30.73
2005	M/Pioneer 33G66	56,300	116	290	117	36.45
2006	S/Pioneer 93M11	370,600	131	276	0	46.9
2007	M/Pioneer 33H26	62,088	121	309	125	60.22
2008	S/Pioneer 93M11	369,500	134	282	0	64.06
2009	M/Pioneer 33T57	61,800	112	315	110	55.82
2010	S/Pioneer 93M11	370,600	139	279	0	60.35
2011	M/DeKalb 61-72RR	56,800	122	291	138	51.98
2012	S/Pioneer 93M43	370,600	136	275	0	20.22

Table 2.2. Soil characteristics of the experimental sites at Mead, NE. Field capacity and wilting point were measured at matric potentials of -33 and -1,500 kPa, respectively.

Site	Measurement depth	Bulk Density	Saturation	Field Capacity	Wilting Point
	cm	g/cm^3	---------- cm/cm ----------		
ICM	10	1.39	0.48	0.37	0.20
	25	1.35	0.49	0.41	0.22
	50	1.44	0.46	0.40	0.22
	100	1.45	0.45	0.41	0.27
IMS	10	1.49	0.44	0.39	0.24
	25	1.49	0.44	0.41	0.26
	50	1.41	0.47	0.42	0.27
	100	1.41	0.47	0.42	0.27
RMS	10	1.41	0.47	0.39	0.23
	25	1.33	0.50	0.40	0.24
	50	1.36	0.49	0.39	0.25
	100	1.31	0.51	0.39	0.22

Table 2.3. Parameters used in model simulations. RUE_{TB} is the radiation use efficiency of total biomass; GLWR is the green leaf weight ratio; GLAI is the green leaf area index; and SLA is the specific leaf area.

	Maize at Mead, NE	**Maize at Bondville, IL**	**Soybean at Mead, NE**	**Soybean at Bondville, IL**	**Winter wheat at Ponca city, OK**
RUE_{TB} (g biomass m^{-2} $langley^{-1}$ PAR)	0.16 (Pioneer), 0.14 (DeKalb)ǂ	0.16	0.08	0.09	0.13
Initial biomass at emergence (g m^{-2})	0.9	1.0	1.4 (2002), 3.0 (2004), 0.4 (2006, 2008, 2010, 2012)	2.5	10.0
Ceiling GLWR at early development stage	0.9	0.9	0.7	0.7	0.5
Intercept of the second stage linear equation at emergence	0.9	0.9	0.85	0.85	0.9
GLWR at maximum GLAI	0.3	0.3	0.3	0.3	0.2
GLWR at physiological maturity	0.02	0.02	0	0	0
SLA (m^2 g^{-1})	0.02	0.02	0.025	0.025	0.025
Extinction coefficient	0.6	0.6	0.6	0.6	0.7

ǂ For rainfed treatment, these values have been adjusted for smaller planting density.

Table 2.4. Statistics of green leaf area index (GLAI) simulation by the modified model. R^2 is coefficient of determination and RMSE is root mean square error.

	Irrigated sites		**Rainfed sites**	
	R^2	RMSE	R^2	RMSE
Mead, NE				
Maize	0.87	0.61	0.82	0.63
Soybean	0.85	0.53	0.84	0.50
Bondville, IL				
Maize			0.72	0.96
Soybean			0.83	0.69
Ponca City, OK				
Winter wheat			0.83	0.53

Table 2.5. R^2 of the simulated evapotranspiration (ET) for three periods in a year and volumetric soil water content (SWC) at 4 depths for the irrigated sites and the rainfed site at Mead, NE. R^2 (coefficient of determination) value is the average of each year.

	Irrigated sites		**Rainfed site**	
	Original	Modified	Original	Modified
ET				
non-growing season	0.27	0.28	0.30	0.34
early and middle season	0.76	0.84	0.62	0.74
late season	0.68	0.87	0.38	0.72
SWC				
10 cm	0.28	0.32	0.57	0.71
25 cm	0.27	0.35	0.56	0.73
50 cm	0.27	0.28	0.51	0.60
100 cm	0.26	0.27	0.36	0.39

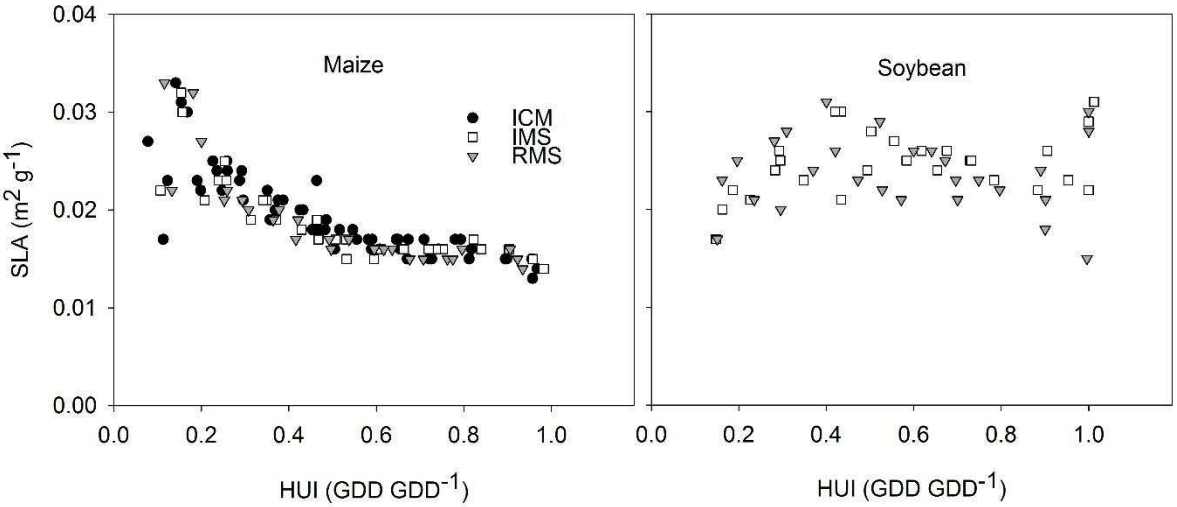

Fig. 2.1. Measured specific leaf area (SLA) of maize (top) and soybean (bottom) at three experiment treatments at Mead, NE from 2001 to 2007. Heat unit index is calculated as ratio of cumulated growing degree days to the amount of growing degree days at physiological maturity. Treatments were irrigated continuous maize (ICM), irrigated maize-soybean (IMS) and rainfed maize-soybean (RMS).

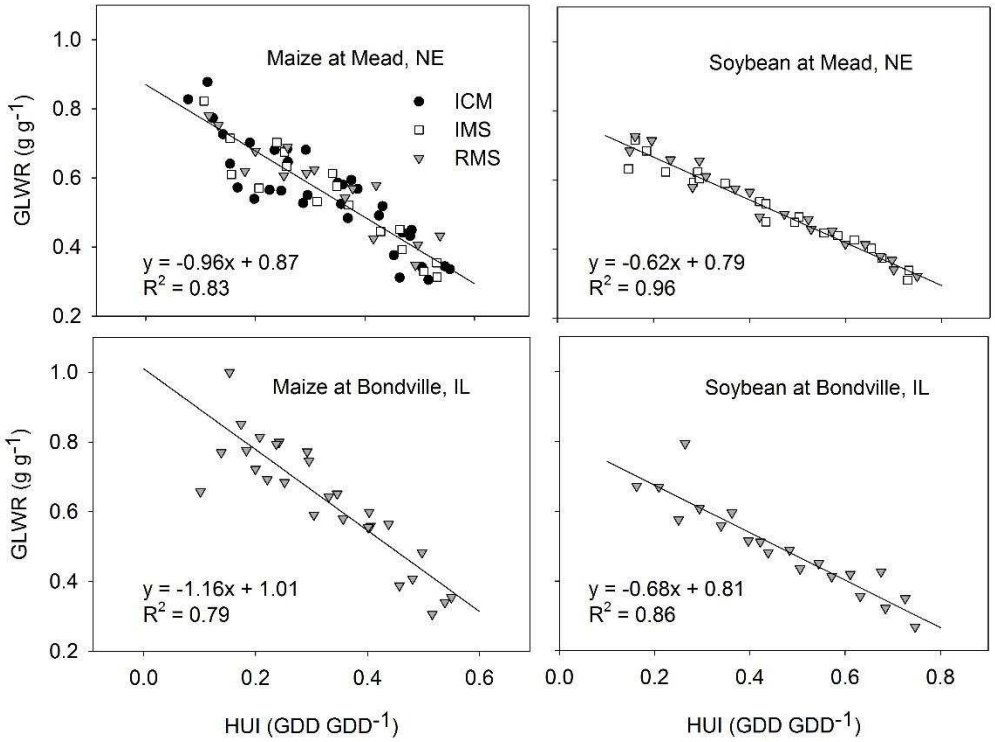

Fig. 2.2. Measured green leaf weight ratio (GLWR) of maize and soybean at two locations from emergence to the development stage of maximum green leaf area index, as a function of the heat unit index (HUI).

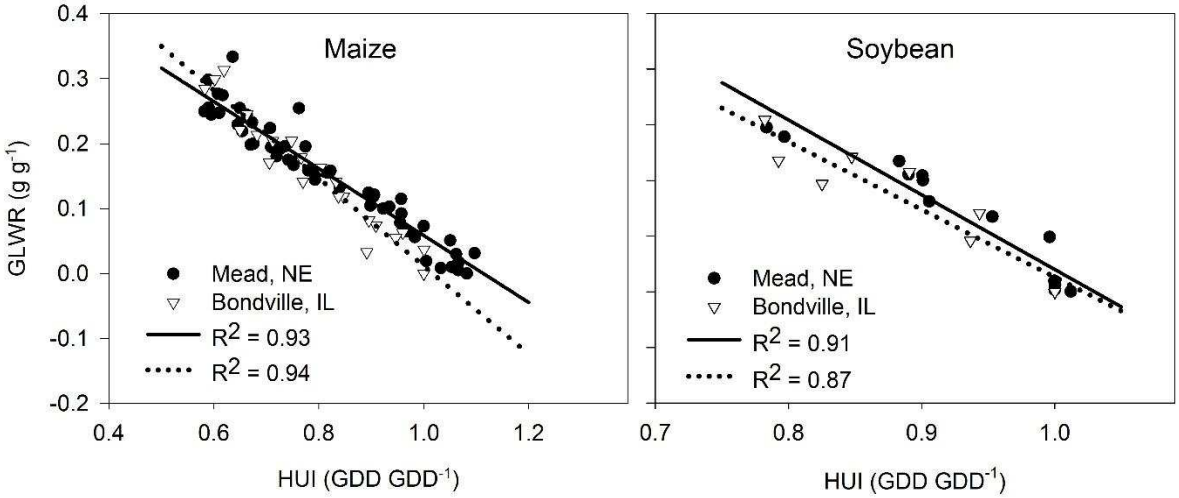

Fig. 2.3. Measured green leaf weight ratio (GLWR) of maize and soybean of two locations from the development stage of maximum green leaf area index to end of growing season.

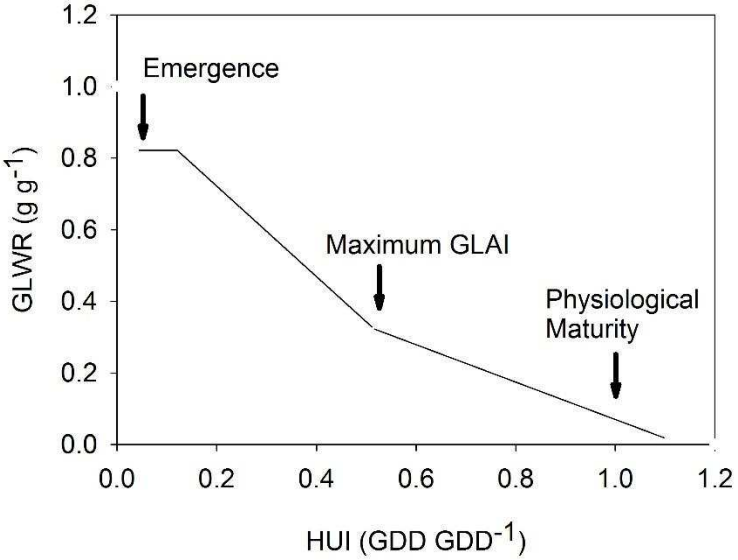

Fig. 2.4 The schematic representation of the new method for green leaf weight ratio (GLWR) modeling.

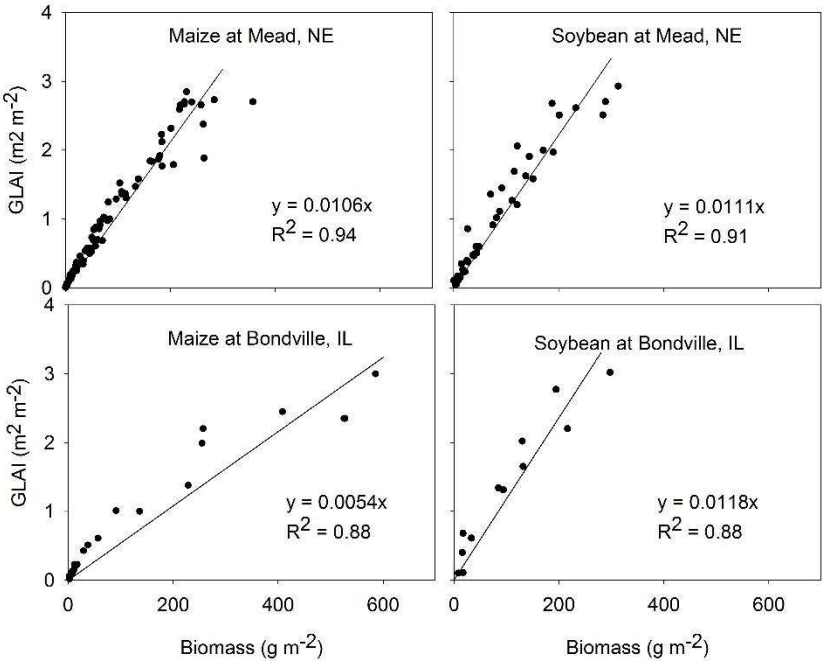

Fig. 2.5 Regression of measured green leaf area index (GLAI) vs. measured aboveground biomass of maize and soybean at two locations.

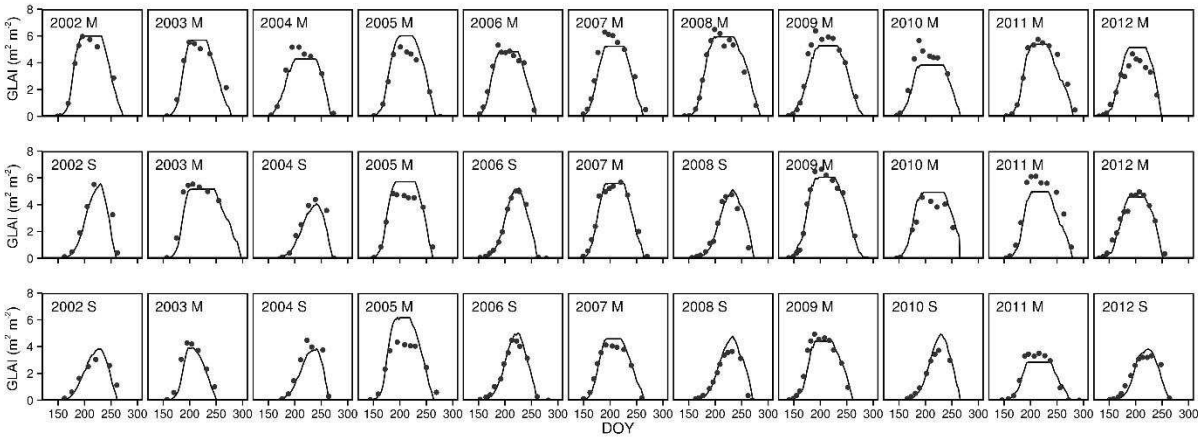

Fig. 2.6. Measured (dot) and simulated green leaf area index (GLAI) by the modified model (solid line) at ICM site (top row), IMS site (middle row), and RMS (bottom row) from 2002 to 2012. M and S stands for maize and soybean, respectively.

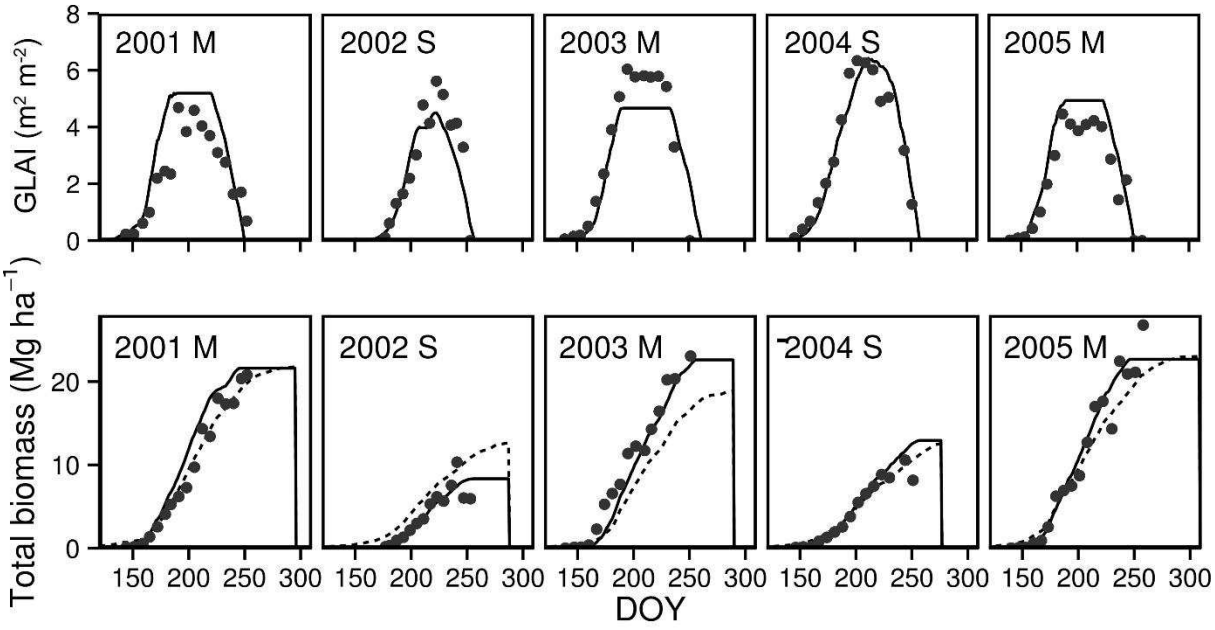

Fig. 2.7. Comparison of measured (dot) and simulated total biomass for experiment at Bondville, IL by original (dashed line) and modified (solid line) models. M and S stands for maize and soybean respectively.

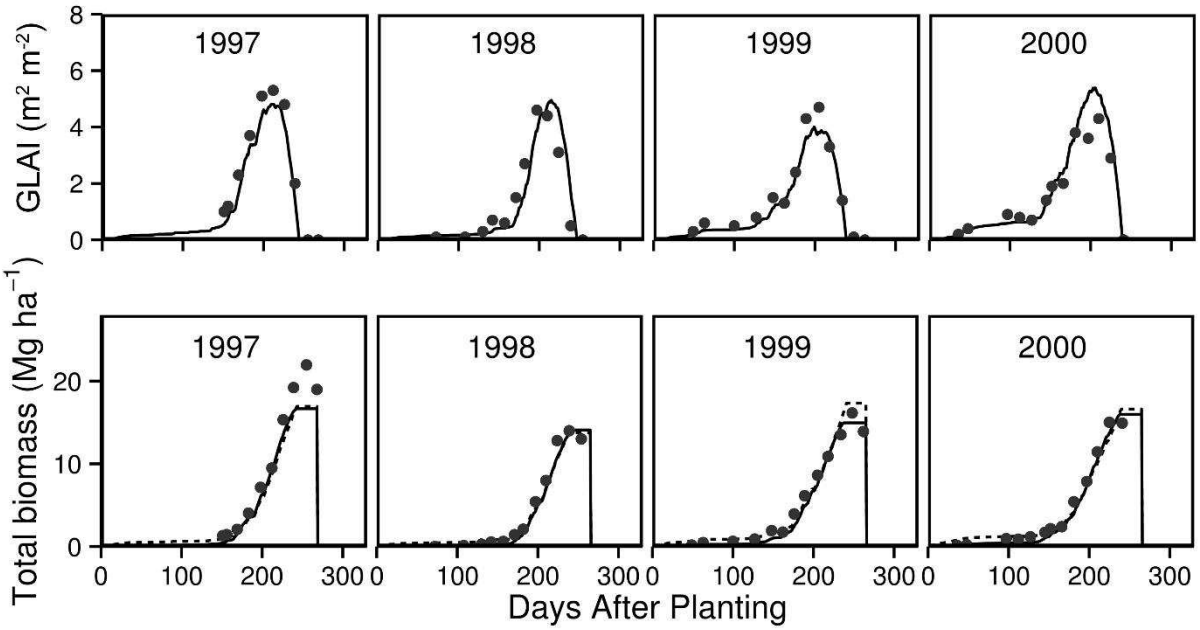

Fig. 2.8. Comparison of measured (dot) and simulated total biomass of winter wheat for experiment at Ponca City, OK by original (dashed line) and modified (solid line) models.

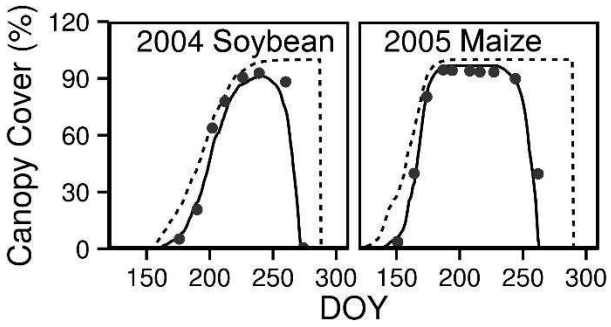

Fig. 2.9. Comparison of measured (dot) and simulated canopy cover of soybean in 2004 and maize in 2005 at IMS site by original (dashed line) and modified (solid line) models.

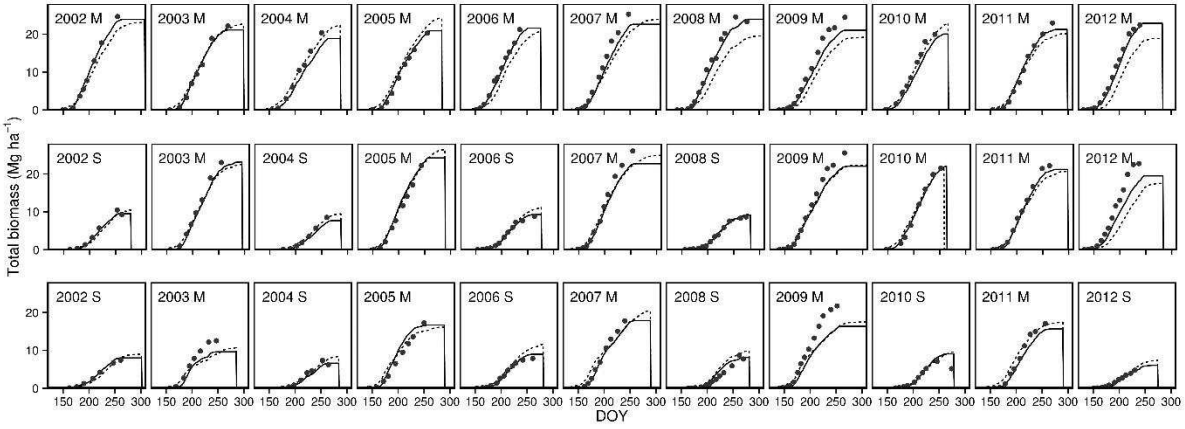

Fig. 2.10. Measured (dot) and simulated total biomass by original (dashed line) and modified (solid line) models at ICM site (top row), IMS site (middle row), and RMS (bottom row) from 2002 to 2012. M and S stands for maize and soybean respectively.

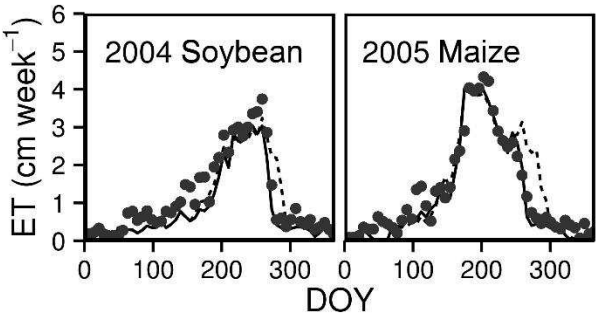

Fig. 2.11. Measured (dot) and simulated weekly cumulative ET of soybean in 2004 and maize in 2005 at IMS site by original (dashed line) and modified (solid line) models.

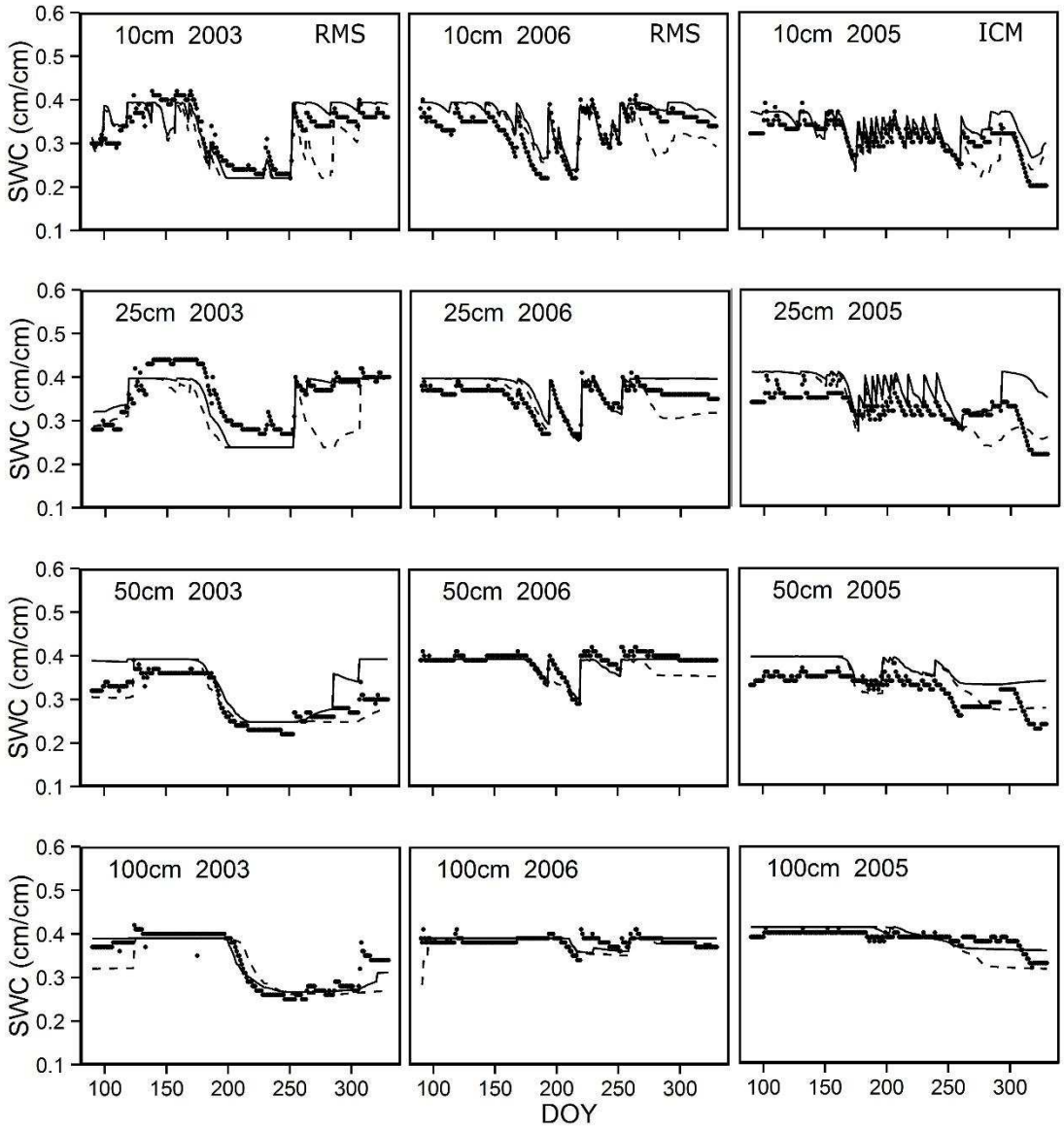

Fig. 2.12. Simulated and measured SWC at 4 depths in three years. Solid line is the simulated result by the modified model and dashed line is the simulated result by the original model. Solid points indicate the measured values. The first two columns of the figure are from the rainfed site and represent a relative dry year (2003) and a year (2006) with growing season precipitation close to long-term average. The third column is from ICM site (irrigated continuous maize).

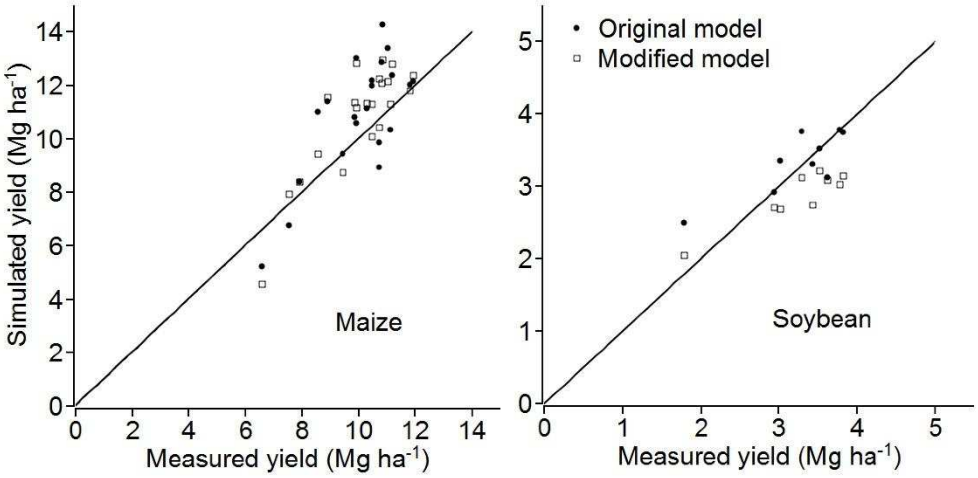

Fig. 2.13. Simulated and measured grain yield for maize and soybean of two experiments. Yield has been adjusted to 0% of moisture.

REFERENCES

Aase, J.K., 1978. Relationship between leaf area and dry-matter in winter-wheat. Agronomy Journal, 70(4): 563-565.

Abe, K. and Suge, H., 1993. Role of gravitropic response in the dry-matter production of rice (Oryza-Sativa L) - an experiment with a line having lazy gene. Journal of Plant Research, 106(1084): 337-343.

Ahuja, L.R., K.W. Rojas, J.D. Hanson, M.J. Shafer and Ma., L., 2000. Root Zone Water Quality Model. Modeling management effects on water quality and crop production. Water Resources Publ., Highlands Ranch, CO.

Allen, R.G., L.S. Pereira, D. Raes and Smith, M., 1998. Crop evapotranspiration: Guidelines for computing crop requirements. FAO Irrigation and Drainage Paper No. 56, Rome, Italy.

Amanullah, M.J.H., Nawab, K. and Ali, A., 2007. Response of specific leaf area (SLA), leaf area index (LAI) and leaf area ratio (LAR) of maize (Zea mays L.) to plant density, rate and timing of nitrogen application. World Applied Sciences Journal, 2(3): 235-243.

Ashley, D.A., Doss, B.D. and Bennett, O.L., 1965. Relation of cotton leaf area index to plant growth and fruiting. Agron. J., 57(1): 61-64.

Borrell, A., Hammer, G. and Van Oosterom, E., 2001. Stay-green: A consequence of the balance between supply and demand for nitrogen during grain filling? Annals of Applied Biology, 138(1): 91-95.

Bullock, D.G., Nielsen, R.L. and Nyquist, W.E., 1988. A growth analysis comparison of corn grown in conventional and equidistant plant spacing. Crop Science, 28(2): 254-258.

Dale, R.F., Coelho, D.T. and Gallo, K.P., 1980. Prediction of daily green leaf-area index for corn. Agronomy Journal, 72(6): 999-1005.

de la Vega, A.J. et al., 2011. Canopy stay-green and yield in non-stressed sunflower. Field Crops Research, 121(1): 175-185.

Del Grosso, S.J., Halvorson, A.D. and Parton, W.J., 2008. Testing DAYCENT model simulations of corn yields and nitrous oxide emissions in irrigated tillage systems in Colorado. Journal of Environmental Quality, 37(4): 1383-1389.

Del Grosso, S.J. et al., 2006. DAYCENT national-scale simulations of nitrous oxide emissions from cropped soils in the United States. Journal of Environmental Quality, 35(4): 1451-1460.

Donatelli, M., Stockle, C., Ceotto, E. and Rinaldi, M., 1997. Evaluation of CropSyst for cropping systems at two locations of northern and southern Italy. European Journal of Agronomy, 6(1-2): 35-45.

Farahani, H.J., Howell, T.A., Shuttleworth, W.J. and Bausch, W.C., 2007. Evapotranspiration: Progress in measurement and modeling in agriculture. Transactions of the Asabe, 50(5): 1627-1638.

Fraisse, C.W., Sudduth, K.A. and Kitchen, N.R., 2001. Calibration of the CERES-Maize model for simulating site-specific crop development and yield on claypan soils. Applied Engineering in Agriculture, 17(4): 547-556.

Grant, R.F. et al., 2007. Net biome productivity of irrigated and rainfed maize-soybean rotations: Modeling vs. measurements. Agronomy Journal, 99(6): 1404-1423.

Hanan, N.P. et al., 2002. Inversion of net ecosystem CO2 flux measurements for estimation of canopy PAR absorption. Global Change Biology, 8(6): 563-574.

Heinemann, A.B., Maia, A.D., Dourado-Neto, D., Ingram, K.T. and Hoogenboom, C., 2006. Soybean (Glycine max (L.) Merr.) growth and development response to CO2 enrichment under different temperature regimes. European Journal of Agronomy, 24(1): 52-61.

Heng, L.K., Hsiao, T., Evett, S., Howell, T. and Steduto, P., 2009. Validating the fao aquacrop model for irrigated and water deficient field maize. Agronomy Journal, 101(3): 488-498.

Jarecki, M.K., Parkin, T.B., Chan, A.S.K., Hatfield, J.L. and Jones, R., 2008. Comparison of DAYCENT-simulated and measured nitrous oxide emissions from a corn field. Journal of Environmental Quality, 37(5): 1685-1690.

Jeuffroy, M.H. and Recous, S., 1999. Azodyn: a simple model simulating the date of nitrogen deficiency for decision support in wheat fertilization. European Journal of Agronomy, 10(2): 129-144.

Koller, H.R., Nyquist, W.E. and Chorush, I.S., 1970. Growth analysis of soybean community. Crop Science, 10(4): 407-412.

Kozak, J.A., Ma, L., Ahuja, L.R., Flerchinger, G. and Nielsen, D.C., 2006. Evaluating various water stress calculations in RZWQM and RZ-SHAW for corn and soybean production. Agronomy Journal, 98(4): 1146-1155.

Kumudini, S., Hume, D.J. and Chu, G., 2001. Genetic improvement in short season soybeans: I. Dry matter accumulation, partitioning, and leaf area duration. Crop Science, 41(2): 391-398.

Lafarge, T.A. and Hammer, G.L., 2002. Predicting plant leaf area production: shoot assimilate accumulation and partitioning, and leaf area ratio, are stable for a wide range of sorghum population densities. Field Crops Research, 77(2-3): 137-151.

Lizaso, J.I., Batchelor, W.D. and Westgate, M.E., 2003. A leaf area model to simulate cultivar-specific expansion and senescence of maize leaves. Field Crops Research, 80(1): 1-17.

Maas, S.J., 1993. Parameterized model of gramineous crop growth .1. leaf-area and dry mass simulation. Agronomy Journal, 85(2): 348-353.

Mallott, P.G. and Davy, A.J., 1978. Analysis of effects of bird cherry-oat aphid on growth of barley - unrestricted infestation. New Phytologist, 80(1): 209-218.

Meyers, T.P. and Hollinger, S.E., 2004. An assessment of storage terms in the surface energy balance of maize and soybean. Agricultural and Forest Meteorology, 125(1-2): 105-115.

Miller, J.E., Patterson, R.P., Heagle, A.S., Pursley, W.A. and Heck, W.W., 1988. Growth of cotton under chronic ozone stress at 2 levels of soil-moisture. Journal of Environmental Quality, 17(4): 635-643.

Monsi, M. and Saeki, T., 1953. The light factor in plant communities and its significance for dry matter production. Japanese Journal of Botany 14: 22-52.

Morgan, J.A., 1988. Growth and canopy carbon-dioxide exchange-rate of spring wheat as affected by nitrogen status. Crop Science, 28(1): 95-100.

Oleary, G.J., Connor, D.J. and White, D.H., 1985. A simulation-model of the development, growth and yield of the wheat crop. Agricultural Systems, 17(1): 1-26.

Parton, W.J., Hartman, M., Ojima, D. and Schimel, D., 1998. DAYCENT and its land surface submodel: description and testing. Global and Planetary Change, 19(1-4): 35-48.

Parton, W.J., Schimel, D.S., Cole, C.V. and Ojima, D.S., 1987. Analysis of factors controlling soil organic-matter levels in great-plains grasslands. Soil Science Society of America Journal, 51(5): 1173-1179.

Ranatunga, K., Nation, E.R. and Barratt, D.G., 2008. Review of soil water models and their applications in Australia. Environmental Modelling & Software, 23(9): 1182-1206.

Richards, L.A., 1931. Capillary conduction of liquids through porous mediums. Physics-a Journal of General and Applied Physics, 1(1): 318-333.

Sadras, V.O. and Milroy, S.P., 1996. Soil-water thresholds for the responses of leaf expansion and gas exchange: A review. Field Crops Research, 47(2-3): 253-266.

Scott, H.D. and Batchelor, J.T., 1979. Dry-weight and leaf area production-rates of irrigated determinate soybeans. Agronomy Journal, 71(5): 776-782.

Sellers, P.J., 1985. Canopy reflectance, photosynthesis and transpiration. International Journal of Remote Sensing, 6(8): 1335-1372.

Sionit, N., Hellmers, H. and Strain, B.R., 1982. Interaction of atmospheric co2 enrichment and irradiance on plant-growth. Agronomy Journal, 74(4): 721-725.

Smith, W.N. et al., 2008. Evaluation of two process-based models to estimate soil N2O emissions in Eastern Canada. Canadian Journal of Soil Science, 88(2): 251-260.

Soltani, A. and Sinclair, T.R., 2012. Modeling Physiology of crop development, growth and yield. CABI International, Wallingford, UK.

Spaeth, S.C., Randall, H.C., Sinclair, T.R. and Vendeland, J.S., 1984. Stability of soybean harvest index. Agronomy Journal, 76(3): 482-486.

Steduto, P., Hsiao, T.C., Raes, D. and Fereres, E., 2009. AquaCrop-The FAO crop model to simulate yield response to water: I. Concepts and underlying principles. Agronomy Journal, 101(3): 426-437.

Steiner, J.L., 1989. Tillage and surface residue effects on evaporation from soils. Soil Science Society of America Journal, 53(3): 911-916.

Stockle, C.O., Martin, S.A. and Campbell, G.S., 1994. CropSyst, a cropping systems simulation-model - water nitrogen budgets and crop yield. Agricultural Systems, 46(3): 335-359.

Subedi, K.D. and Ma, B.L., 2005. Nitrogen uptake and partitioning in stay-green and leafy maize hybrids. Crop Science, 45(2): 740-747.

Sudar, R.A., Saxton, K.E. and Spomer, R.G., 1981. A predictive model of water-stress in corn and soybeans. Transactions of the Asae, 24(1): 97-102.

Suyker, A.E. and Verma, S.B., 2009. Evapotranspiration of irrigated and rainfed maize-soybean cropping systems. Agricultural and Forest Meteorology, 149(3-4): 443-452.

Tardieu, F., Granier, C. and Muller, B., 1999. Modelling leaf expansion in a fluctuating environment: are changes in specific leaf area a consequence of changes in expansion rate? New Phytologist, 143(1): 33-44.

Todorovic, M. et al., 2009. Assessment of AquaCrop, CropSyst, and WOFOST models in the simulation of sunflower growth under different water regimes. Agronomy Journal, 101(3): 509-521.

Unsworth, M.H., Lesser, V.M. and Heagle, A.S., 1984. Radiation interception and the growth of soybeans exposed to ozone in open-top field chambers. Journal of Applied Ecology, 21(3): 1059-1077.

Vandiepen, C.A., Wolf, J., Vankeulen, H. and Rappoldt, C., 1989. WOFOST - A simulation-model of crop production. Soil Use and Management, 5(1): 16-24.

Voldeng, H.D. and Blackman, G.E., 1973. Analysis of components of growth which determine course of development under field conditions of selected inbreds and their hybrids of Zea mays. Annals of Botany, 37(151): 539-552.

Wallace, D. and Munger, H., 1965. Studies of the physiological basis for yield differences. I. Growth analysis of six dry bean varieties. Crop Science, 5(4): 343-348.

Williams, J.W., Izaurralde, R.C. and Steglich, E.M., 2008. Agricultural policy/environmental extender model: Theoretical documentation, Version 0604.

Xie, Y., Kiniry, J.R., Nedbalek, V. and Rosenthal, W.D., 2001. Maize and sorghum simulations with CERES-maize, SORKAM, and ALMANAC under water-limiting conditions. Agronomy Journal, 93(5): 1148-1155.

Yuan, F.M., Meixner, T., Fenn, M.E. and Simunek, J., 2011. Impact of transient soil water simulation to estimated nitrogen leaching and emission at high- and low-deposition forest sites in Southern California. Journal of Geophysical Research-Biogeosciences, 116.

Zhang, Y., Qian, Y.L., Bremer, D.J. and Kaye, J.P., 2013. Simulation of nitrous oxide emissions and estimation of global warming potential in turfgrass systems using the DAYCENT model. Journal of Environmental Quality, 42(4): 1100-1108.

CHAPTER 3. MODELING DEFICIT IRRIGATION OF MAIZE WITH THE DAYCENT MODEL

3.1. SUMMARY

Dramatic increase in water demand in municipal and industrial sections results in less water available for crop irrigation in semi-arid region of U.S. Limited irrigation strategy is seen as one of the promising solutions to close this water demand and supply gap. To estimate crop water use and production under limited irrigation is challenging. Dynamic models have been designed to understand the impact of limited irrigation and provide information on decision making. In this study, we presented the parameterization and validation results on three limited irrigation experiments using a recently improved version of the DayCent ecosystem model. We also compared the stress coefficient (K_s) method of the original DAYCENT model with the one described in the FAO 56 paper. Overall, the new leaf area method provided fairly accurate estimation of green leaf area index (GLAI) for full and limited irrigation treatments. The method tends to over-predict the GLAI at late vegetative growth period of the limited irrigation treatments. GLAI, biomass, and grain yields compared well with the measured values. There is little difference between the two K_s methods in the output variables. In summary, the DAYCENT model could simulate the response of maize under water deficit conditions and could be used as a guide for application of limited irrigation strategies for water saving.

3.2. INTRODUCTION

Dramatically increased water demand from municipal and industrial users will create bigger water shortage in the future in arid and semi-arid regions of U.S; in semi-arid Colorado, the projected water demand and supply analysis showed that the state's water shortage gap is between 0.23 and 0.78 km^3 by 2050 which is 3.5% to 11.9% of current annual consumption (Colorado Water Conservation Board, 2010; Vorosmarty et al., 2000). To meet this demand, one of the strategies is to transfer water from agriculture (composes 86% water supply at 2010). The Colorado Water Conservation Board (2010)

projected a significant loss of irrigated agriculture and the associated wetlands by 2050; which means about 40% of the South Platte Basin and 30% of the Arkansas Basin would dry up. One of the alternatives is to apply limited irrigation to reduce irrigation water use and maintain certain amount of crop yields (Fereres and Soriano, 2007). However, to estimate crop water use and production under limited irrigation is challenging. In order to gain more understanding of limited irrigation and provide predictions for decision support, field experiments and modeling exercises are very necessary (Fereres and Soriano, 2007; Saseendran et al., 2014; Trout et al., 2010).

Lack of irrigation results in substantial crop yield reduction in semi-arid and arid regions (Doorenbos and Kassam, 1979). The mechanism is well studied that water stress causes leaf stomatal closure to prevent loss of water through transpiration, which also results in reduction of the inward transportation rate of CO_2 (Hsiao, 1973). Thus, the CO_2 assimilation of photosynthesis is reduced. Persistent drought also leads to reduced leaf area and further reduce the amount of light intercepted by canopy for photosynthesis. Other changes due to drought include leaf rolling, the partitioning of assimilate among root and shoot, the rate of nutrient uptake and transport, etc. (Hsiao, 1973).

Our understanding of drought effect on crop growth and production has been incorporated into crop models for hypothesis testing and yield predictions (Ma et al., 2003; Todorovic et al., 2009; Xie et al., 2001). The DAYCENT model (Del Grosso et al., 2011; Del Grosso et al., 2000; Parton et al., 1998) is an ecosystem model which has been widely used for estimation of soil carbon and nitrogen, and greenhouse gas emission in agro-ecosystems. It contains a crop growth/production sub-model and has been applied in simulations of agricultural lands not only in the U.S. but also globally (Del Grosso et al., 2008; Lee et al., 2012; Stehfest et al., 2007). Recently, we found soil water use of crop lands was not properly simulated due to its simple method for canopy development. The original model assumed full canopy cover for middle and late growing season which was not valid in severe water or nutrient stress environments. The lack of senescence process in late growing season resulted in over-prediction of transpiration. To improve the model, a new green leaf area index (GLAI) simulation method was developed and implemented into the DayCent model which is characterized as simple, robust, and easy

for parameterizing (Chapter 2). The improved model has been applied to irrigated and rain-fed conditions (Chapter 2). Results showed simulated ET, SWC, GLAI, biomass and yield of maize, soybean, and wheat were compared well with measured values. It suggested this version of model simulated crop response to water stress better than the original model. However, there was no comprehensive and systematic validation of the modeled drought effect.

To estimate the drought effect on transpiration, DayCent model simulated stress coefficient (K_s) as a function of relative soil water content (RSWC) of the wettest soil layer. An exponential function was used to describe the relationship. This approach was similar to the one documented in FAO Irrigation and Drainage Paper No. 56 (Allen et al., 1998). In contrast, the relationship of RSWC and K_s was modeled using linear equations, which was very easy to parameterize. Additionally, the RSWC in FAO 56 was calculated based on the soil water in entire root zone. While in theory, both K_s methods might be proper and they have been used in various models, some field studies (Meyer and Green, 1981; Shouse et al., 1982) indicated the linear method provided better fit to measurements. It is not clear on the accuracy of simulated drought effect on transpiration and crop production by these two methods in dynamic models.

To further evaluate the new version of DayCent model and improve the simulated water stress effect, three data sets of limited irrigation experiments of corn conducted in Colorado were used in this study. The objectives are to: 1) simulate and test the new GLAI method in DayCent model using measured GLAI under water limited conditions; 2) examine the predictions of crop growth, biomass accumulation, grain yield and soil water dynamics; 3) compare the simulated drought effect on transpiration and production using two stress coefficients (K_s) methods.

3.3. MATERIALS AND METHODS

3.3.1. Field Experiment

3.3.1.1. Greeley, Colorado

The first field experiment was conducted near Greeley, Colorado (Ma et al., 2012; Trout et al., 2010) which was designed to study limited irrigation strategy on crop production. From 2008 to 2011, maize hybrid ‘Dekalb 52-59’ was planted in May (Table 3.2). Dripping irrigation was applied through

surface drip tubing adjacent to each row. As described in Saseendran et al. (2014), six irrigation treatments (numbered from 1 to 6) are to apply certain percentage of potential crop ET requirements: 100%, 85%V, 70%, 70%V, 55%V, and 40%V (Table 3.2). Letter V denotes that 20% of the calculated amounts of irrigation were withheld and added to the reproductive growth period on a weekly basis. Fertilizer was applied several times every year to meet the potential need of crop for nutrients.

The soil of this site is a sandy loam with three soil types Nunn (Fine, smectitic, mesic Aridic Argiustolls), Olney (Fine-loamy, mixed, superactive, mesic Ustic Haplargids), and Otero (Coarse-loamy, mixed, superactive, calcareous, mesic Aridic Ustorthents). An on-site standard Colorado Agriculture Meteorological Network weather station was established for measurement. Aboveground biomass was only sampled at harvest and LAI was measured weekly using LI-3000C portable leaf area meter (non-destructive method) in 2010 in 4 treatments only. Green canopy cover was estimated using nadir-view digital camera mounted on a mobile platform weekly. Soil water content near surface (0 – 15 cm) was measured with a portable TDR senor (MiniTrase, Soil Moisture Equipment Corp.). Neutron probe (503 DR Hydroprobe moisture gauge, Campbell Pacific Nuclear) was used for measurement from 30 to 200 cm at 30 cm increment.

3.3.1.2. Fort Collins, Colorado

This field experiment was conducted at Agricultural Research, Development and Education Center of Colorado State University near Fort Collins, Colorado from 2006 to 2010. Maize was irrigated with linear move sprinkler system and two treatments were studied: full irrigation and limited irrigation. Full irrigation was to meet crop water need in entire growing season based on crop ET requirement which is similar to the Greeley experiment. For the limited irrigation treatment, no irrigation was applied before V12 stage and full irrigation was started afterwards. To ensure uniform germination, early irrigation was supplied as necessary in both treatments. Fertilizer has been applied according to crop need and details of management can be found in DeJonge et al.(2012).

Soil at this site is a Fort Collins Loam (fine-loamy, mixed, superactive, mesic Aridic Haplustalf). Gravimetric soil water content was sampled weekly in 2008 to a depth of 40 cm and less frequently to 90

cm. In 2007, 2008, and 2009 growing seasons, LAI was sampled by a non-destructive method (DeJonge et al., 2011). Crop yield of 2008 reported here has been corrected for hail damage occurred on 14 August 2008. An on-site standard Colorado Agriculture Meteorological Network weather station (FTC03) was used for weather recording.

3.3.1.3. Akron, Colorado

Limited irrigation experiment was conducted at the USDA Central Great Plains Research Station near Akron, Colorado. Maize of Pioneer Hybrid 3732 was planted in May during 1984, 1985, and 1986 three growing seasons. A line-source gradient irrigation system (Nielsen, 1997) was designed to apply water linearly declining with distance from the line. Four levels (only three in 1984) of irrigation were conducted and irrigation catch gauges were placed in sampling sub-plots for measurement of irrigation amount. Irrigation was not applied before tasseling; the amount of irrigation of all treatments is in Table 2.1. Fertilizer of ammonium nitrate was applied before each planting at 168 kg N ha^{-1}.

The soil type is a Rago silt loam (fine, smectitic, mesic Pachic Argiustoll); detailed soil texture information can be found in Ma et al. (2003). Neutron probe readings of soil moisture were made several times from planting to harvest in 1985. The measurement depth was from 15 cm to 165 cm with 30 cm increment. Aboveground biomass and leaf area measurements were made periodically in 1984 and 1985 by the destructive method from 1 m of crop row sampling. Weather data are available from an automated station about 300 m from the experimental site.

3.3.2. The DAYCENT Model

3.3.2.1. Overall description of DayCent model

The DayCent model is the daily time step version of the CENTURY model which was widely used for simulation of soil carbon and nitrogen cycling (Parton et al., 1987). The DayCent simulates major ecosystem processes including plant production, changes in soil water, soil organic matter dynamics, and trace gas emissions, etc. The main inputs include soil property, daily weather data, plant type, and management practices.

In this study, modified DAYCENT model (Chapter 2) was used. The most notable change in this testing version is the new method for leaf area simulation. The new method can be described as

$$GLAI = Biomass_{aboveground} * GLWR * SLA \quad (3.1)$$

where GLAI is green leaf area index; GLWR is the green leaf weigh ratio; and SLA is specific leaf area. In the modified model, SLA is kept as constant while GLWR changes from emergence to maturity. The change of GLWR is modeled using three linear equations as shown in Fig. 3.1. Unlike some crop models, this method does not intend to explain the allocation of daily carbon supply among organs in a physiological way but assumes there is a kind of regulation mechanism of crop that regulates the amount of green leaf biomass as a fraction of its total biomass. This leaf area method has been validated for maize and soybean in two locations in the Corn Belt and for winter wheat in northern Oklahoma (Chapter 2). Under drought stressed conditions, we assume there is no direct water stress effect on either GLWR or SLA in current version of the model. In DAYCENT model, phenology of the reproductive stages is modeled as accelerated by water stress. So indirectly, enhanced leaf senescence under drought is modeled as a result of faster development of phenology. The importance of GLAI is that it provides prediction on canopy cover (CC) which is used in the plant production sub-model for estimating the amount of light intercepted by the leaves and also in the soil water sub-model for partitioning PET into soil evaporation and plant transpiration. In DAYCENT, CC is calculated simply by Beer's equation as a function of GLAI.

$$CC = 1 - \exp(-k * GLAI) \quad (3.2)$$

where k is the extinction coefficient.

3.3.2.1. Plant production sub-model

In this testing version of DAYCENT, daily potential production (PP) is a function of intercepted light using the concept of radiation use efficiency (RUE).

$$PP = CC * PAR * RUE \quad (3.3)$$

where CC is short for canopy cover; PAR is the photosynthetic radiation which is assumed half of the measured short wave radiation. Actual production (AP) is calculated considering temperature, water and nutrients effect.

$$AP = \min(PP * T_e * W_e , PP_{nutrient}) \quad (3.4)$$

where T_e and W_e are temperature and water effect; $PP_{nutrient}$ is the maximum production can be supported by available nutrients. There are no explicit pools for stem, leaf, and grain for crops in the model. Grain biomass is calculated using predicted harvest index (HI) which is the fraction of grain to total aboveground biomass.

Soil water sub-model

The DAYCENT model uses a method incorporating the field capacity concept of the tipping-bucket approach and applies Richards' equation for water re-distribution after the dainage from saturation to field capacity; details can be found in Parton et al.(1998). At the beginning of daily loop, PET is calculated from climatic inputs and crop coefficent (fixed value and equivilent to $K_{c\ mid}$ in FAO 56). CC is used to estimate the propotion of potential transpiration:

$$PT = PET * CC \quad (3.5)$$

where, PT is potential transpiration and PET is crop potential evapotranspiration. Actual transpiration is firstly estimated using a stress coefficient that is a function of the soil water status (discussed later). And the actual root water uptake in each soil layer is based on the root uptake coefficients in that layer (reflecting the amount of root in that layer and ability for water uptake) and soil water potential. The water stress effect on daily production is fraction of AT to PT in the modified version of DAYCENT. So the prediction for AT under limited soil water condition is critical for the model to simulate the biomass and yield of the limited irrigation experiments.

Stress coefficient of transpiration

The soil water status used in the DAYCENT model for estimating the stress coefficient of transpiration is the relative soil water content (RSWC) of the wettest soil layer in the root zone.

$$RSWC_i = (SWC_i – WP_i)/(FC_i – WP_i) \quad (3.6)$$

$$RSWC_{wettest} = \max(RSWC_i) \quad (3.7)$$

where SWC, FC, and WP are the soil water content, field capacity, and wilting point of soil layer i; $RSWC_{wet}$ is the RSWC of the wettest soil layer in the root zone. The stress coefficient is a function of $RSWC_{wettest}$ (Fig. 3.2):

$$K_s = 1.0 - \exp(-b * RSWC_{wettest}) \quad (3.8)$$

where b is a coefficient of the curve and is set 3.0 as default in DAYCENT.

In this study, we compared the DAYCENT default method on K_s to the FAO 56 method (Allen et al., 1998). The FAO 56 method of K_s is based on the water depletion in the entire root zone. First, the total available soil water in the current root zone (TAW) is calculated each day.

$$TAW = (FC - WP) * Z_r \quad (3.9)$$

where Z_r the rooting depth. To apply this equation in DAYCENT, we calculate (FC – WP) and multiply by layer width for each soil layer in root zone and summed them up. The relation of K_s and the fraction of soil water depletion (D_r) to TAW is shown in Fig. 3.2. The turning point of the FAO 56 curve is (1 – p); p is "the fraction of TAW that a crop can extract from the root zone without suffering water stress is the readily available soil water". Factor p is adjusted for ET demand using an empirical equation:

$$p = p_{Table} + 0.04 * (0.5cm - ET_c) \quad (3.10)$$

where, p_{Table} is the recommended p value for a crop type in the table of FAO 56 paper; ET_c is the crop ET of FAO 56 method. In our calculation, ET_c was replaced with PT which represents the demand of water for root uptake.

3.3.3. Model calibration

The model with original K_s method and the one with FAO 56 K_s method were calibrated separately. For the experiment at Greeley, CO, the measurement from the full irrigation treatment of 2010 was used to calibrate the model because LAI data were only available in 2010. Two brands of hybrids were used in the experiment at Fort Collins, CO. We calibrated Garst 8827 with measurement of full irrigation treatment in 2007 and hybrids of Pioneer with data of 2010. Although different hybrids of Pioneer were used from 2008 to 2010, we used the same set of parameters as little information was

available about the difference of the hybrids. Data in 1985 of treatment 4 in the Akron, CO experiment was used for calibration as SWC was measured only in 1985. The crop coefficient of ET at mid-season of 1.2 based on recommendation of FAO 56 was used for all locations. The factor p_{Table} is set 0.55 for maize according to FAO 56. Parameters and values used in the simulations are listed in Table 3.2. Nitrogen stress effect was not simulated as ample nitrogen fertilizer was applied in all the experiments for stress-free growth and no nutrient deficit symptoms were observed in fields.

Statistics

To compare model predictions to measurements and between simulation models, we selected root mean square error (RMSE) and coefficient of determination (R^2) as evaluation criteria.

$$RMSE = \sqrt{\frac{1}{n}\sum_{i=1}^{n}(O_i - P_i)^2} \quad (3.11)$$

$$R^2 = 1 - \frac{\sum_{i=1}^{n}(O_i - P_i)^2}{\sum_{i=1}^{n}(O_i - \overline{O})^2} \quad (3.12)$$

Where O_i is the observed value, P_i is the predicted value, n is the total number of observations, and $\overline{O}$ is the average of the observed values. These two criteria are commonly reported in modeling studies and provide good evaluation of model performance.

3.4. RESULTS AND DISCUSSION

3.4.1. Greeley, CO

Simulated K_s represents the drought effect on transpiration. Taking Treatment 6 (lowest irrigation water) in 2008 as an example, severe water stress was simulated around DOY 200 (Fig. 3.3a) which resulted in low actual transpiration rate in the same period (Fig. 3.3b). There was not substantial difference in simulated K_s values using the DAYCENT Ks method and the FAO 56 method (Fig. 3.3a). This resulted in the similar simulated daily actual transpiration rates (Fig. 3.3b). As shown in Fig. 3.2, when $RSWC_{wettest}$ was at 1.0, the corresponding K_s value was 0.95 for the DAYCENT method and 1.0 for the FAO 56 K_s method. In theory, if plenty water is in root zone, there should be no water stress for plant and maximum K_s is expected to be 1.0. The coefficients of equation used in DAYCENT were originally fitted with field measurements and not theoretically perfect. Using treatment 6 in 2008 as an example

(Fig. 3.3a), between Day 150 and Day 190, simulated K_s value by DAYCENT Ks method was 0.95 which was lower than 1.0 of the FAO 56 K_s method. As a result, slightly more actual transpiration (3% more than the DAYCENT K_s method) was simulated by FAO 56 K_s method between Day 150 and Day 190 (Fig. 3.3b). Because more water lost during the period between Day 150 and Day 190, the simulated K_s (Fig. 3.3b) was lower in FAO 56 method around Day 200. The overall difference in the growing season was little. Under no stressed condition where K_s was at its maximum, potential production is always lower in the DAYCENT K_s method if same reference RUE was used. So we calibrated RUE to be slightly higher in the DAYCENT K_s method in order to achieve same potential production (Table 3.2).

Leaf area determines the amount of light intercepted for photosynthesis and the percentage of actual transpiration relative to full canopy. In this experiment, the measurement of GLAI was only conducted for 4 of the 6 treatments in 2010. Regarding the model prediction of GLAI, both DAYCENT K_s method and FAO 56 K_s method accurately simulated GLAI of the full irrigation treatment (Fig. 3.4). For the limited irrigation treatment 4 and 5, both methods slightly over-predicted GLAI in the later part of the vegetative growth period. One of the reasonable guesses was that water stress causes SLA decreasing in the field while the model assumes SLA as constant (Tardieu et al., 1999). However, in another experiment conducted at the same site at Greeley, CO in 2013, measured SLA at three weeks before silking showed a trend of increase under mild drought stress (Fig. 3.5; not significant between treatments at 0.05 level using LSD test; unpublished data). Similarly, unchanged SLA in maize under water deficit was reported by Tardieu et al. (1999) although they showed decreased SLA in sunflower leaves under mild water stress. Another possible reason was that the leaf structure change due to water deficit (leaf rolling) was not modeled. Our field observation showed obvious change in leaf structure in the stressed treatments. Under drought, leaves became more erect and rolls inward to reduce the amount of light intercepted by canopy thus reduce biomass production and leaf area. In modeling, leaf rolling can be simulated as change in extinction coefficient of Beer's Law (Equation 3.2). Cavero et al. (2000) reported a decrease of the extinction coefficient of their field measurement of maize due to water stress and found

improved simulation results after making the fixed coefficient as a function water stress in their modified EPICphase model.

Drought stress substantially inhibited the biomass production in the field (Fig. 3.6). The drought stress effect was well simulated by both K_s methods in our model in all four years (Fig. 3.6). The FAO 56 K_s method was slightly better than the DAYCENT K_s method in this simulation (1129 kg ha^{-1} of FAO 56 method comparing to 1537 kg ha^{-1} of the DAYCENT K_s method). Both methods over-predicted the biomass in 2010 for the Treatment 4, 5 and 6. Similar to our result, Ma et al. (2012) found the RZWQM2 model over-predicted the biomass of the same treatments in 2010. Regarding grain yield (Fig. 3.7), model predictions provided very good fit to the observations. Our prediction of grain yields was similar to those from RZWQM2 model (Ma et al., 2012). Overall, DAYCENT model with both methods could simulate the effect of water stress on production at this site.

The SWC was simulated by the DAYCENT model with fair accuracy. The RMSE of comparison to neutron probe measurement at 30, 60, 90, and 120 cm measurement depths were 0.033, 0.026, 0.028, and 0.026 cm cm^{-1}, respectively; and R^2 were 0.43, 0.44, 0.25, and 0.16. The statistics of both the DAYCETN K_s method and FAO 56 K_s method were almost the same; thus result of only one model was presented. These statistics were similar to those of two irrigated experimental sites at eastern Nebraska in Chapter 1. The comparison of SWC of top 15 cm was not shown because the same potable TDR devices were found relatively low accuracy in another experiment at a site near Fort Collins, CO (Erika Foster, personal communication, 2015).

3.4.2. Fort Collins, CO

Measurement of GLAI in this experiment was made in 2007, 2008, and 2009 in vegetative growth period only. Again, the model accurately simulated the GLAI under the full irrigation treatment for both K_s methods (Fig. 3.8; full irrigation treatment in 2007 and 2008 were used for calibration). For the limited irrigation treatment, the accuracy was slightly lower. Similar to the simulated GLAI at Greeley, CO, the GLAI of the limited irrigation treatment at late vegetative growth was over-predicted in 2007. In 2008, the GLAI in the whole vegetative growth period was over-predicted for the limited

irrigation treatment. The reason might be that the stressed crop was slower to recover from adversity. As stated in DeJonge et al. (2011), a tornado that occurred in in nearby Windsor, CO on 22 May 2008 likely delayed the leaf development following this period. In 2009, the observed GLAI of limited irrigation was even higher than the full irrigation treatment which might due to the large variations in the field; thus, it appeared that the model under-predicted the GLAI for the limited treatment in this year. Overall, the new leaf area method provided accurate estimation of leaf development under both non-stress and drought stress conditions.

The predictions of grain yields of the full irrigation treatment were fairly well for this site. They were within 12% of the measured values in the five years (Fig. 3.9; RMSE of 668 and 837 kg ha^{-1} for DAYCENT Ks method and FAO 56 K_s method). Both K_s methods under-predicted the yield of limited irrigation treatment (10.3% and 13.7% lower in average for the DAYCENT and FAO 56 methods). Similarly, DeJonge et al. (2012) simulated this experiment with the CERES-Maize model and found the original model under-predicted the yield of limited irrigation by 12.9%. Although the modified CERE-Maize provides better yield prediction of five-year average, the RMSE (1451 kg ha^{-1}) was larger than those of the DAYCENT model (834 and 1114 kg ha^{-1} for DAYCENT Ks method and FAO 56 method).

Regarding soil water, both K_s methods resulted in good predictions of SWC (Fig. 3.10). The difference of predicted SWC between the two K_s methods was negligible. The R^2 was higher in the limited irrigation treatment (0.67) than the full irrigation treatment (0.41). In Chapter 1, we found similar results and concluded that irrigation uniformity and spatial variations in soil likely resulted in the lower agreement with observations of full irrigation.

3.4.3. Akron, CO

There was no full irrigation treatment in the experiment at Akron, CO. All treatments started to receive irrigation just prior to tasseling (stage VT). Thus, observed peak GLAI was less than 4 in both 1984 and 1985 due to the drought stress at the vegetative growth period. The new GLAI method implemented in DAYCENT model accurately simulated the development of leaf area for both K_s methods (Fig. 3.11). Regarding biomass, simulated results were fairly accurate and the difference of the two K_s is

small (Fig. 3.12). The two K_s methods slightly under-predicted finial biomass at harvest for treatment 1 and 3 in 1984. In 1985, we observed large variation in the measured biomass at the vegetative period. Measured biomass values were constantly higher in treatment 2 and 3 than that in treatment 1 and 4. As no irrigation was initiated at that period, we would expect similar amount of biomass.

Grain yield was correctly simulated in 1985 for all treatments (Fig. 3.13; treatment 4 of 1985 was used for calibration). In 1984, the predicted yield of treatment 3 was close to the measurement but the yields of treatment 1 and 2 were largely over-predicted (about twice of the measurement) by both K_s methods. As we see in Fig. 3.12, the predicted final biomass was fairly well; thus the model failed to predict HI correctly. The observed HI values of treatment 1 and 2 in 1984 were only 0.20 and 0.22 while model predictions are 0.41 and 0.42 by both K_s methods. The reason was likely that although water stress effect on HI was simulated by DAYCENT, the inhibition of pollination resulted from severe stress was not considered in the model. In the AquaCrop model, Raes et al. (2009) described a method introducing a water stress coefficient for pollination in addition to the simulated reduction of HI due to reduced photosynthesis rate. Similar method can be added to DAYCENT model to improve simulation on HI under severe water stress. For the grain yields in 1986, both K_s methods under-predicted the values by 18% in average of four treatments. It was hard to determine the reason as there was no measurement of biomass and HI in 1986. Ma et al. (2003) simulated the same experiment using the RZWQM model. In their simulation, yields of Treatment 1, 2 and 3, were overestimated by 23% and 35%, and overestimated by 18% in 1984, respectively. In 1985, yields were predicted well. In 1986, the model under-predicted the yield values ranging from 10% to 24%. These results were in high agreement with the predictions from our DAYCENT model.

SWC was well simulated by both K_s methods (Table 3.3) in 1985. The R^2 was lower at 15 cm depth than the deeper depths which may due to the high spatial variations in crop residue cover in the field according to Saseendran et al.(2008). Saseendran et al.(2008) simulated the same experiment using the CERES-maize model. The RMSE of SWC simulation using DAYCENT was slightly lower than the reported value of 0.025 of the simulation using CERES-maize.

3.5. CONCLUSIONS

The new leaf area method implemented in DAYCENT model provided relatively accurate estimation of GLAI of maize grown in Colorado regarding its simplicity. The changes in GLAI in response to water deficit were well represented, although the GLAI of the limited irrigation treatments at late vegetative growth period was slightly over-predicted. Both the DAYCENT K_s method and FAO 56 K_s method provided similar predictions on actual transpiration and leads to similar results of simulated SWC, biomass production and grain yields. The accuracy of predictions of these variables was fairly high. It is hard to conclude which method is superior than the other based on the results of this study; however, the FAO 56 56 K_s method is easier for parameterization. Comparing these predictions of the new DayCent model with simulations of the same experiments by some other crop models, the performance of DAYCENT is at the same level. The advantages of the new DayCent model is the simplicity and that the most of input parameters can be directly measured. With further testing on other crop types and conditions in the future, the new DayCent model can be used as a tool to provide decision-support and forecasting capabilities for agricultural producers and water managers.

Table 3.1 Crop management for the three sites in Colorado.

Site/ Year	Crop/cultivar	Plant population (plants ha^{-1})	Planting time (DOY)	Harvest time (DOY)	Rainfall in growing season (cm)	Total irrigation (cm)
Greeley, Colorado						
2008	Dekalb 52-59	81,000	133	311	23	43.8, 33.8, 28.2, 27.2,18.1, and 13.7Ɨ
2009	Dekalb 52-59	81,000	131	306	22.9	41.8, 34.8, 30, 25, 16.8, and 10.9Ɨ
2010	Dekalb 52-59	81,000	131	305	20	36.5, 29, 24.7, 22, 15.9, and 11.2Ɨ
2011	Dekalb 52-59	81,000	123	298	17.6	48.5, 38.8, 32.9, 30.6, 22.1, and 15.7Ɨ
Akron, Colorado						
1984	Pioneer 3732	72,400	133	275	26.5	2.3, 6.8, and 10.6ǂ
1985	Pioneer 3732	76,100	123	270	30.8	7.2, 9.8, 15.1, and 18.8ǂ
1986	Pioneer 3732	76,100	121	288	22.6	14.6, 20.3, 25.8, and 29.9ǂ
Fort Collins, Colorado						
2006	Garst 8827	79,100, and 59,300§	130	308	8.3	50.0, and 25.9§
2007	Garst 8827	79,800, and 59,300§	128	317	20.1	36.2 and 21.0§
2008	Pioneer 38P	79,100	121	324	24.1	40.6 and 20.3§
2009	Pioneer P9512XR	79,100	133	317	20.2	29.2, and 19.1§
2010	Producers Hybrids 5004VT3	79,100	124	289	15.2	40.0 and 21.0§

Ɨ Treatments are 100%, 85%V, 70%, 70%V, 55%V, and 40%V (percentage of potential crop ET). Letter V denotes that 20% of the calculated amounts of irrigation were withheld and added to the reproductive growth period on a weekly basis.
ǂ Irrigation levels from treatment 1 to treatment 4. There is no treatment 4 in 1984.
§ Treatments are full irrigation and limited irrigation.

Table 3.2. Calibrated parameters used in simulations.

Parameters	Dekalb 52-59 Greeley	Pioneer 3732 Akron	Garst 8827 Fort Collins	Pioneer Fort Collins
RUE (g biomass m^{-2} $langley^{-1}$ PAR)	0.15 (DAYCENT), 0.14 (FAO 56)	0.165 (DAYCENT) 0.16 (FAO 56)	0.17 (DAYCENT), 0.16 (FAO 56)	0.165 (DAYCENT), 0.155 (FAO 56)
Optimum temperature for production (^{0}C)	27			
Initial biomass at emergence (g m^{-2})	0.4	0.1	0.4 Ɨ	0.1
Ceiling GLWR at early development stage	0.9			
Intercept of the second stage linear equation at emergence	0.9			
GLWR at maximum GLAI	0.25			
GLWR at physiological maturity	0.02			
SLA (m^2 g^{-1})	0.02			
Extinction coefficient	0.55 ǂ			

Ɨ For limited irrigation treatment, this value have been adjusted for smaller planting density.
ǂ Calibrated using measured canopy cover and GLAI in 2010 of the experiment at Greeley, CO.

Table 3.3 Statistics of simulated soil water content at 4 depths across treatments in 1985 at Akron, CO.

Depth (cm)	DAYCENT Ks method		FAO Ks method	
	RMSE	R^2	RMSE	R^2
15	0.03	0.46	0.03	0.47
45	0.03	0.73	0.03	0.73
75	0.03	0.63	0.04	0.68
105	0.02	0.78	0.03	0.73

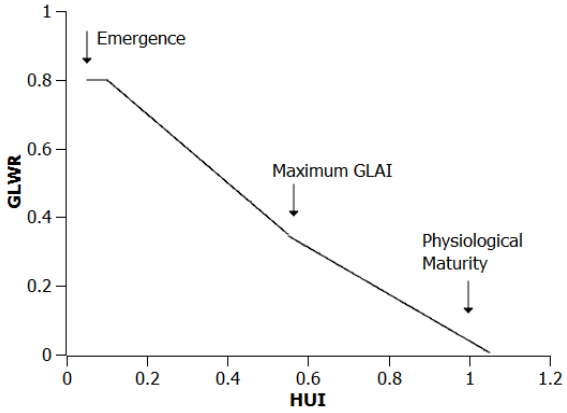

Fig. 3.1. The schematic representation of the new method for green leaf weight ratio (GLWR) modeling in Chapter 2.

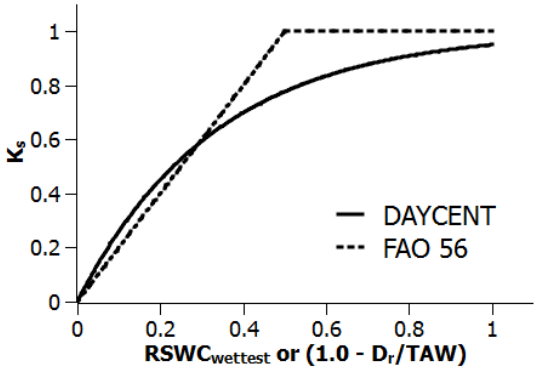

Fig. 3.2. Water stress coefficient (K_s) response function to the relative soil water content of the wettest soil layer ($RSWC_{wettest}$) in DAYCENT model and the relative depletion in soil water content (D_r/TAW) of the FAO 56 method.

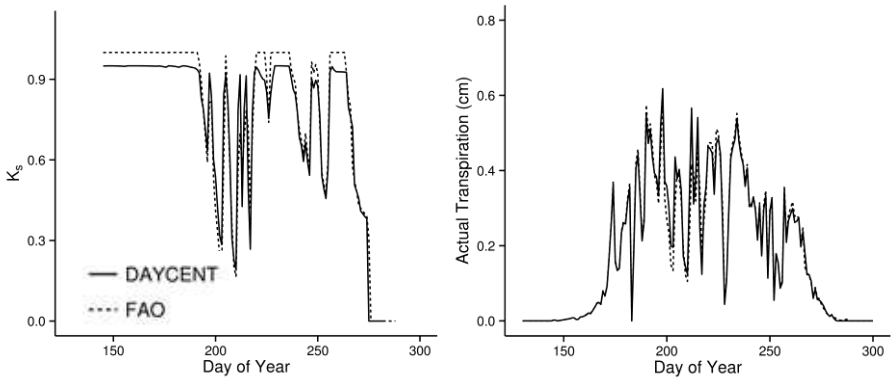

Fig. 3.3. Example of simulated a) stress coefficient (K_s) and b) actual transpiration of Treatment 6 in 2008 of the Greeley experiment by the DAYCENT K_s method and FAO 56 K_s method.

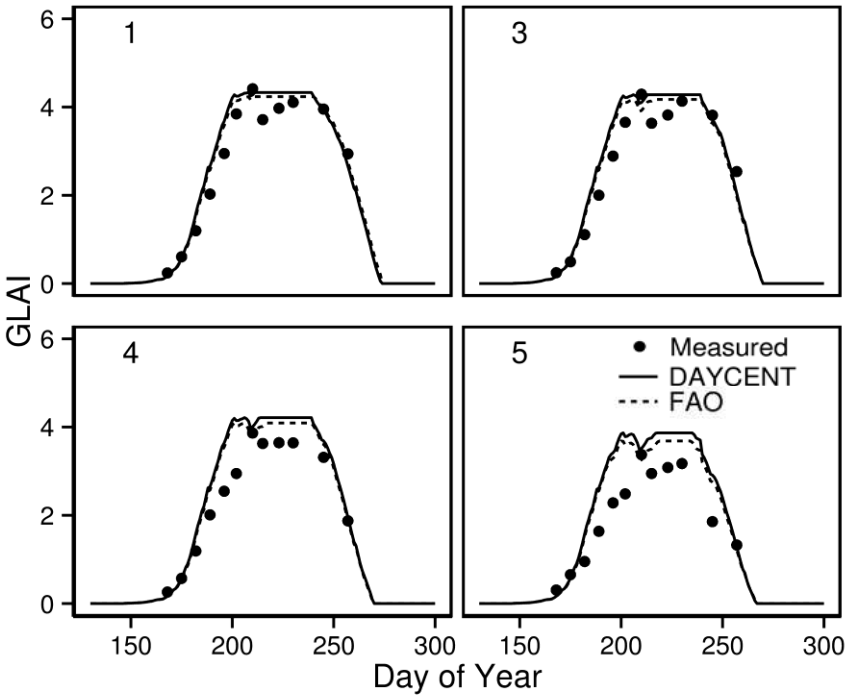

Fig. 3.4. Comparison of measured green leaf area index (GLAI) of Treatment 1, 3, 4, and 5 in 2010 of the experiment at Greeley, CO and simulated values by the DAYCENT K_s method and FAO 56 K_s method.

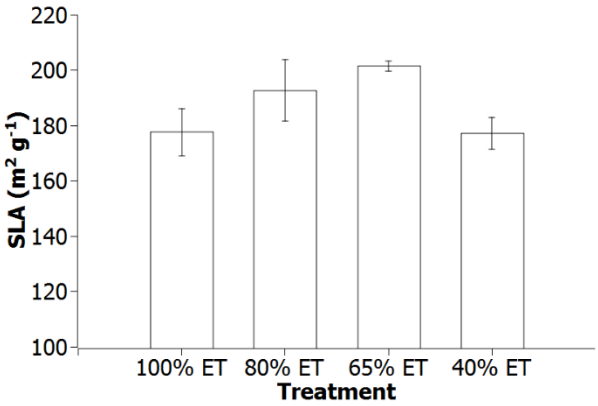

Fig. 3.5. Measure specific leaf area (SLA) in a limited irrigation experiment at Greeley, CO in 2013 (unpublished data). Measurement was taken about three weeks before silking.

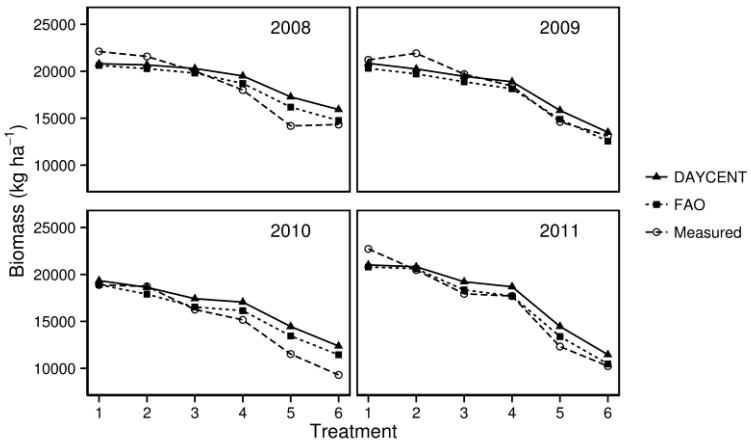

Fig. 3.6. Comparison of measured final aboveground biomass at harvest of the experiment at Greeley, CO and simulated values by DAYCENT K_s method and FAO 56 K_s method. Irrigation amount decreases from Treatment 1 to Treatment 6.

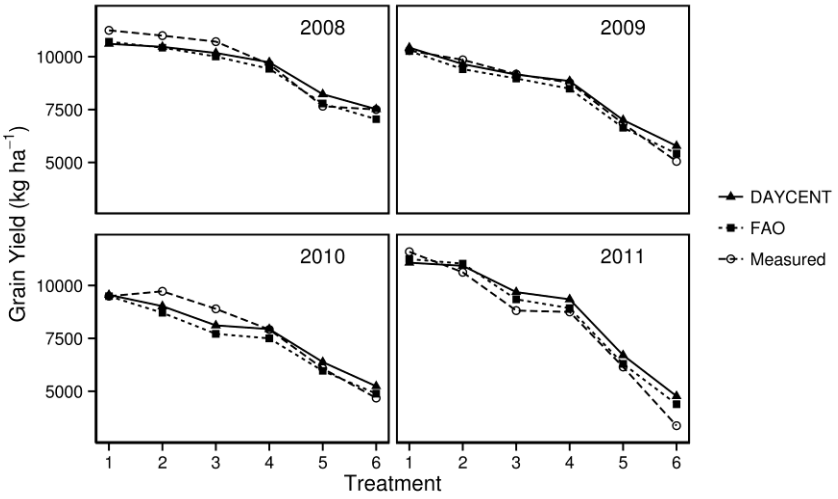

Fig. 3.7. Comparison of measured grain yields (0% moisture) of the experiment at Greeley, CO and simulated values by DAYCENT K_s method and FAO 56 K_s method. Irrigation amount decreases from Treatment 1 to Treatment 6.

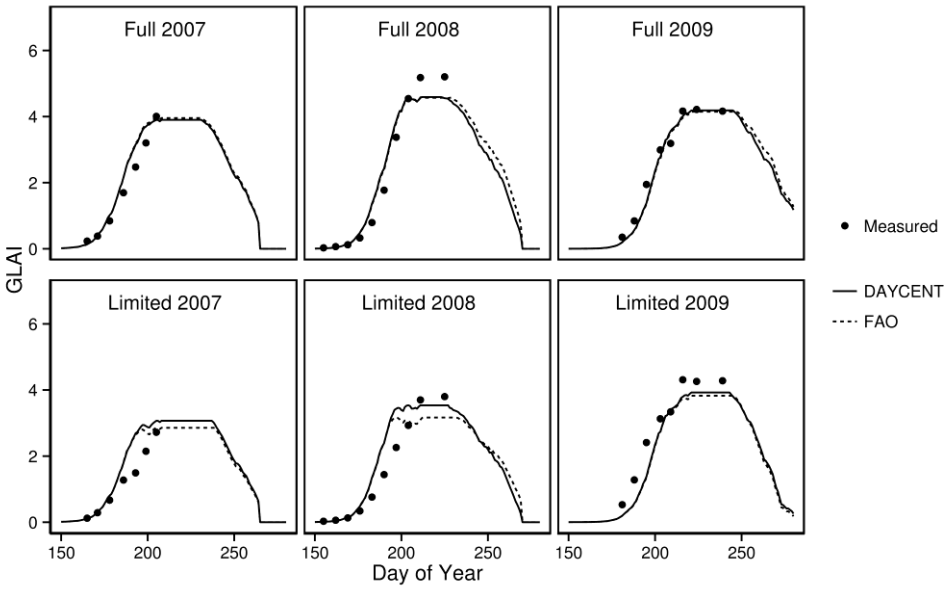

Fig. 3.8. Comparison between measured green leaf area index (GLAI) of the full and limited irrigation treatments of the experiment at Fort Collins, CO and simulated values by the DAYCENT K_s method and FAO 56 K_s method.

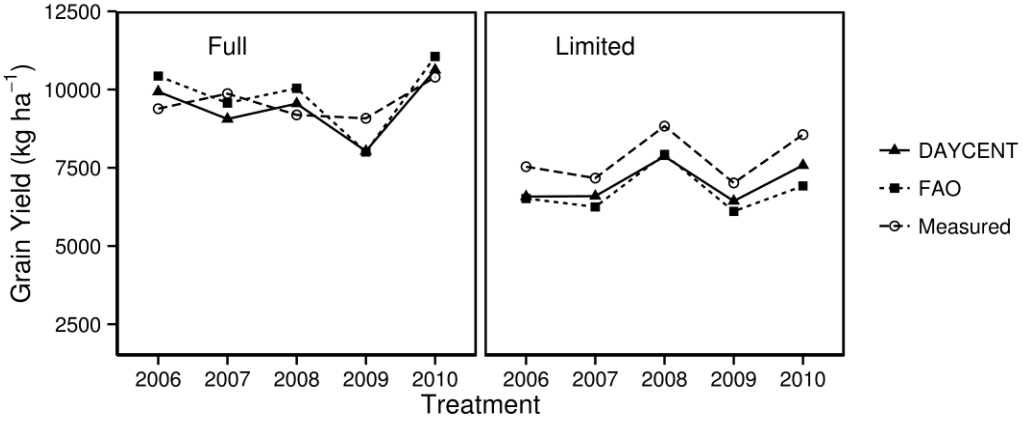

Fig. 3.9. Comparison of measured grain yields (0% moisture) of the experiment at Fort Collins, CO and simulated values by DAYCENT K_s method and FAO 56 K_s method for full and limited irrigation treatments.

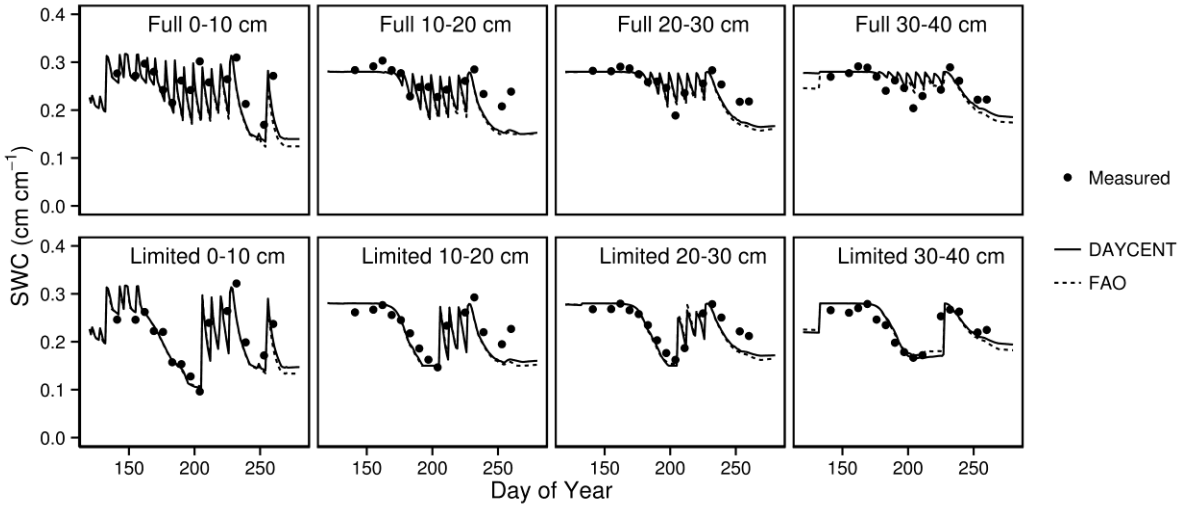

Fig. 3.10. Comparison of measured soil water content (SWC) of four depths in 2008 at Fort Collins, CO and simulated values by DAYCENT K_s method and FAO 56 K_s method for full and limited irrigation treatments.

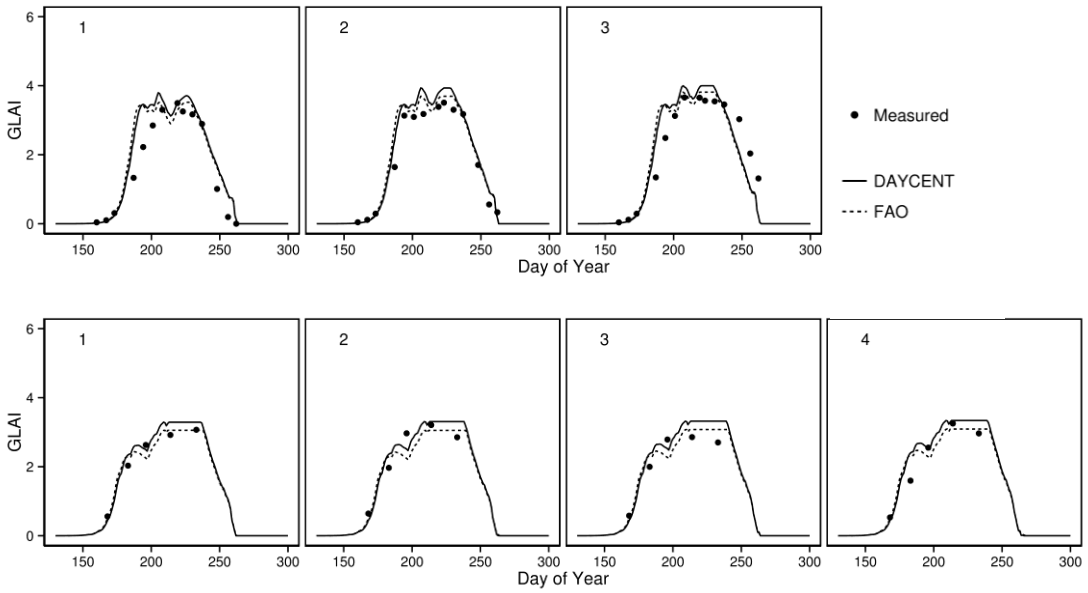

Fig. 3.11. Comparison between measured green leaf area index (GLAI) of the 4 treatments (only 3 in 1984) of the experiment at Akron, CO and simulated values by the DAYCENT K_s method and FAO 56 K_s method.

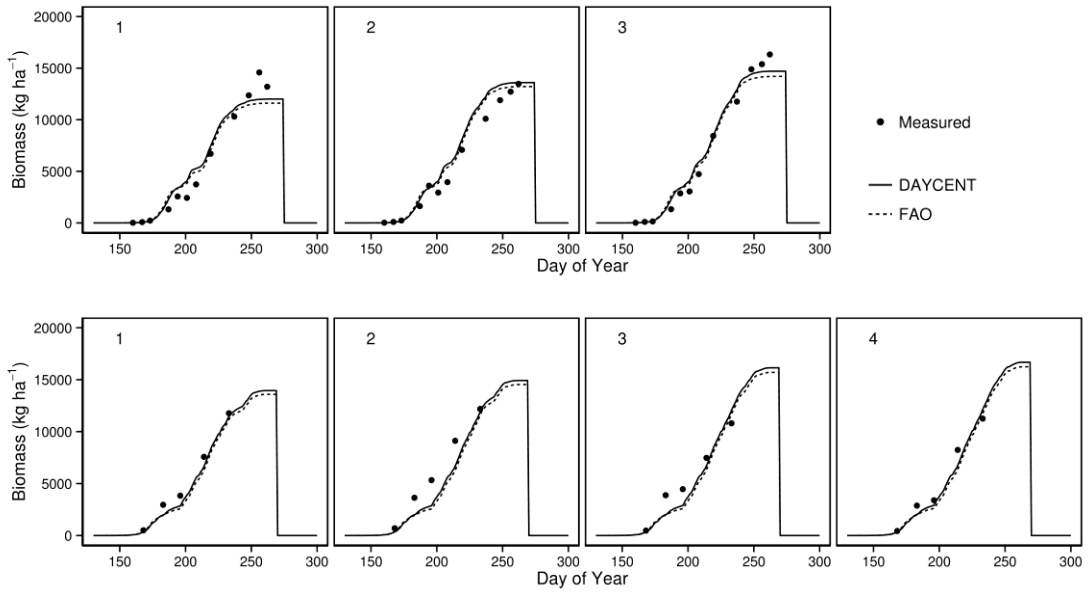

Fig. 3.12. Comparison between measured aboveground biomass of the 4 treatments (only 3 in 1984) of the experiment at Akron, CO and simulated values by the DAYCENT K_s method and FAO 56 K_s method.

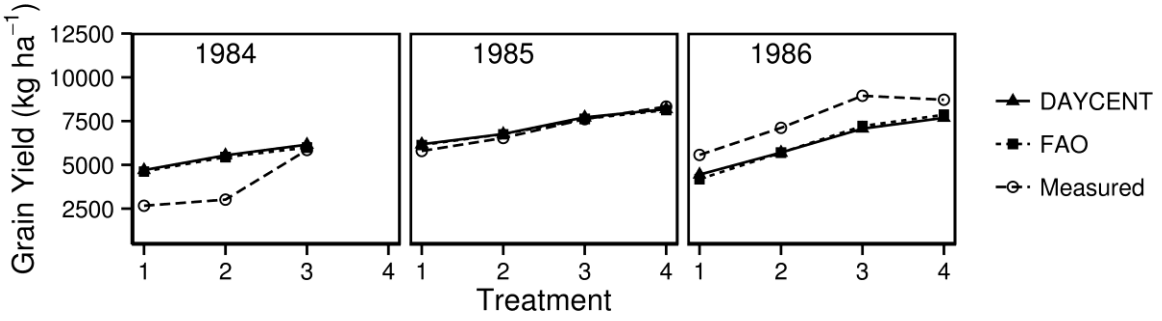

Fig. 3.13. Comparison between measured grain yield (0% moisture) of the 4 treatments (only 3 in 1984) of the experiment at Akron, CO and simulated values by the DAYCENT K_s method and FAO 56 K_s method.

REFERENCES

Allen, R. G., L.S. Pereira, D. Raes, and Smith, M. (1998). Crop evapotranspiration: Guidelines for computing crop requirements. FAO Irrigation and Drainage Paper No. 56. Rome, Italy.

Cavero, J., Farre, I., Debaeke, P., and Faci, J. M. (2000). Simulation of maize yield under water stress with the EPICphase and CROPWAT models. *Agronomy Journal* **92**, 679-690.

Colorado Water Conservation Board (2010). Colorado's Water Supply Future. SWSI 2010 Mission Statement, Key Findings, and Recommendations. (D. o. n. resources, ed.). State of Colorado.

DeJonge, K. C., Andales, A. A., Ascough, J. C., II, and Hansen, N. C. (2011). MODELING OF FULL AND LIMITED IRRIGATION SCENARIOS FOR CORN IN A SEMIARID ENVIRONMENT. *Transactions of the Asabe* **54**, 481-492.

DeJonge, K. C., Ascough, J. C., II, Andales, A. A., Hansen, N. C., Garcia, L. A., and Arabi, M. (2012). Improving evapotranspiration simulations in the CERES-Maize model under limited irrigation. *Agricultural Water Management* **115**, 92-103.

Del Grosso, S. J., Halvorson, A. D., and Parton, W. J. (2008). Testing DAYCENT model simulations of corn yields and nitrous oxide emissions in irrigated tillage systems in Colorado. *Journal of Environmental Quality* **37**, 1383-1389.

Del Grosso, S. J., Parton, W. J., Keough, C. A., and Reyes-Fox, M. (2011). Special Features of the DayCent Modeling Package and Additional Procedures for Parameterization, Calibration, Validation, and Applications. *In* "Methods of Introducing System Models into Agricultural Research" (L. R. Ahuja and L. Ma, eds.), pp. 155-176. American Society of Agronomy, Crop Science Society of America, Soil Science Society of America.

Del Grosso, S. J., Parton, W. J., Mosier, A. R., Ojima, D. S., Kulmala, A. E., and Phongpan, S. (2000). General model for N2O and N-2 gas emissions from soils due to dentrification. *Global Biogeochemical Cycles* **14**, 1045-1060.

Doorenbos, J., and Kassam, A. (1979). Yield response to water. *Irrigation and drainage paper* **33**, 257.

Fereres, E., and Soriano, M. A. (2007). Deficit irrigation for reducing agricultural water use. *Journal of Experimental Botany* **58**, 147-159.

Hsiao, T. C. (1973). Plant responses to water stress. *Annual review of plant physiology* **24**, 519-570.

Lee, J., Pedroso, G., Linquist, B. A., Putnam, D., van Kessel, C., and Six, J. (2012). Simulating switchgrass biomass production across ecoregions using the DAYCENT model. *Global Change Biology Bioenergy* **4**, 521-533.

Ma, L., Nielsen, D. C., Ahuja, L. R., Malone, R. W., Saseendran, S. A., Rojas, K. W., Hanson, J. D., and Benjamin, J. G. (2003). Evaluation of RZWQM under varying irrigation levels in eastern Colorado. *Transactions of the Asae* **46**, 39-49.

Ma, L., Trout, T. J., Ahuja, L. R., Bausch, W. C., Saseendran, S. A., Malone, R. W., and Nielsen, D. C. (2012). Calibrating RZWQM2 model for maize responses to deficit irrigation. *Agricultural Water Management* **103**, 140-149.

Meyer, W. S., and Green, G. C. (1981). PLANT INDICATORS OF WHEAT AND SOYBEAN CROP WATER-STRESS. *Irrigation Science* **2**, 167-176.

Nielsen, D. C. (1997). Water use and yield of canola under dryland conditions in the central Great Plains. *Journal of Production Agriculture* **10**, 307-313.

Parton, W. J., Hartman, M., Ojima, D., and Schimel, D. (1998). DAYCENT and its land surface submodel: description and testing. *Global and Planetary Change* **19**, 35-48.

Parton, W. J., Schimel, D. S., Cole, C. V., and Ojima, D. S. (1987). ANALYSIS OF FACTORS CONTROLLING SOIL ORGANIC-MATTER LEVELS IN GREAT-PLAINS GRASSLANDS. *Soil Science Society of America Journal* **51**, 1173-1179.

Raes, D., Steduto, P., Hsiao, T. C., and Fereres, E. (2009). AquaCrop-The FAO Crop Model to Simulate Yield Response to Water: II. Main Algorithms and Software Description. *Agronomy Journal* **101**, 438-447.

Saseendran, S., Ahuja, L. R., Ma, L., Trout, T. J., McMaster, G. S., Nielsen, D. C., Ham, J. M., Andales, A. A., Halvorson, A. D., and Chávez, J. L. (2014). Developing and normalizing average corn crop

water production functions across years and locations using a system model. *Agricultural Water Management*.

Saseendran, S. A., Ahuja, L. R., Nielsen, D. C., Trout, T. J., and Ma, L. (2008). Use of crop simulation models to evaluate limited irrigation management options for corn in a semiarid environment. *Water Resources Research* **44**.

Shouse, P., Jury, W. A., Stolzy, L. H., and Dasberg, S. (1982). FIELD MEASUREMENT AND MODELING OF COWPEA WATER-USE AND YIELD UNDER STRESSED AND WELL-WATERED GROWTH-CONDITIONS. *Hilgardia* **50**, 1-25.

Stehfest, E., Heistermann, M., Priess, J. A., Ojima, D. S., and Alcamo, J. (2007). Simulation of global crop production with the ecosystem model DayCent. *Ecological Modelling* **209**, 203-219.

Tardieu, F., Granier, C., and Muller, B. (1999). Modelling leaf expansion in a fluctuating environment: are changes in specific leaf area a consequence of changes in expansion rate? *New Phytologist* **143**, 33-44.

Todorovic, M., Albrizio, R., Zivotic, L., Saab, M.-T. A., Stockle, C., and Steduto, P. (2009). Assessment of AquaCrop, CropSyst, and WOFOST Models in the Simulation of Sunflower Growth under Different Water Regimes. *Agronomy Journal* **101**, 509-521.

Trout, T. J., Bausch, W. C., and Buchleiter, G. (2010). Water production functions for Central Plains crops. *In* "5th National Decennial Irrigation Conference Proceedings", pp. 5-8, Phoenix, AZ.

Vorosmarty, C. J., Green, P., Salisbury, J., and Lammers, R. B. (2000). Global water resources: Vulnerability from climate change and population growth. *Science* **289**, 284-288.

Xie, Y., Kiniry, J. R., Nedbalek, V., and Rosenthal, W. D. (2001). Maize and sorghum simulations with CERES-maize, SORKAM, and ALMANAC under water-limiting conditions. *Agronomy Journal* **93**, 1148-1155.

CHAPTER 4. QUANTIFYING THE PARAMETER UNCERTAINTY IN MODEL PREDICTED CROP WATER PRODUCTION FUNCTIONS

4.1. SUMMARY

In semi-arid west U.S, the amount of water for agricultural irrigation is dramatically decreasing as a result of increasing demand from municipal users and other industrial and environmental users. Using dynamic models to characterize crop water production functions is helpful for decision making for reducing the water footprint of agricultural crop while maintaining production levels. However, there is uncertainty associated with the model predicted water production functions. In this study, we investigated the uncertainty in crop production functions due to parameter uncertainty using DayCent model. First a global sensitivity analysis was carried out for 24 parameters; we found growth/production related parameters in DayCent have relative more impact on grain yield, GLAI, and biomass than ET and soil water related parameters in both rainfed and irrigated conditions. A MCMC method DREAM was used to characterize the posterior distribution of 12 most sensitive parameters. In order to reach desired 95% inclusion rate, the unknown parameter σ_ε in the likelihood function was increased from the estimated optimal value. Using 440% of the optimal σ_ε, the inclusion rate of the training and testing datasets reached 95% and 96%, respectively. To quantify predictive uncertainty of crop water production functions, scenarios of six levels of irrigation for 12-year period was created. The model generated yield response to irrigation levels was found similar to previous field and modeling studies. The standard deviation of predicted yield for each scenario was found to increase as irrigation increased. However, CV was found very stable (averaged at 0.097) regardless of climatic differences in each year, which implies that the uncertainty of a water production function can be roughly estimated using a CV value if no resources available for a complete uncertainty analysis.

4.2. INTRODUCTION

In arid and semiarid regions, such as the western United States, water poses the greatest limitation in agricultural production as rainfall in these regions does not meet the evaporative demand (Doorenbos and Kassam, 1979; Feddes et al., 1978). Large amounts of water from surface and underground sources are applied for irrigation every year to maintain high crop yield. The total irrigation withdraws were estimated as 0.435 km^3/day in U.S. in 2010, which accounted for 38 percent of total freshwater withdrawals (Maupin et al., 2014). The increasing demand for water from municipal users due to rapid population growth and urbanization as well as demands from other industrial and environmental users pose a great threat to availability of water for agriculture (Colorado Water Conservation Board, 2010; Vorosmarty et al., 2000). Extended drought periods in a changing climate and declining groundwater levels are expected to only exacerbate the situation (Colorado Water Conservation Board, 2010; McGuire, 2014). Understanding the response of cropping systems to changes in irrigation levels is essential for reducing the water footprint of agricultural crops while maintaining production levels (Fereres and Soriano, 2007; Saseendran et al., 2014; Trout et al., 2010).

Characterization of crop water production functions, i.e. the relationship between crop yield and irrigation water amount, is necessary in order to simultaneously optimize economic return of crop production and achieve desired water allocation levels (English, 1990; Reca et al., 2001). Dynamic crop models are valuable tools for the estimation of water production functions specific to a crop at a specific location (Brumbelow and Georgakakos, 2007; Garcia-Vila and Fereres, 2012; Saseendran et al., 2014). However, simulation models are approximate representations of the real world systems and bear uncertainties in simulating the behavior of the system under study. Quantification of modeling uncertainties is needed particularly when their outputs are used in decision making (Vose, 1996). The predictions of dynamic crop models are influenced by meteorological, soil, and land use inputs, uncertain model parameters, the limitation of the mathematical representation of real world processes, and uncertainty in observed data that are used for calibration purposes. Consequently, the uncertainty in crop model predictions should be better investigated (Confalonieri et al., 2016). However, to the authors'

knowledge, no previous studies have investigated how modeling uncertainties propagate forward into estimated crop production functions.

Sources of modeling uncertainties include input, parameter, and structural uncertainties (Haefner, 2005). Input uncertainty is from errors in input forcing (e.g. precipitation or soil texture of a field). When input data are obtained from predictions of another model, like the projected future climate or model generated weather, input uncertainty can be from the predictive uncertainty of the model producing the forcing inputs. Model structures are invariably incomplete due to approximation of real world processes, lack of knowledge about some processes, and neglecting to include some processes that are deemed insignificant for pragmatic considerations. Finally, model parameters, time-invariant coefficients that are treated as constants and are estimated by means of calibration to observed data, could beat considerable uncertainty.

For a single model structure, the uncertainty due to model parameters can be estimated using Bayesian methods by conditioning the model behavior on measurements. Literature is replete with methods for uncertainty analysis based on Bayesian formalism, particularly in hydrological studies (e.g. Beven and Binley, 1992). Some Bayesian methods have been applied for uncertainty analysis of crop models. The Generalized Likelihood Uncertainty Estimation (GLUE) method (Beven and Binley, 1992) has been used for the estimation of posterior parameter distributions in studies of wheat using STICS-wheat model (Varella et al., 2010), sweet corn using CERES-Maize model (He et al., 2009), and cotton using CSM-CROPGRO-Cotton model (Pathak et al., 2012). Despite computational simplicity and popularity of the GLUE method, concerns about using informal Bayesian likelihood functions in GLUE have been the subject of extensive scientific discourse (Stedinger et al., 2008; Vrugt et al., 2009b).

Alternatively, formal Bayesian methods using the Markov-Chain Monte-Carlo (MCMS) techniques have been developed. In crop modeling, MCMC methods have been applied to quantify the uncertainty in predicted phenological development of maize in Slovenia using WOFOST model (Ceglar et al., 2011). More recently, the Differential Evolution Adaptive Metropolis (DREAM) method was applied to characterize uncertainties in simulations of winter wheat using STICS model (Dumont et al.,

2014). Another recent study applied MCMC method with SALUS model to simulate maize, peanut, and cotton (Dzotsi et al., 2015). The predictive uncertainty of output variables was also examined with validation data sets in both later studies and were found useful as a method for quantifying uncertainty.

Parameter sensitivity analysis (SA) is usually performed prior to uncertainty analysis to evaluate the importance of model parameters (Ceglar et al., 2011; He et al., 2009; Laloy et al., 2010; Pathak et al., 2012). While several local and global methods are available, global SA methods are more informative since they account for interactions between parameters (Saltelli et al., 2000). Furthermore, global SA can provide information for examination of the structure of the model residuals, which is essential the implementation of formal Bayesian techniques for uncertainty analysis (Ahmadi et al., 2014).

The DayCent model (Parton et al., 1998) is one of the most commonly-use agroecosystem models for crop yield, soil carbon, nitrous oxide emission, and other ecosystem responses (Chang et al., 2013; Del Grosso et al., 2008; Del Grosso et al., 2006; Jarecki et al., 2008; Stehfest et al., 2007; Zhang et al., 2013). A few previous studies have been carried out to assess the predictive uncertainty of DayCent due to parameter uncertainty (De Gryze et al., 2010; Del Grosso et al., 2010; Fitton et al., 2014; Lee et al., 2011). Two studies, in particular, analyzed the parameter uncertainty on trace gas emissions using Bayesian methods (van Oijen et al., 2011; Wang and Chen, 2012).

Despite the importance of understanding the crop response to irrigation under various climatic conditions, no previous study has investigated the uncertainty in crop production functions due to parameter uncertainty. The overall goal of this study is to enhance understanding of the uncertainty in crop yield and production functions using the DayCent agroecosystem and ecological model. The objectives are to: (i) understand the importance of parameters and processes they represent in DayCent model through Global sensitivity analysis; (ii) characterize the uncertainty of important parameters; and (iii) propagate parameter uncertainty forward into estimation of crop production functions.

Quantifying uncertainty of model predictions is particularly important when their outputs are used in decision making. This study will illustrate how predictive uncertainty changes at different irrigation

levels in crop production functions due to parameter uncertainty, which has not been previously investigated by others.

4.3. METHODS

The DayCent agroecosystem model (Parton et al 1998) was used to simulate agroecosystem processes. Maize measurement data from a field experiment conducted in Mead, NE were used in this study, which include three treatments of irrigated continuous maize, irrigated maize soybean rotation, and rainfed maize soybean rotation. First, the Sobol's global sensitivity analysis was applied to identify the importance of the DayCent model parameters for model responses of annual grain yield, monthly GLAI, and monthly aboveground biomass; and the model outputs from sensitivity analysis were used to investigate the structure of model errors using measurement data (six year*treatment). Posterior distribution of the model parameters for one maize hybrid was identified using the DREAM technique. The predictive uncertainty of training dataset (three from six year*treatment) was quantified and analyzed for its spread and inclusion rate using the posterior distribution of the parameters. The predictive uncertainty of testing (the rest three year*treatment) datasets was estimated. To assess uncertainty in predicted crop production functions, we created 6 scenarios of different levels of irrigation using 13-year weather data. The distribution of the predicted grain yield was analyzed and standard deviation and coefficient of variation was quantified.

4.3.1. Field experiment

The field data used in this study was obtained from a field experiment conducted at the University of Nebraska Agricultural Research and Development Center near Mead, NE. Detailed experimental design can be found in Suyker and Verma (2009). Although it is not a limited irrigation experiment, the irrigated treatment and rainfed treatment provide enough information for the study of water stress. The experiment was initialized in 2001. Two of the treatments were irrigated and one was rainfed. Each treatment is a large production field (49 – 65 ha). One of the irrigated treatment was planted in maize (*Zea mays* L.) continuously (ICM). The other irrigated treatment was in maize/soybean (*Glycine max* L.) rotation (IMS). The rainfed treatment was also in maize/soybean rotation (RMS). These treatments have

been managed using standard best management practices in this region. These managements include fertilizer, herbicide, and pesticide applications. During the experimental period, different hybrids of maize were grown with different planting date depending on the relative maturity and weather/soil conditions (Chapter 2.). Hybrid Pioneer 33B51 was planted in 2001, 2003, 2004 and 2005 (Table 4.2); measurement data of this hybrid were selected to use in this study.

Within each treatment, six 20 m by 20 m measurement areas (intensive measurement zones) were established for detailed measurement of leaf area, aboveground biomass and other important ecosystem variables (Verma et al., 2005). Grain yields were recorded from the measurement of combine harvest of each entire treatment field. In this study, LAI, aboveground biomass and grain yield measurements were used. Leaf area and aboveground biomass were sampled destructively on an average of 11-day basis at each intensive measurement zone of each treatment.

The soil of the three treatments is deep silty clay loam with very gentle slope. Soil characteristics were measured for four depths and details can be found in Chapter1. Weather data of temperature, solar radiation, relative humidity, and wind speed for model simulation are from a local weather station (station name MEADAGROFARM; High Plains Regional Climate Center, Lincoln, Nebraska). Precipitation and irrigation amounts were from the direct measurement within each treatment field using rain gauges.

4.3.2 Agroecosystem Model

The DayCent ecosystem (cropland, forest, grassland and savanna) model (Parton et al., 1998) was used in this study. The model is the daily time step version of the widely used monthly time step model Century (Parton et al., 1987). The major sub-models of DayCent include plant growth, soil water, soil organic matter decomposition, trace gas emission. Major inputs for the model are daily weather, soil property, plant type, and management practices. The model has been in continuous development and improvement. Recently, Zhang et al. (Chapter1) has incorporated a new method to simulate the canopy dynamics of annual crop along with other modifications. The field experiment used in this study has been previously simulated with the improved model using manually calibrated parameters (Chapter1). The results show improved green leaf area index (GLAI) simulation and better fit in late season

evapotranspiration rate in comparison with the original model. And this version of model has also been successfully applied to simulate limited irrigation experiments in eastern Colorado (Chapter 3) with accurate prediction for the GLAI, biomass and grain yield.

A brief discussion of the theory, concepts and methods used in the improved model are presented in this study. In DayCent, crop daily potential production is simulated as the product of radiation use efficiency and intercepted photo synthetically active radiation (*PAR*).

$$PP_i = CC_i \times PAR_i \times RUETB \quad (4.1)$$

where PP_i is the potential production on the ith day, CC_i is the fraction of radiation intercepted by canopy on the ith day and *RUETB* is the radiation use efficiency of total biomass production (aboveground and belowground). The CC_i is calculated using Beer's Law (MONSI and SAEKI, 1953; Sellers, 1985).

$$CC_i = 1 - exp(-KLIGHT \times GLAI_i) \quad (4.2)$$

where *KLIGHT* is the extinction coefficient of vegetation. The actual production is affected by temperature, water, and nutrient. Daily actual production is allocated to above and below-ground based on the development stage and stress (water and nitrogen). Phenology of growth is estimated by growing degree day (GDD) method. Temperature effect (T_e) on PP_i (close to bell-shape) is as following

$$T_e = \left(\frac{PPDF2 - T_{mean}}{PPDF2 - PPDF1}\right)^{PPDF3} \times \exp\{\frac{PPDF3}{PPDF4} \times [1 - \left(\frac{PPDF2 - T_{mean}}{PPDF2 - PPDF1}\right)^{PPDF4}]\} \quad (4.3)$$

where *PPDF1, PPDF2, PPDF3, PPDF4* are parameters to control the shape of the curve; T_{mean} is the daily mean temperature.

The soil water sub-model simulates 1-dimension water balance including precipitation, irrigation, ET, runoff, and percolation (Parton et al., 1998). Potential ET is simulated by calculated reference ET and crop coefficient (Allen et al., 1998). Potential ET is partitioned to potential evaporation of soil and transpiration of plant based on GLAI.

Both growth/production sub-model and soil water sub-model require prediction of GLAI. The newly added improved GLAI method is described in Chapter 2. Briefly, GLAI is converted from green

leaf biomass using constant specific leaf area (*SLA*). Green leaf biomass is simulated using green leaf weight ratio (*GLWR*; as a function of GDD) and aboveground biomass.

$$GLAI_i = AgBiomass_i \times GLWR_i \times SLA \quad (4.4)$$

4.3.3. Global sensitivity analysis

Global sensitivity analysis (GSA) apportions the uncertainty in model outputs to the uncertainty in individual inputs and interactions thereof (Saltelli et al., 2000). The 'Sobol' method (Sobol, 1993) is arguably the most comprehensive GSA methods due to its sampling design for the exploration of the parameter space. The decomposition of variance of the model outputs $\mathrm{Var}(\widehat{\mathrm{Y}})$ for *k* parameters (θ) is written:

$$var(\hat{Y}) = \sum_{i=1}^{k} D_i + \sum_{i<j} D_{ij} + \cdots + D_{1\ldots k} \quad (4.5)$$

where D_i is the main effect of input parameter θ_i. The terms of $D_{ij}, \ldots, \mathrm{D}_{1\ldots\mathrm{k}}$ correspond to the interactions between parameters.

The sensitivity indices are given by

$$S_{i_1,\ldots,i_s} = D_{i_1,\ldots,i_s}/var(\hat{Y}) \quad (4.6)$$

So the first order sensitivity indices (main effects) for each parameter are

$$S_i = D_i/var(\hat{Y}) \quad (4.7)$$

And total order indices are

$$TS_i = S_i + \sum_{j\neq i} S_{ij} + \cdots + S_{1\ldots k} \quad (4.8)$$

Twenty-four crop growth and water stress related parameters in the improved version of DayCent model were used in sensitivity analysis (Table 4.1). These parameters can be summarized into two groups: i) crop growth/production related parameters, which are species or cultivar specific; and ii) parameters representing ET and soil water processes. Non-informative uniform distribution was assumed for the prior parameter distributions. The ranges of model parameters were selected based on field measurements or previous studies.

Global sensitivity analysis using the method of Sobol requires independency of parameters. However, parameters *MNDDHRV* (minimum number of degree days from anthesis to harvest) and

MXDDHRV (maximum number of degree days from anthesis to harvest) are not independent. A new parameter *GAPMNDD*, the difference between *MNDDHRV* and *MXDDHRV*, was defined as a random variable. *MNDDHRV* was then calculated based on the *MXDDHRV* and *GAPMNDD*. Additionally, a wider range of 0.9 – 1.3 for the crop coefficient for evapotranspiration (*KCET*) parameter was used because field measurements indicated smaller values (1.03 ± 0.07, (Suyker and Verma, 2009) values than the those reported by FAO (Allen et al., 1998). Soil parameters including saturation point, field capacity, wilting point, and saturated conductivity were estimated by soil texture using the Saxton equation (Saxton et al., 1986). The sand content, clay content, and bulk density were varied within the ranges of a silty clay loam (U.S. soil texture triangle) by assuming only one soil texture in the experimental fields.

In this study, a sample size of 25,600 were generated using the SimLab software (Joint Research Center of the European Commission, 2004). This sample size meets the requirement of $n \times (k + 2)$ (with *n* in range of 500 to 1000 typically) to ensure numerical stability (Saltelli et al., 2005; Saltelli et al., 1999). These samples of parameter sets were used to run simulation of hybrid Pioneer 33B51 (total six year*treatment; Table 4.2). The model responses examined in the sensitivity analysis are annual grain yield, monthly aboveground biomass and monthly GLAI. Monthly averages of aboveground biomass and GLAI in May, July and September were examined for the differences of sensitivity in early, middle, and late growing seasons.

Important model parameters were then included in parameter and predictive uncertainty analysis. The criterion for classifying parameters as "important" was sensitivity indices greater than 0.05 for monthly aboveground biomass, monthly GLAI, or annual grain yield.

4.3.4. Bayesian parameter uncertainty analysis using DREAM

Using Bayesian formalism, the posterior distribution $P(\theta_i|D)$ of a set of parameters θ of model responses ($\hat{Y}$) conditioned on observed data *Y* is:

$$P(\theta|Y) = \frac{P(Y|\theta)\,P(\theta)}{\int P(\hat{Y}|\theta)\;P(\theta)\,d\theta} \tag{4.9}$$

where $P(Y|\theta)$ represents the likelihood of the data, $P(\theta)$ is the prior distribution of parameters. The likelihood $P(Y|\theta)$ is determined from the probability distribution of the residuals between observed (Y) and modeled ($\hat{Y}$) responses. Residuals are often assumed to be uncorrelated, independent identically normally distributed (Box and Tiao, 1992), hence yielding the likelihood function:

$$L(\theta|Y) = \prod_{i=1}^{n}(2\pi\,\sigma_{\varepsilon}^{2})^{-1/2} \times \exp\left(-\frac{1}{2\,\sigma_{\varepsilon}^{2}}\left[\hat{Y}_i(\theta) - Y_i\right]^2\right) \quad (4.10)$$

where σ_{ε} is the standard deviation of model errors and *n* is the number of observed responses. Assuming homoscedastic model residuals, the log likelihood function is:

$$\mathcal{L}(\theta|Y) = -\frac{n}{2}\ln(2\pi) - 2n\,\ln(\sigma_{\varepsilon}) - \frac{1}{2\sigma_{\varepsilon}^{2}}\sum_{i=1}^{n}\left[Y_i - \hat{Y}_i(\theta)\right]^2 \quad (4.11)$$

When model residuals are not homoscedastic, observed and model responses are typically transformed using appropriate transformations, e.g. Box-Cox transformation (Box and Cox, 1964), prior to computation of the likelihood function. Similarly, autoregressive time series models, e.g. AR(1), may be applied to remove model error autocorrelation (Sorooshian and Darcup, 1980; Ahmadi et al., 2014; Vrugt, 2016).

MCMC simulations are commonly used for estimation of posterior parameter distributions as a formal Bayesian method. The DREAM algorithm (Vrugt, 2016; Vrugt et al., 2008; Vrugt et al., 2009a) was selected for this study. The advantage of this approach is the efficiency in mitigating issues with high-dimensionality, multimodality, nonlinearity, and local optima with proved ergodicity comparing to some traditional MCMC algorithms. Vurgt (2016) presents a complete review of the theory, concepts, and MATLAB implementation for the DREAM approach.

4.3.5. Identification of the structure of model residuals

DayCent model residuals were investigated for homoscedasticity, normality, and uncorrelated residuals. From the 25,600 GSA run, outputs were extracted and residuals were calculated for each run using measurement data of annual grain yield, multiple in-season GLAI and in-season aboveground biomass of hybrid Pioneer 33B51. Residuals for the "best" model, selected based on the minimum root mean squared error (RMSE), were explored. Model residuals of the three responses were examined for

heteroscedasticity using the chi-square test for normality. Since the GLAI and biomass are only continuously measured within each year, graphical assessment of partial autocorrelation in each year was also assessed.

4.3.6. Implementation of the DayCent linkage with DREAM

The R package for DREAM (Guillaume and Andrews, 2012) was integrated with the DayCent model to conduct the parameter uncertainty analysis. A script was written in R to compute the likelihood function required as input by the DREAM package. Twelve MCMC chains were used in this study. The Gelman and Rubin (1992) statistic ($\hat{R}$) of 1.2 was used for convergence. The first 50% of simulations were treated as the burin-in runs.

The measurement data used in residual analysis were divided into two datasets for training and testing. Data from the ICM treatment in 2004, IMS treatments in 2005, and RMS treatment in 2001 were used for training since these data covered variations in planting dates, water stress (irrigated vs non-irrigated), and growing season temperature. This data set contained 28 measurements of GLAI, 26 measurements of aboveground biomass, and 3 measurements of annual grain yield. For testing purpose, measurements from the three treatments in 2003 were used. The measurement data included 24 measurements of monthly GLAI, 24 measurements of monthly aboveground biomass, and 3 measurements of annual grain yield.

Field measurements are associated with uncertainty largely because of the natural variation of the soil, precipitation, and management inputs. Since these variations were not included in our simulation, the measurement uncertainty of uniform fields was estimated using data from a well-managed field experiment conducted on maize in Colorado (Trout et al., 2010) which characterized as uniform in soil property, irrigation (dripping system) and other managements. The coefficient of variation (CV) of the well irrigated treatments (less affected by the non-uniformity of soil and precipitation) ranged from 1.44% to 12.1%. A repressive value of 3% was used in this study.

Predictive uncertainty for GLAI, aboveground biomass, and annual grain yield were computed using the last 10% of parameter sets from DREAM algorithm. The performance of the predictive

uncertainty analysis technique was then corroborated using the "inclusion rate" and "spread". The inclusion rate was computed as the percentage of data points within the 95% prediction interval (P.I.). To account for measurement uncertainty, an observed data point was considered as included in the 95% P.I. if the 95% measurement uncertainty band had an overlap with the model 95% P.I. The spread was defined as the average width of the corresponding uncertainty band.

The sensitivity of the inclusion rate and spread of the model 95% P.I. to σ_ε was examined by altering σ_ε at 20% intervals. The purpose of this experiment was to identify the value of σ_ε that results in minimum spread with inclusion rate above 95%. The posterior distributions of parameters from the selected σ were used for testing and predictive uncertainty of water production functions.

4.3.7 Uncertainty in the prediction of crop production function

A 13-year analysis period from January 2001 to December 2012 was used to generate crop production functions. The analysis period was selected such that dry and wet climatic conditions were encompassed. The planting date was fixed at Day of Year (DOY) 130. Simulation were conducted with no nutrient stress to be able to discern the effects of water stress at varying irrigation levels under dry to wet climatic conditions. Soil data from the rainfed treatment was used.

The optimal DayCent parameter set from DREAM computational experiments was used to estimate irrigation amount requirements to meet crop consumptive use in each year within the analysis period. Subsequently, the uncertainty of model responses was evaluated for limited irrigation treatments at 0 (i.e. rainfed), 20, 40, 60, and 80 percent of full irrigation requirements.

4.4. RESULT AND DISCUSSION

4.4.1. Important DayCent parameters and critical crop growth processes

Figure 4.1 presents a summary of the main effects and total effects of DayCent model parameters on the estimated average annual grain yield for the ICM, IMS, and RMS treatments. The most important parameters were crop growth/production related parameters. The total sensitivity indices for ET and soil water related parameters were very small even under rainfed treatment (RMS).

Parameters *PPDF1*, *RUETB*, and *KLIGHT* were the most important parameters for all treatments. Results suggest that more attention should be paid to the optimum temperature for production (PPDF1) when using DayCent, which is typically not adjusted. Radiation use efficiency (RUETB) is the primary parameter that controls the crop production response in DayCent and was found to have very high sensitivity indices. These results corroborated similar finding for other crop models with similar scientific theory and conceptualization for crop growth simulation, including CERES-Maize (DeJonge et al., 2012) and EPIC (Wang et al., 2005). Extinction coefficient parameter (*KLIGHT*) is another parameter widely used by crop models which determines how much light can be intercepted by the canopy for photosynthesis; thus it is expected to be very influential on yield (Pathak et al., 2007).

Results indicated that the soil texture parameters (*BD*, $P_{sand,}$ and P_{clay}) for a given texture class had relatively small influence on simulated average annual crop yields, which justifies the use of texture class information in regional studies, or field level studies where detailed soil information are not available. Similarly, the soil property parameters of CERES-Maize model were found with relatively low sensitivity on grain yield of corn in both full and limited irrigation treatments. The *KCET* parameter in the rainfed treatment was more important than the two irrigated treatments. This result is plausible since higher potential ET rate (higher *KCET* value) indicates higher actual ET and subsequently higher drought stress when irrigation is not available to mitigate water stress.

Sensitivity of seasonal or monthly crop response variables has not been investigated in previous studies. Understanding the importance of model parameters and processes they represent on inter-annual responses enhances the knowledge about interactions and feedback among various processes that must be adequately represented within the model structure (Passioura, 1996). The enhanced understanding is also vital for proper parameterization of models in response to the temporal variability of climatic conditions. Figure 4.2 shows the total sensitivity indices for months May, July and September in the rainfed treatment corresponding to early, middle and late growing season. Results are depicted for only important parameters with indices greater than 0.05 for monthly *GLAI* and aboveground biomass. The ranking of indices of the two irrigated treatments is similar except the parameter *GAPMNDD*, which tends to be

more important in rainfed treatment since it represents the change of GDD requirement from anthesis to maturity under drought stress. The three most important parameters for grain yield (PPDF1, RUETB, and KLIGHT) were also important in most of months for GLAI and aboveground biomass. In some months, a single parameter was shown to be most influential. For example, in May, the sensitivity indices for *DDEMERG* for both GLAI and aboveground biomass were higher than 0.4, conforming to the intuition that early crop growth is largely affected by the time of emergence after planting while late emergence produces less biomass.

4.4.2. Analysis of residuals from Sobol GSA

Model residuals for the GSA simulation with lowest RMSE were analyzed to identify a proper likelihood function for uncertainty analysis (Figure 4.3). Heteroscedasticity was not detected in model residuals using Brown-Forsythe test (p values for GLAI and biomass were 0.246 and 0.462, respectively; grain yield was not test because of only six observations). Residuals for all three responses (monthly GLAI, monthly aboveground biomass, and annual grain yield) were normally distributed based on the chi-square test for normality at 0.05 significance level (*p* values for GLAI, biomass, and grain yield were 0.918, 0.088, and 0.059, respectively). The partial autocorrelation plots of each year and treatment showed no significant correlation at any lag. The estimated optimal σ_ε values corresponding to the GSA simulations with minimum RMSE were 0.51 m^2 m^{-2}, 119.30 kg ha^{-1}, and 38.67 kg ha^{-1} for GLAI, aboveground biomass, and grain yield respectively.

4.4.3. The influence of residual standard deviation on the performance of DREAM

DREAM failed to converge within 50,000 model evaluations for the optimal σ_ε values obtained from the GSA. Hence, the σ_ε for the three response variables were altered at 20% incremental increase for all three responses until the convergence criteria were met. For computation simplicity, we did not investigate altering σ_ε the three responses differently. Convergence was achieved when σ_ε was increased to 160% of the optimal values. Figure 4.4 provides a summary of the results from uncertainty analysis using different values for σ_ε. With increasing σ_ε, DREAM generally tended to require lower number of model evaluations before convergence, while the spread of the 95% P.I. for all three response variables

increased substantially. Desired inclusion rate (above 95%) was obtained when 440% σ_ε was used. As we know, σ_ε which is the standard deviation of errors is unknown in most cases and need to be estimated. The errors which σ_ε represented including measurement, model input, and model structural errors, some of which are usually very difficult to quantify. Figure 4.5 shows the change of σ_ε on log likelihood values (calculated using Equation 4.11) for two arbitrarily picked residual levels. The difference between the log likelihood values dramatically reduces when σ_ε increases. Since the MCMC algorithm was based on maximizing log likelihood, there was more probability for model runs resulting large residuals. Moreover, log likelihood from different model responses (GLAI, biomass and grain yield) were combined in Equation 4.11. At small σ_ε, a very low log likelihood value from one response could dominate the overall combined likelihood (Figure 4.5); this effect would be much smaller when σ_ε is large. Large σ_ε results in more parameter samples potentially get accepted in the MCMC algorithm, which leads to less evaluations for convergence and larger spread of predictions.

4.4.4. Posterior distribution of parameters

Figure 4.6 depicts the posterior cumulative distribution function (CDF), i.e. nonexceedance probabilities, for the 12 important DayCent parameters from DREAM at three levels of σ_ε (160%, 300%, and 440%). The straight line depicts the prior CDF from the uniform distribution. The summary of the basic statistics and the optimal value for each parameter was shown in Table 4.3. Interestingly, the standard deviation of the posterior distribution of most DayCent parameters increased monotonically with increasing σ_ε values for yield, aboveground biomass, and GLAI responses. As discussed previously, when σ_ε is larger, more parameter samples would be potentially accepted in the MCMC algorithm, which leads to a parameter posterior distribution with larger standard deviation.

Figure 4.7 illustrates the correlation structure between posterior parameters from DREAM analysis. A high positive correlation of 0.58 was evident between parameters *PPDF1* and *PPDF2*, which is realistic because the two parameters jointly influence temperature effects on production (Equation 4.3). A high negative correlation was computed between parameters *BMINI* and *KLIGHT* with a correlation

coefficient of -0.57. The parameter *BMINI* determines the *GLAI* at early stages of growth, while *GLAI* and *KLIGHT* jointly influence canopy cover (Equation 4.2). Hence, the high negative correlation between *BMINI* and *KLIGHT* is to be expected. Another strong negative correlation was evident between *RUETB* and *KLIGHT*. This observation can be explained because to produce same amount of biomass when more light is intercepted (i.e. larger *KLIGHT*) the radiation use efficiency would have to decrease (i.e. smaller *RUETB*). High negative correlation was also computed between *DDBASE* and *LEAFMX*. When the time of maximum *GLAI* is delayed, the *LEAFMX* (*GLWR* at maximum *GLAI*) decreases because the linear function with negative slope used in the revised DayCent model (Chapter 2). The correlations between other parameters are relatively small and negligible.

4.4.5. Predictive uncertainty for the training data

Figure 4.8 shows the 95% P.I. for the response variables GLAI, aboveground biomass, and annual grain yield, with σ_ε values (440% of optimal values) 2.24 m^2 m^{-2}, 230.96 kg ha^{-1}, and 74.9 kg ha^{-1}, respectively. For the two irrigated treatments (field experiments ICM and IMS), the inclusion rate was 100% for aboveground biomass, GLAI and grain yield. In the rainfed treatment (field experiment RMS), two measurements in the late growing season were not covered, indicating that water stress was over-predicted by the model. One of the reasons might be the precipitation inputs were not representative of the whole field as rainfall varies spatially. In this study, no input uncertainty was included because it would largely increase the complexity of the assessment. Also, DayCent includes a one-dimension water sub-model with only daily precipitation input to simulate runoff and run-on within the filed, which may be inadequate in capturing all important processes, responses and interactions.

The width of the P.I. was wider comparing to that of the training dataset presented by Dumont et al. (2014) for winter wheat using the STICS crop model and DREAM algorithm, although Dumont et al. (2014) did not report the corresponding inclusion rate. The width of the 95% P.I. for grain yield in the rainfed treatment was slightly narrower than those of the two irrigated treatments (Figure 4.8). The reason might be that the predictions were more limited by water stress than the uncertainty in parameters.

4.4.6. Predictive uncertainty for the testing data

For each irrigation scenario in 12 years, distribution of predictions of yields were plotted using boxplot (Figure 4.10). In dry years (2001, 2002, 2003, 2005, and 2012; annual precipitation less than 60 cm), the response of yield to irrigation was very clear (except 2005 which has large storage of water from previous year). The medium values of predicted yield of non-irrigated scenario were less than half of those of full irrigation scenario in extremely dry year of 2012. In wet years, there was little difference in predicted medium of yield between irrigation levels because precipitation could meet most water demand for crop growth. In these years, standard deviations of different irrigation levels within the same year was similar, while they were significantly different in dry years. There was a trend of increase in standard deviations as irrigation level increased in dry years. This may be due to the limiting effect of drought stress on production over-whelmed the effect of parameter uncertainty. In most years and irrigation levels, the predicted yields using the optimal parameter set were close to the medium but they are frequently outside the range of first and third quantiles. In all 100% irrigation level scenarios, the predictions using optimal parameter set were less the medium of predictions. It may be because irrigation used in the calibration dataset was slightly less than the actual demand; predictions of yield from some parameter sets were constrained by water stress. In our irrigation scenarios, as the constrain removed, over-predictions using these parameter sets were expected.

Coefficient of variation (CV) which is a standardized measure of dispersion of a distribution, was shown in Figure 4.11 for each scenario of 12 years. Relative stable CV (slope of fitted line was -0.0002) were found regardless of dry and wet years and irrigation levels with a mean value of 0.097. The two obvious outliers in irrigation levels of 0 and 20% were from 2001, which likely be that it was the first year of simulation which started with the same soil water content in all irrigation levels and resulted in large amount of available water in the begging of growing season in low irrigation level scenarios. As CV was found relative stable, it indicated that in situation when uncertainty analysis was not performed due to reasons like lacking of computation power or regional analysis with large amount of simulations, a rough estimation of uncertainty interval can be made using predictions from optimal parameter set and the mean of CV.

4.5. CONCLUSION

In this study, parameter sensitivity, parameter uncertainty, and predictive uncertainty were analyzed using DayCent model for one hybrid of corn. Among the 24 parameters tested, growth/production related parameters in DayCent had relative more impact on grain yield, GLAI, and biomass than ET and soil water related parameters at both rainfed and irrigated conditions. Additionally, sensitivity indices can be dramatically different for each month of simulated GLAI and biomass. Using the MCMC method DREAM, posterior distributions of 12 most sensitive parameters were obtained and used for estimation of predictive uncertainty. In the predictive uncertainty analysis, both inclusion rate and spread increased when the unknown parameter σ_ε (in likelihood function) increased. Using 440% of the optimal σ_ε, the inclusion rate of the training and testing datasets reached 95% and 96%, respectively. Scenarios of six levels of irrigation for 12-year period was created to quantify the predictive uncertainty of grain yield. The DayCent model generated yield response to irrigation levels was similar to previous field and modeling studies. Regardless of climatic differences in each year, relative stable CV averaging 0.097 was found, which implies that the uncertainty of a water production function can be roughly estimated using a CV value if no resources available for a complete uncertainty analysis.

Table 4.1. The input parameters for the sensitivity analysis.

Name	Definition	Unit	Lower bound	Upper bound	Reference #	Reference
Growth and production						
RUETB	Radiation use efficiency for total biomass production	g m^{-2} $langley^{-1}$ PAR	0.12	0.2	1	Chapter 1 and 2
PPDF1	Optimal temperature for production	(^{0}C)	25	32	2	Necpálová et al. (2015) and Chapter 2
PPDF2	Maximum temperature for production	(^{0}C)	35	50	3	Necpálová et al. (2015) and Chapter 2
DDEMERG	GDDs from planting to emergence	Degree-day	50	120	4	Field measurement
DDBASE	GDDs from planting to anthesis	Degree-day	600	900	5	Field measurement
MXDDHRV	The maximum number of degree days from anthesis to harvest	Degree-day	650	850	6	Field measurement
GAPMNDD[1]	The difference between MNDDHRV* and MXDDHRV	Degree-day	0	600	7	Field measurement
BMINI	Initial biomass at emergence	g m^{-2}	0.1	2	8	Field measurement
SLA	Specific leaf area	m^2 g^{-1}	0.015	0.025	9	Field measurement
LEAFEMERG	Intercept of the second stage linear equation at emergence	g g^{-1}	0.8	0.95	10	Field measurement
LEAFMX	Green leaf weight ratio at maximum GLAI	g g^{-1}	0.2	0.35	11	Field measurement
LEAFPM	Green leaf weight ratio at physiological maturity	g g^{-1}	0	0.1	12	Field measurement
FRTC1	Fraction of C allocated to roots at planting, with no water or nutrient stress,	g g^{-1}	0.3	0.5	13	Developers' suggestion
FRTC2	Fraction of C allocated to roots when reaches maximum root depth	g g^{-1}	0.05	0.2	14	Developers' suggestion
FRTC3	Time after planting at which the FRTC2 value is reached	days	70	110	15	Developers' suggestion
FRTC4	The maximum increase in the fraction of C going to the roots due to water stress	g g^{-1}	0.01	0.3	16	Developers' suggestion
HIMAX	The maximum harvest index	g g^{-1}	0.5	0.6	17	Field measurement
HIWSF	Water stress factor on harvest index	-	0.3	0.7	18	Developers' suggestion
KLIGHT	Extinction coefficient of Beer's Law	-	0.4	0.8	19	Developers' suggestion
ET and soil water						
KCET	Crop coefficient for evapotranspiration	-	0.9	1.3	20	Allen et al. (1998) and Suyker and Verma (2009)
dmpflux	The damping factor for soil water flux is a multiplier used to reduce (or dampen) the upward and downward	-	1E-7	1E-5	21	Developers' suggestion

	soil water fluxes between two soil layers in a Darcy's Law calculation.					
BD	Bulk density	g m^{-3}	1.3	1.5	22	USDA NRCS[2]
P_{sand}	Sand content	-	0.05	0.2	23	USDA NRCS
P_{clay}	Clay content	-	0.27	0.4	24	USDA NRCS

1. GAPMNDD is not a real parameter in the model. MNDDHRV is the minimum number of degree days from anthesis to harvest.
2. USDA Natural Resources Conservation Service soil texture triangle.

Table 4.2. Crop management for the three treatments of Pioneer 33B51 at Mead, NE.

Treatment/ Year	Plant population (plants ha^{-1})	Planting time (DOY)	Harvest time (DOY)	Irrigation and rainfall from planting to harvest (cm)
Irrigated continuous maize (ICM)				
2003	77,000	135	300	62.9
2004	79,800	125	288	61.3
Irrigated maize-soybean rotation (IMS)				
2003	78,000	134	296	63.3
2005	81,000	122	290	63.6
Rainfed maize-soybean rotation (RMS)				
2001	62,000	134	302	35.5
2003	57,600	133	286	29.2

Table. 4.3 Summary of the statistics of parameter uncertainty analysis

Parameter	Optimal	Mean	SD
RUETB	0.199	0.176	0.015
PPDF1	27.370	27.261	1.694
PPDF2	43.448	44.279	3.828
DDEMERG	118.412	87.987	19.230
DDBASE	604.618	707.255	68.320
MXDDHRV	650.024	713.417	51.010
GAPMNDD	440.270	258.663	165.800
BMINI	0.268	1.040	0.530
SLA	0.025	0.022	0.002
LEAFMX	0.330	0.295	0.037
LEAFPM	0.001	0.028	0.021
KLIGHT	0.588	0.585	0.111

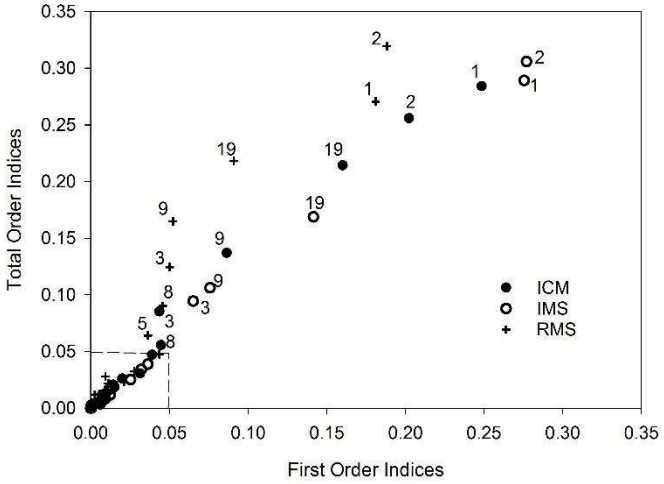

Fig. 4.1 Comparison of first order and total order sensitivity indices of Sobol for DayCent output of grain yield of maize of three treatments. Treatments were irrigated continuous maize (ICM), irrigated maize-soybean (IMS) and rainfed maize-soybean (RMS). The numerical numbers are references for parameters in Table 4.1. Dashed line indicates the criterion for selection of important parameters.

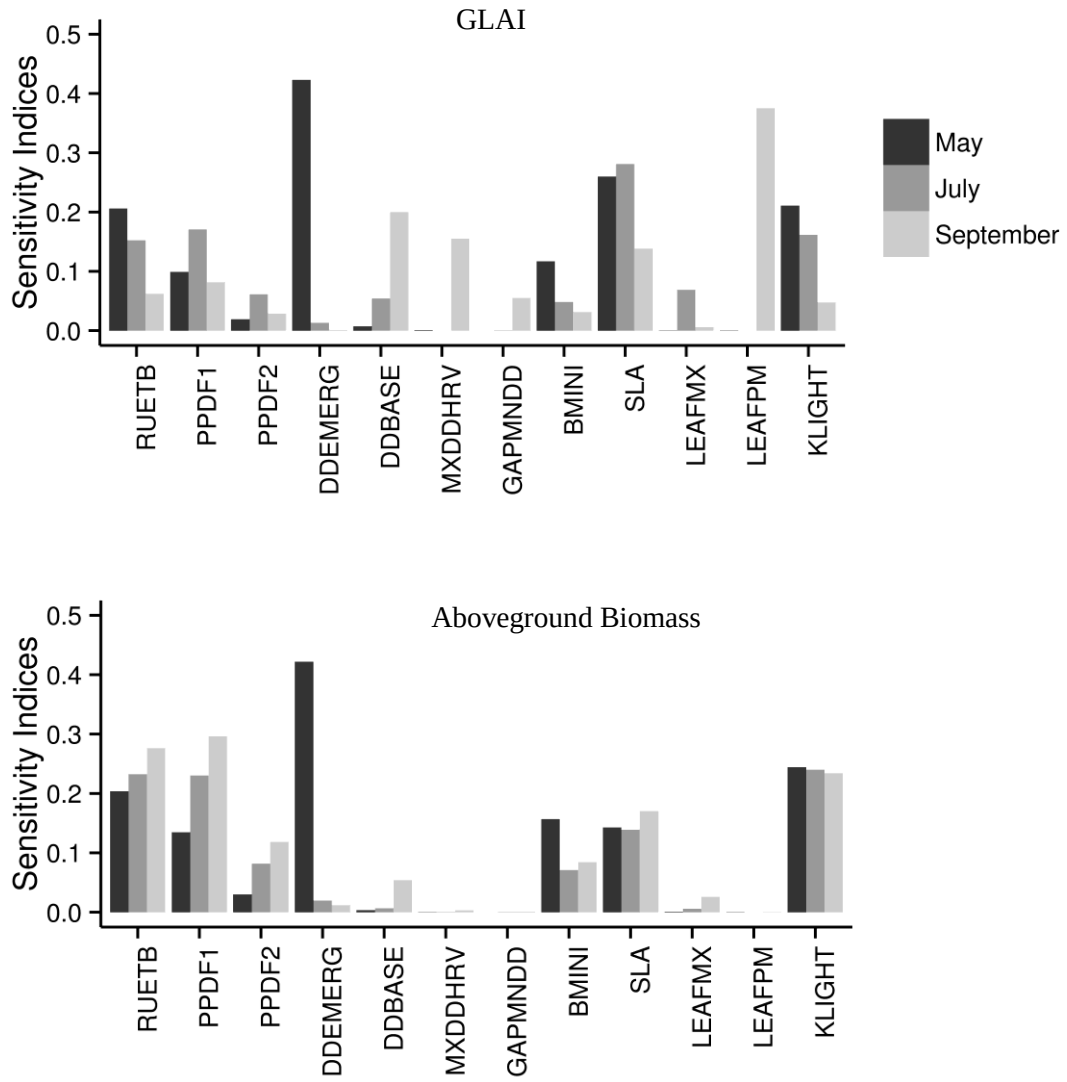

Fig. 4.2 Total sensitivity indices for DayCent output of GLAI and aboveground biomass in May, July, and September representing early, middle, and late growing season, respectively. Only input parameters with total sensitivity indices higher than 0.05 in at least one month were shown.

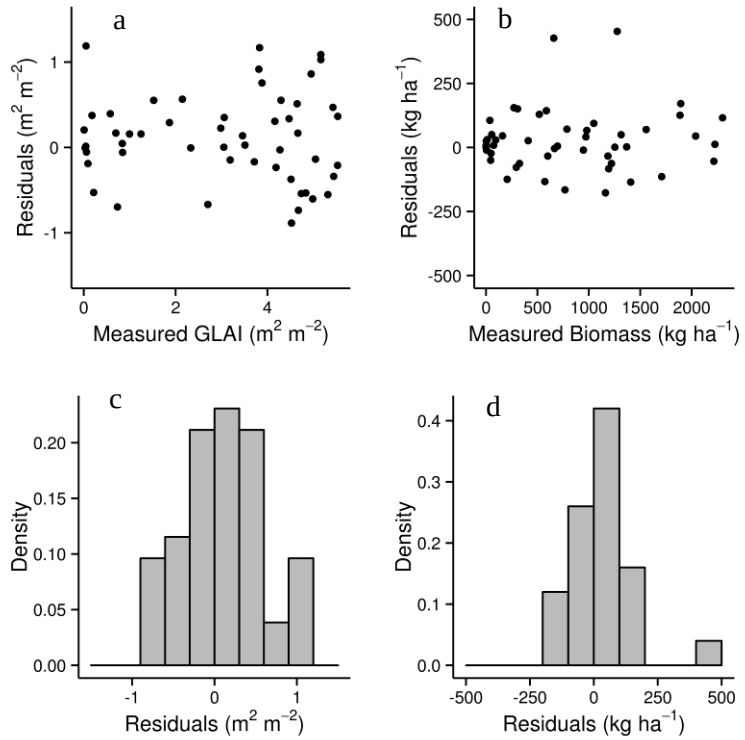

Fig. 4.3 Modeled residuals plotted against a) measured GLAI and b) measured aboveground biomass. The density plot of residuals for c) GLAI and d) aboveground biomass.

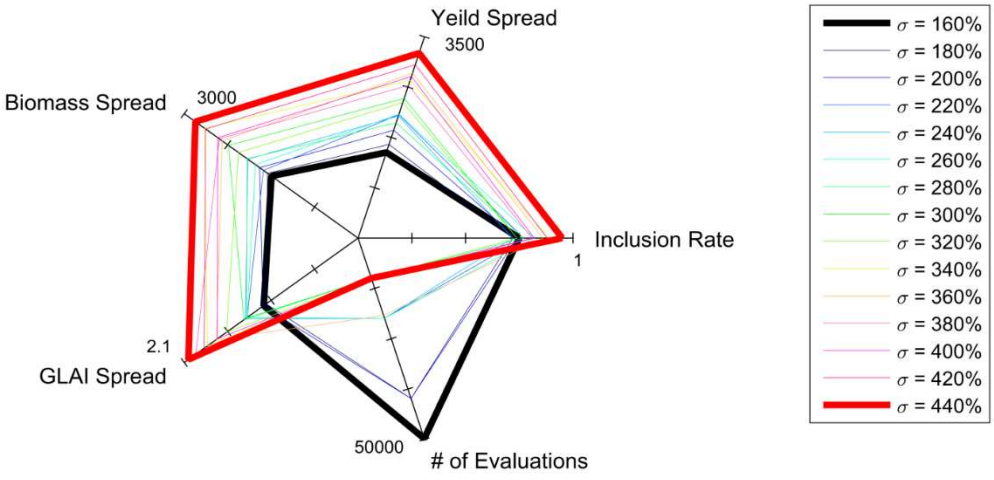

Fig. 4.4. Tradeoffs between spread, inclusion rate and DREAM conversion.

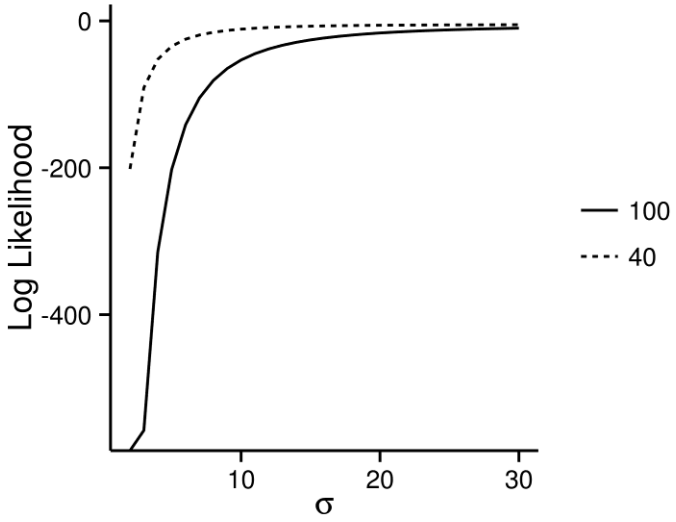

Fig. 4.5 Simple illustration of changes in log likelihood as a function of σ at two levels of residuals.

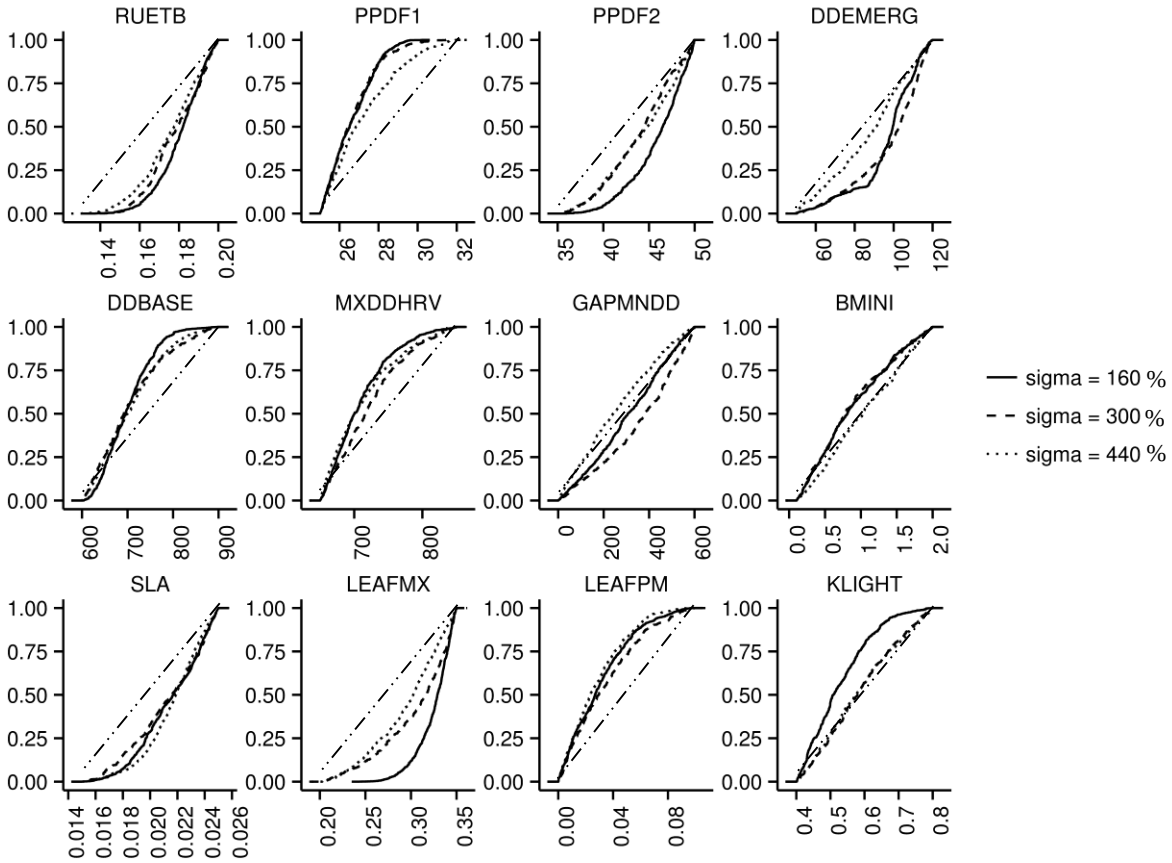

Fig. 4.6 The cumulative distribution functions (CDFs) for posterior distribution of the parameters for three levels of σ_ε used in DREAM algorithm. The straight line depicts the prior CDF from the uniform distribution.

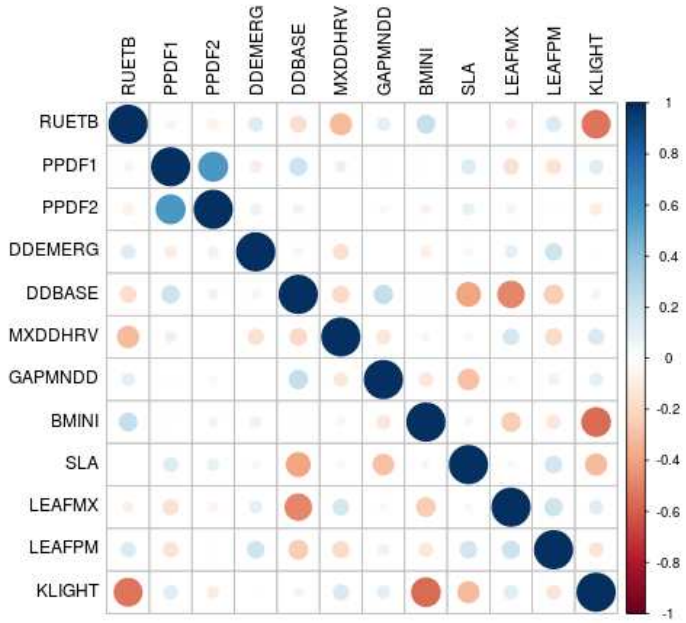

Fig. 4.7 The correlation of the parameters from the analysis using DREAM algorithm.

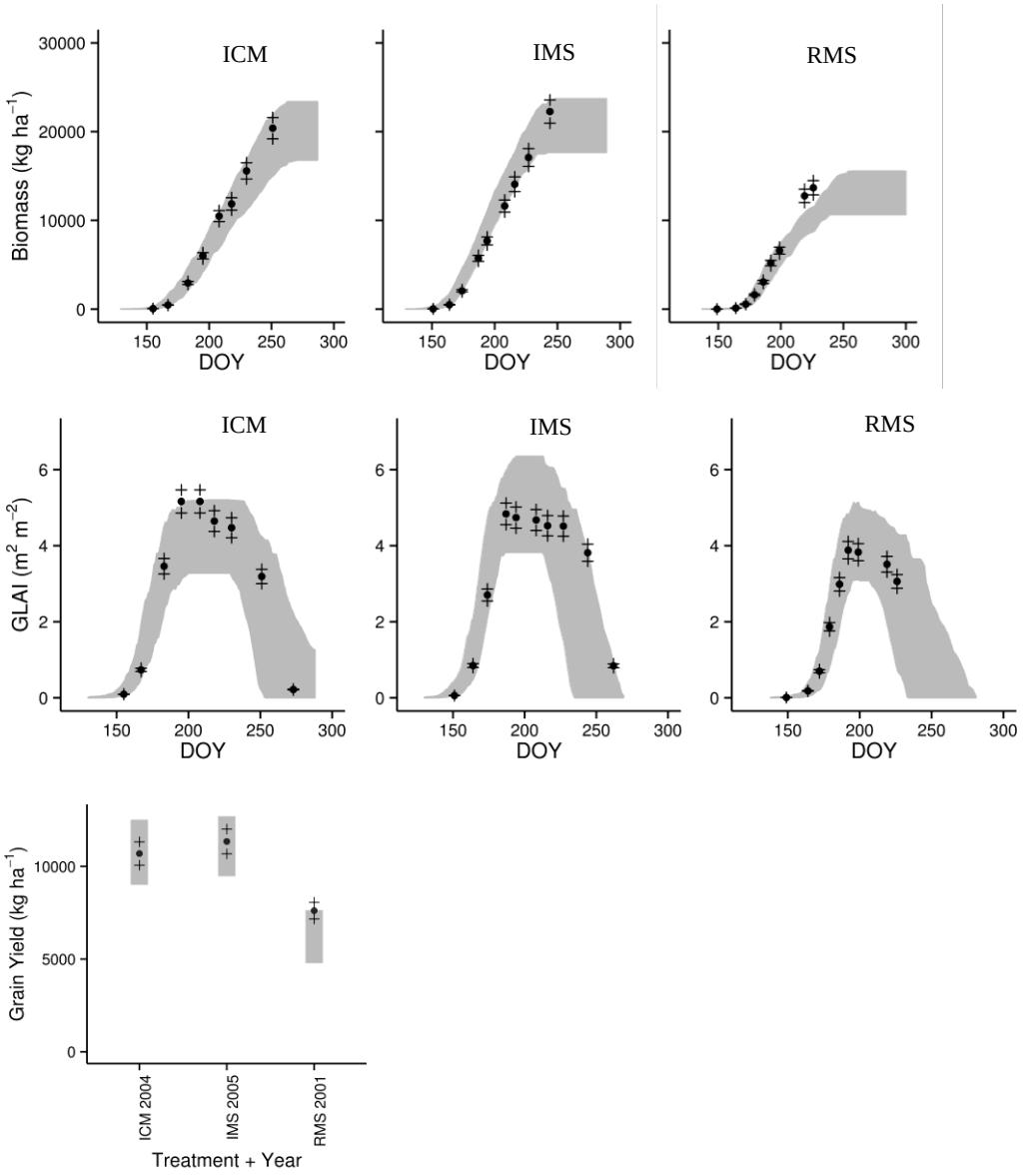

Fig. 4.8 Comparison of predictive 95% uncertainty (gray band) with measured data (dots) of the calibration dataset of aboveground biomass, GLAI and grain yields for 3 treatments in 3 years. Plus signs indicate the measurement 95% uncertainty intervals assuming 3% of coefficient of variation.

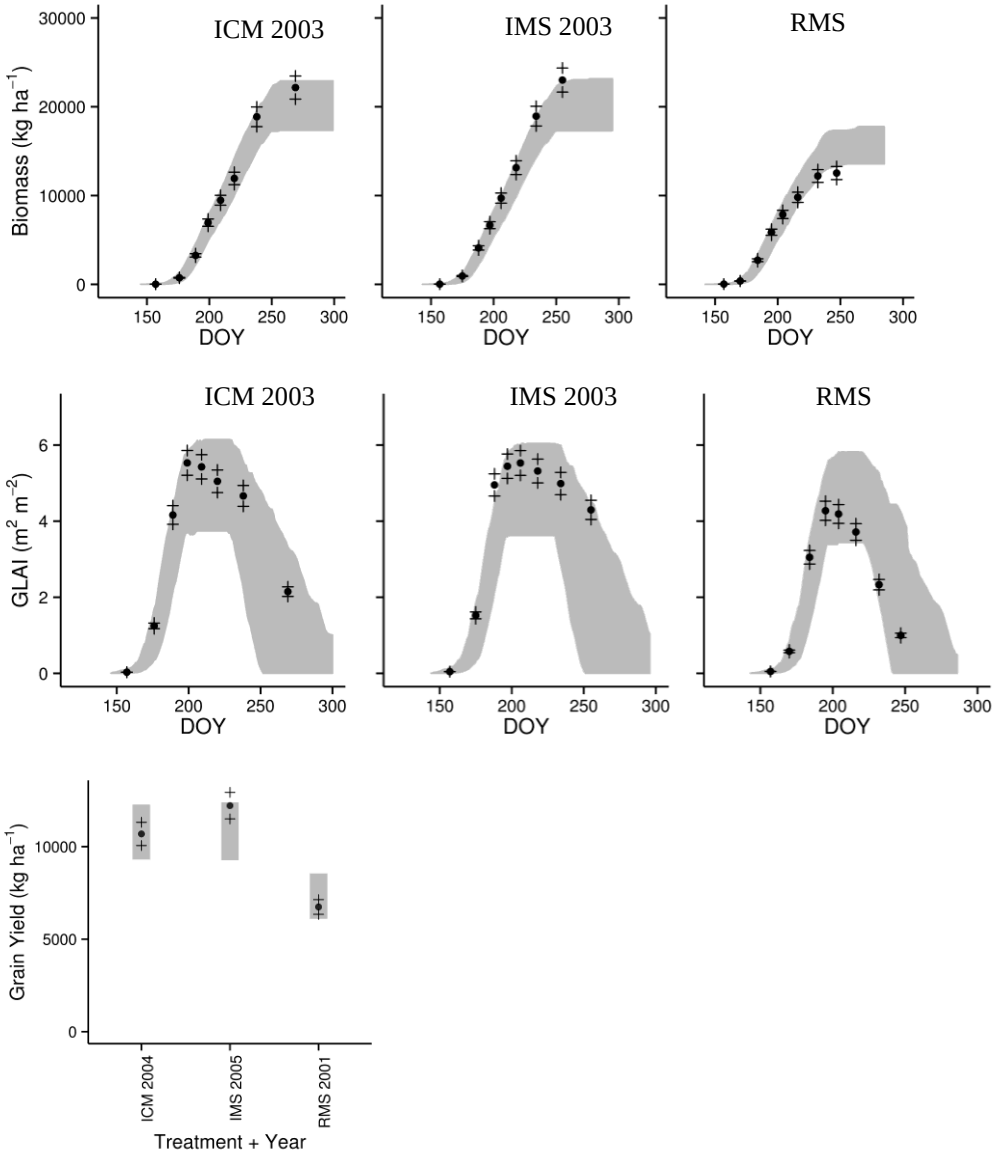

Fig. 4.9 Comparison of predictive 95% uncertainty (gray band) with measured data (dots) of the validation dataset of aboveground biomass, GLAI and grain yields for 3 treatments in 3 years. Plus signs indicate the measurement 95% uncertainty intervals assuming 3% of coefficient of variation.

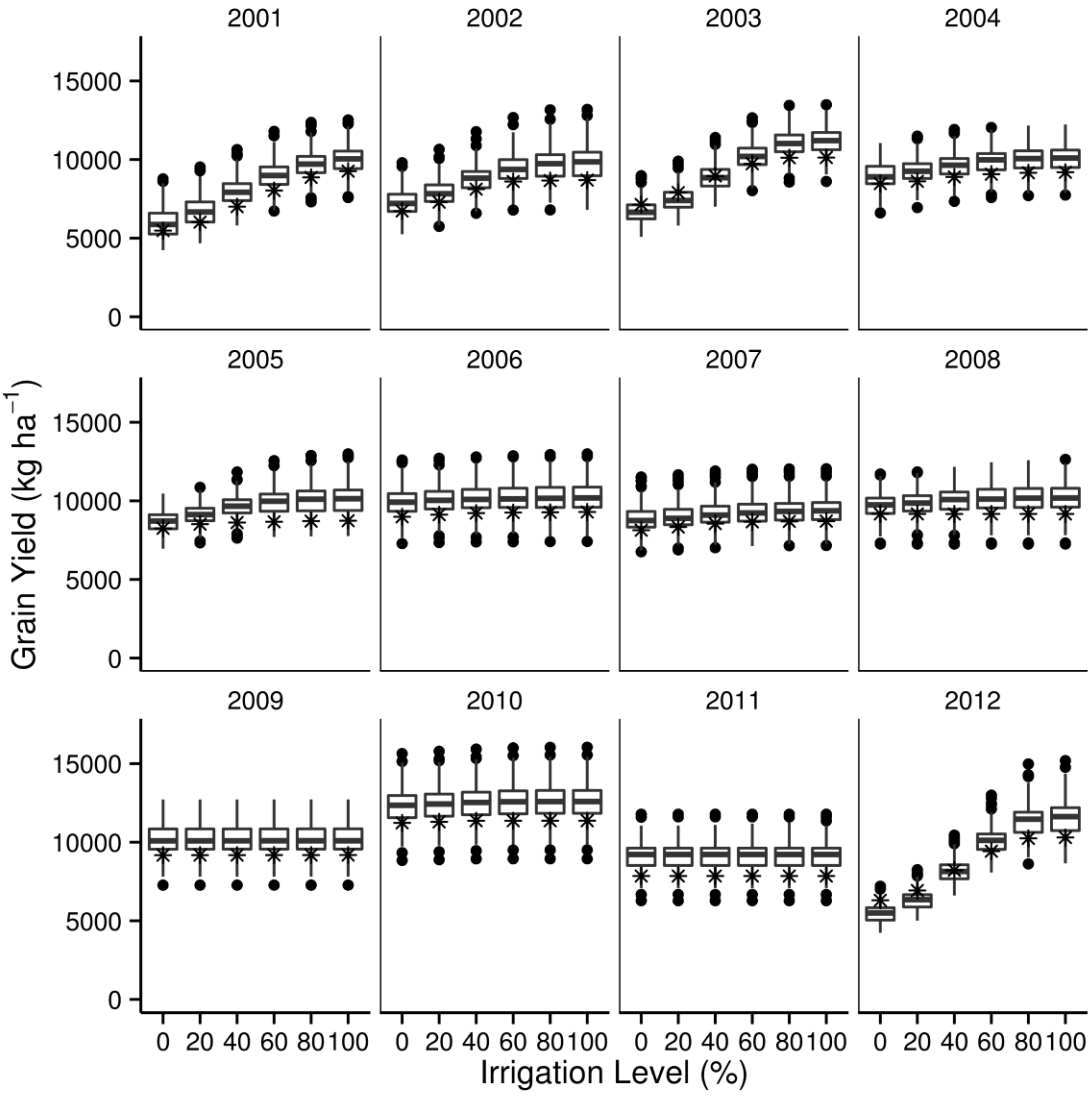

Fig. 4.10 The box plots of the predicted grain yield using parameter sets from DREAM algorithm for six irrigation levels (percentage of the 100% full irrigation scenario) for 12 years at Mead, NE. The asterisk symbols represent the predictions using the optimal set of parameters.

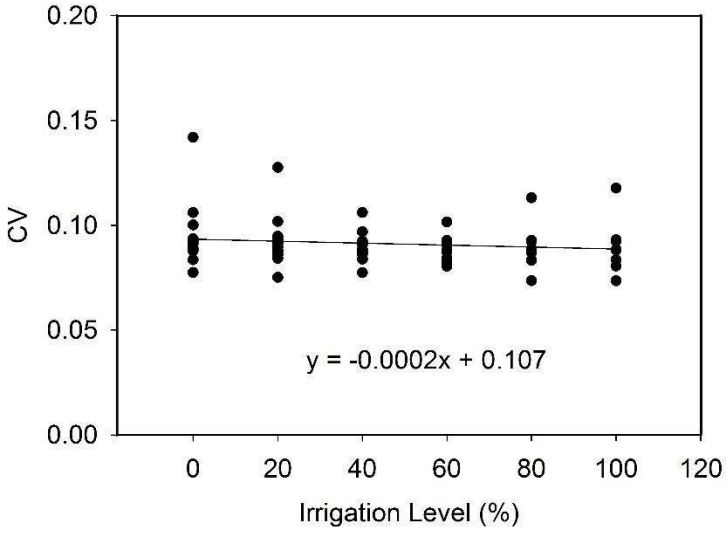

Fig. 4.11 The coefficient of variation (CV) of the predicted grain yield of the four dry years at six irrigation levels (percentage of the 100% full irrigation scenario).

REFERENCES

Ahmadi, M., Ascough, J.C., II, DeJonge, K.C. and Arabi, M., 2014. Multisite-multivariable sensitivity analysis of distributed watershed models: Enhancing the perceptions from computationally frugal methods. Ecological Modelling, 279: 54-67.

Allen, R.G., L.S. Pereira, D. Raes and Smith, M., 1998. Crop evapotranspiration: Guidelines for computing crop requirements. FAO Irrigation and Drainage Paper No. 56, Rome, Italy.

Beven, K. and Binley, A., 1992. THE FUTURE OF DISTRIBUTED MODELS - MODEL CALIBRATION AND UNCERTAINTY PREDICTION. Hydrological Processes, 6(3): 279-298.

Box, G. and Tiao, G., 1992. Bayesian Inference in Statistical Analysis. Wiley.

Brumbelow, K. and Georgakakos, A., 2007. Determining crop-water production functions using yield-irrigation gradient algorithms. Agricultural Water Management, 87(2): 151-161.

Ceglar, A., Crepinsek, Z., Kajfez-Bogataj, L. and Pogacar, T., 2011. The simulation of phenological development in dynamic crop model The Bayesian comparison of different methods. Agricultural and Forest Meteorology, 151(1): 101-115.

Chang, K.-H., Warland, J., Voroney, P., Bartlett, P. and Wagner-Riddle, C., 2013. Using DayCENT to Simulate Carbon Dynamics in Conventional and No-Till Agriculture. Soil Science Society of America Journal, 77(3): 941-950.

Colorado Water Conservation Board, 2010. Colorado's Water Supply Future. SWSI 2010 Mission Statement, Key Findings, and Recommendations. In: D.o.n. resources (Editor). State of Colorado.

Confalonieri, R. et al., 2016. Uncertainty in crop model predictions: What is the role of users? Environmental Modelling & Software, 81: 165-173.

De Gryze, S. et al., 2010. Simulating greenhouse gas budgets of four California cropping systems under conventional and alternative management. Ecological Applications, 20(7): 1805-1819.

DeJonge, K.C., Ascough, J.C., II, Ahmadi, M., Andales, A.A. and Arabi, M., 2012. Global sensitivity and uncertainty analysis of a dynamic agroecosystem model under different irrigation treatments. Ecological Modelling, 231: 113-125.

Del Grosso, S.J., Halvorson, A.D. and Parton, W.J., 2008. Testing DAYCENT model simulations of corn yields and nitrous oxide emissions in irrigated tillage systems in Colorado. Journal of Environmental Quality, 37(4): 1383-1389.

Del Grosso, S.J., Ogle, S.M., Parton, W.J. and Breidt, F.J., 2010. Estimating uncertainty in N2O emissions from US cropland soils. Global Biogeochemical Cycles, 24.

Del Grosso, S.J. et al., 2006. DAYCENT national-scale simulations of nitrous oxide emissions from cropped soils in the United States. Journal of Environmental Quality, 35(4): 1451-1460.

Doorenbos, J. and Kassam, A., 1979. Yield response to water. Irrigation and drainage paper, 33: 257.

Dumont, B. et al., 2014. Parameter identification of the STICS crop model, using an accelerated formal MCMC approach. Environmental Modelling & Software, 52: 121-135.

Dzotsi, K.A., Basso, B. and Jones, J.W., 2015. Parameter and uncertainty estimation for maize, peanut and cotton using the SALUS crop model. Agricultural Systems, 135: 31-47.

English, M., 1990. Deficit Irrigation. I: Analytical Framework. Journal of Irrigation and Drainage Engineering, 116(3): 399-412.

Feddes, R.A., Kowalik, P.J. and Zaradny, H., 1978. Simulation of field water use and crop yield. Centre for Agricultural Publishing and Documentation.

Fereres, E. and Soriano, M.A., 2007. Deficit irrigation for reducing agricultural water use. Journal of Experimental Botany, 58(2): 147-159.

Fitton, N. et al., 2014. Assessing the sensitivity of modelled estimates of N2O emissions and yield to input uncertainty at a UK cropland experimental site using the DailyDayCent model. Nutrient Cycling in Agroecosystems, 99(1-3): 119-133.

Garcia-Vila, M. and Fereres, E., 2012. Combining the simulation crop model AquaCrop with an economic model for the optimization of irrigation management at farm level. European Journal of Agronomy, 36(1): 21-31.

Gelman, A. and Rubin, D.B., 1992. Inference from Iterative Simulation Using Multiple Sequences. Statistical Science, 7(4): 457-472.

Guillaume, J. and Andrews, F., 2012. dream: DiffeRential Evolution Adaptive Metropolis. R package version 0.4-2. URL http://CRAN.R-project.org/package=dream.

Haefner, J.W., 2005. Modeling Biological Systems: Principles and Applications. Springer Science & Business Media.

He, J., Dukes, M.D., Jones, J.W., Graham, W.D. and Judge, J., 2009. APPLYING GLUE FOR ESTIMATING CERES-MAIZE GENETIC AND SOIL PARAMETERS FOR SWEET CORN PRODUCTION. Transactions of the Asabe, 52(6): 1907-1921.

Jarecki, M.K., Parkin, T.B., Chan, A.S.K., Hatfield, J.L. and Jones, R., 2008. Comparison of DAYCENT-simulated and measured nitrous oxide emissions from a corn field. Journal of Environmental Quality, 37(5): 1685-1690.

Joint Research Center of the European Commission, 2004. SIMLAB V2.2 - Simulation Environment for Uncertainty and Sensitivity Analysis. European Commission - Institute for the Protection and Security of the Citizen.

Laloy, E., Fasbender, D. and Bielders, C.L., 2010. Parameter optimization and uncertainty analysis for plot-scale continuous modeling of runoff using a formal Bayesian approach. Journal of Hydrology, 380(1-2): 82-93.

Lee, J., De Gryze, S. and Six, J., 2011. Effect of climate change on field crop production in California's Central Valley. Climatic Change, 109: 335-353.

Maupin, M.A., Kenny, J.F., Hutson,, S.S., L., J.K., B., N.L., and Linsey, K.S., 2014. Estimated use of water in the United States in 2010: U.S. Geological Survey Circular 1405.

McGuire, V.L., 2014. Water-level changes and change in water in storage in the High Plains aquifer, predevelopment to 2013 and 2011–13: U.S. Geological Survey Scientific Investigations Report 2014–5218.

MONSI, M. and SAEKI, T., 1953. Ueber den Lichtfaktor in den Pflanzengesellschaften und seine Bedeutung für die Stoffproduktion. Japanese Journal of Botany (14): 22-52.

Necpálová, M. et al., 2015. Understanding the DayCent model: Calibration, sensitivity, and identifiability through inverse modeling. Environmental Modelling & Software, 66: 110-130.

Parton, W.J., Hartman, M., Ojima, D. and Schimel, D., 1998. DAYCENT and its land surface submodel: description and testing. Global and Planetary Change, 19(1-4): 35-48.

Parton, W.J., Schimel, D.S., Cole, C.V. and Ojima, D.S., 1987. ANALYSIS OF FACTORS CONTROLLING SOIL ORGANIC-MATTER LEVELS IN GREAT-PLAINS GRASSLANDS. Soil Science Society of America Journal, 51(5): 1173-1179.

Pathak, T.B., Fraisse, C.W., Jones, J.W., Messina, C.D. and Hoogenboom, G., 2007. Use of global sensitivity analysis for CROPGRO cotton model development. Transactions of the Asabe, 50(6): 2295-2302.

Pathak, T.B., Jones, J.W., Fraisse, C.W., Wright, D. and Hoogenboom, G., 2012. Uncertainty Analysis and Parameter Estimation for the CSM-CROPGRO-Cotton Model. Agronomy Journal, 104(5): 1363-1373.

Reca, J., Roldán, J., Alcaide, M., López, R. and Camacho, E., 2001. Optimisation model for water allocation in deficit irrigation systems: I. Description of the model. Agricultural Water Management, 48(2): 103-116.

Saltelli, A., Chan, K. and Scott, E.M., 2000. Sensitivity Analysis: Gauging the Worth of Scientific Models. Wiley.

Saltelli, A., Ratto, M., Tarantola, S. and Campolongo, F., 2005. Sensitivity analysis for chemical models. Chemical Reviews, 105(7): 2811-2827.

Saltelli, A., Tarantola, S. and Chan, K.P.S., 1999. A quantitative model-independent method for global sensitivity analysis of model output. Technometrics, 41(1): 39-56.

Saseendran, S. et al., 2014. Developing and normalizing average corn crop water production functions across years and locations using a system model. Agricultural Water Management.

Saxton, K.E., Rawls, W.J., Romberger, J.S. and Papendick, R.I., 1986. ESTIMATING GENERALIZED SOIL-WATER CHARACTERISTICS FROM TEXTURE. Soil Science Society of America Journal, 50(4): 1031-1036.

Sellers, P.J., 1985. CANOPY REFLECTANCE, PHOTOSYNTHESIS AND TRANSPIRATION. International Journal of Remote Sensing, 6(8): 1335-1372.

Sobol, I.M., 1993. Sensitivity estimates for nonlinear mathematical models. Mathematical Modelling and Computational Experiments, 1(4): 407-414.

Stedinger, J.R., Vogel, R.M., Lee, S.U. and Batchelder, R., 2008. Appraisal of the generalized likelihood uncertainty estimation (GLUE) method. Water Resources Research, 44.

Stehfest, E., Heistermann, M., Priess, J.A., Ojima, D.S. and Alcamo, J., 2007. Simulation of global crop production with the ecosystem model DayCent. Ecological Modelling, 209(2-4): 203-219.

Suyker, A.E. and Verma, S.B., 2009. Evapotranspiration of irrigated and rainfed maize-soybean cropping systems. Agricultural and Forest Meteorology, 149(3-4): 443-452.

Trout, T.J., Bausch, W.C. and Buchleiter, G., 2010. Water production functions for Central Plains crops, 5th National Decennial Irrigation Conference Proceedings, Phoenix, AZ, pp. 5-8.

van Oijen, M. et al., 2011. A Bayesian framework for model calibration, comparison and analysis: Application to four models for the biogeochemistry of a Norway spruce forest. Agricultural and Forest Meteorology, 151(12): 1609-1621.

Varella, H., Guerif, M. and Buis, S., 2010. Global sensitivity analysis measures the quality of parameter estimation: The case of soil parameters and a crop model. Environmental Modelling & Software, 25(3): 310-319.

Verma, S.B. et al., 2005. Annual carbon dioxide exchange in irrigated and rainfed maize-based agroecosystems. Agricultural and Forest Meteorology, 131(1-2): 77-96.

Vorosmarty, C.J., Green, P., Salisbury, J. and Lammers, R.B., 2000. Global water resources: Vulnerability from climate change and population growth. Science, 289(5477): 284-288.

Vose, D., 1996. Quantitative risk analysis: a guide to Monte Carlo simulation modelling. John Wiley & Sons.

Vrugt, J.A., 2016. Markov chain Monte Carlo simulation using the DREAM software package: Theory, concepts, and MATLAB implementation. Environmental Modelling & Software, 75: 273-316.

Vrugt, J.A., ter Braak, C.J.F., Clark, M.P., Hyman, J.M. and Robinson, B.A., 2008. Treatment of input uncertainty in hydrologic modeling: Doing hydrology backward with Markov chain Monte Carlo simulation. Water Resources Research, 44.

Vrugt, J.A. et al., 2009a. Accelerating Markov Chain Monte Carlo Simulation by Differential Evolution with Self-Adaptive Randomized Subspace Sampling. International Journal of Nonlinear Sciences and Numerical Simulation, 10(3): 273-290.

Vrugt, J.A., ter Braak, C.J.F., Gupta, H.V. and Robinson, B.A., 2009b. Equifinality of formal (DREAM) and informal (GLUE) Bayesian approaches in hydrologic modeling? Stochastic Environmental Research and Risk Assessment, 23(7): 1011-1026.

Wang, G. and Chen, S., 2012. A review on parameterization and uncertainty in modeling greenhouse gas emissions from soil. Geoderma, 170: 206-216.

Wang, X., He, X., Williams, J.R., Izaurralde, R.C. and Atwood, J.D., 2005. Sensitivity and uncertainty analyses of crop yields and soil organic carbon simulated with EPIC. Transactions of the Asae, 48(3): 1041-1054.

Zhang, Y., Qian, Y.L., Bremer, D.J. and Kaye, J.P., 2013. Simulation of Nitrous Oxide Emissions and Estimation of Global Warming Potential in Turfgrass Systems Using the DAYCENT Model. Journal of Environmental Quality, 42(4): 1100-1108.

CHAPTER 5. COUNTY LEVEL CORN AND SOYBEAN YIELD PREDICTION FOR CONTINENTAL U.S. USING DAYCENT MODEL

5.1. SUMMARY

To provide better understanding and decision support, dynamic models have been used to access the regional impact of climate, soils and management on crop production, including climate change scenarios. In making future projections, it is critical to first test the performance of these models on regional scale under current climate conditions. In this study, we used 15-year NASS county level yields of corn and soybean of the continental U.S. to validate the performance of a newly revised version of the DayCent ecosystem model. The National Resources Inventory survey data, high resolution weather data (PRISM) and SSURGO soil data were used to derive inputs in our simulations. The predictions of corn and soybean yields in the major production areas of U.S. were generally accurate, which reflected the differences of crop yields to climate, soil, and management drivers. In regions with a high variation in year-to-year yields, the interannual variability in yields was generally well simulated for both crops. Although there are challenges to be addressed, our result indicates that the DayCent model can be useful in accessing crop yield changes under scenarios of climate change in the future.

5.2. INTRODUCTION

Climate change is expected to dramatically affect various ecosystems on our planet, including agricultural cropping systems (Adams et al., 1990; IPCC, 1990). Dynamic simulation models have been used to access the impacts on crop production and other variables at regional scales which policy decisions are usually made on. To ensure reliable assessments of future impacts, methods of regional analysis should be first tested with current climatic conditions.

Regional analysis covers large area with differences in climate, soil, and management practices. Previous work has demonstrated dynamic models could simulate the impact of climatic variations across climate regions especially on crop production (Kiniry et al., 1997; Muchow et al., 1990; Wilson et al.,

1995). It has been shown that the effect of temperature and solar radiation explains the most variation of the potential production of crop in locations of different climate regions, along with the genetics of the crop varieties grown (Muchow et al., 1990). Drought and nutrient deficit are two of major stresses that account for actual production being less that the potential given by radiation and temperature conditions. Many studies have demonstrated accurate predictions on the effect of these two stresses (e.g. Ma et al., 2003). However, previous studies also revealed that a limitation of most, if not all, models is the lack of accounting for stresses from disease, pests, and weeds, which can account for substantial loss of yields in some regions (Jagtap and Jones, 2002).

Simulation models are usually parameterized and tested at field level with detailed input data; to simulate regionally, there are a lot of challenges. Among the biggest challenges are limitations with the spatial and temporal data including weather, soils, management, and crop variety which are the necessary inputs for simulation models. In some previous regional studies, weather data from representative meteorological stations were used (Hodges et al., 1987; Moen et al., 1994) while other studies have used gridded weather data from climate simulation (Irmak et al., 2005; Kucharik, 2003). The gridded weather data are preferable as they use interpolation methods to include locations without weather stations. Soil property data are usually from national or regional soil survey databases but researchers may choose to use one or a few dominant soils for a region or the actual soil type of each parcel of cropland in the database (Hartman et al., 2011; Moen et al., 1994). Management practices vary from farm to farm. Commonly, one or a few sets of representative practices were assumed for each defined sub-region (Jagtap and Jones, 2002). Although many varieties of a crop are available in a certain region, a theoretical variety is usually created in the simulations based on the assumption that high yielding varieties share similar traits (e.g. similar period from planting to maturity).

Many studies have been conducted to evaluate and predict crop yields at different regional scales from state to world level (Irmak et al., 2005; Jagtap and Jones, 2002; Kucharik, 2003; Stehfest et al., 2007; Tan and Shibasaki, 2003). Generally, simulations of small regions were conducted with higher resolution inputs like weather, soil types and details on management. In contrast, national simulations

typically use coarser resolution inputs and model outputs have often been validated using state level or national level of historical yield records. On one hand, we desire large region predictions to provide general estimates for policy and decision making. On the other hand, more fine-grained results are necessary to accurately represent the differences in sub-regions and to capture the pattern of changes, which aid in better understanding the limiting factors for crop yields in different regions. Also, more detailed inputs potentially provide better estimation (Moen et al., 1994). Because of the limitation in input data and computation power, there are few studies using high resolution input data for very large scale regional simulation like continental U.S.

In this study, we utilized the National Resources Inventory (NRI) survey data and high resolution weather and soil data to produce yield estimation of corn and soybean that were then aggregated to county-scale for continental U.S using the DayCent ecosystem model. Our predictions were compared with NASS reported county level yields to help us assess the following questions:

1) Is our dynamic model able to capture the variations in crop production across the climate regions of the continental U.S.?
2) Was the interannual variability of crop yields well simulated?
3) What are the major challenges that we are still facing in simulating crop yields of large regional scale in high resolution?

5.3. METHOD

5.3.1 The DayCent model

The DayCent model is an ecosystem model designed to simulate terrestrial ecosystems of cropland, forest, grassland and savanna (Del Grosso et al., 2011; Del Grosso et al., 2000; Parton et al., 1998). It produces a number of ecosystem output variables including plant productivity, water balance, soil carbon and nitrogen dynamics, nitrous oxide and methane emissions (Cheng et al., 2014; Del Grosso et al., 2006; Stehfest et al., 2007; Zhang et al., 2013a; Zhang et al., 2013b). The model runs on a daily time step using daily weather and also requires basic information on soil physical properties, plant type,

and management practices as input. In recent development, the simulation of crop canopy development has been substantially improved (Chapter 2) and this version of the model is used in this study.

Within DayCent, the crop growth and production submodel is based on the radiation use efficiency approach. The amount of light intercepted by crop canopy is converted into biomass production. For models using such light interception approach, it was found that the accuracy of modeled canopy is very important (Adam et al., 2011). The new version of the DayCent model was implemented with a new canopy method that simulates canopy development using green leaf weight ratio (fraction of green leaf biomass to aboveground biomass) which is a function of growing degree days (GDD). The new version of model has been validated with experimental data of corn, soybean, and winter wheat in different regions, for its performance in simulating GLAI, biomass, grain yield, evapotranspiration (ET), and soil water (Chapter 2 and Chapter 3).

5.3.2 Input Data

The distribution of crop type and management data in our study were derived from the National Resources Inventory (NRI) survey which is a comprehensive long-term survey conducted by the U.S. Department of Agriculture's Natural Resources Conservation Service (NRCS) providing information on the status, condition, and trends of land, soil, water, and related resources on the nation's non-Federal lands (USDA, 2009). It was initiated in 1977 and more than 800,000 locations were sampled before 2007. A stratified two-stage random sample and design-based analysis strategy was used to represent the variation in the large scale (Nusser and Goebel, 1997). Majority sites were visited every 5 years during earlier years in the inventory but the frequency was changed after 2000 to sampling a rotating subset of points every year. An extensive amount of soils, land use, and land management data are collected each time.

In this study, NRI locations that are identified as crop land (about one fourth of the total points) were simulated. The survey data were used to provide information on crop management history (1982-2007) for generating the management schedules for DayCent runs. Simulated results of corn and soybean from 1993 to 2007 were extracted for analysis. The number of records in each county (location and year

combinations) from NRI survey was shown in Fig. 5.1. As NRI data do not include detailed management data like planting date and fertilization amount, we used survey data from other sources. Planting and harvesting dates were derived from the NASS database (NASS, 2010). To simplify the simulation, one set of representative planting and harvesting dates was used for each state (Appendix Table A1). For nutrient management practices, only nitrogen fertilization was simulated in this study and average nitrogen fertilizer rates for each state, subdivided for irrigated and non-irrigated crops, were derived from the chemical use survey from NASS (NASS, 2003). We created an initial scenario of applying the reported nitrogen rates (Appendix Table A1). In a second scenario, nitrogen application rates were doubled in order to eliminate nutrient stress on crop growth to evaluate simulated yields solely as a function of climatic (and radiation) drivers. Irrigation practice was simulated with the automatic irrigation option in DayCent model, assuming that full irrigation to meet crop water demand was the predominant practice. Automatic irrigation was assumed to be triggered when 60% of available water depleted in the root zone (Allen et al., 1998). Cropping histories before 1980, based on analyses of a variety of literature and historical databases developed for the US national greenhouse gas inventory (USEPA, 2015), were used for the model 'spinup' to establish the initial conditions for soil organic matter pools (Basso et al., 2011).

Soil property data of each NRI location were derived from the Soil Survey Geographic database (SSURGO) which is the most detailed soil database of the continental U.S. with information collected at scales ranging from 1:12,000 to 1:63,360 (NRCS, 2009). Soil hydraulic parameters were estimated using the pedotransfer function from Saxton et al. (1986).

Recent published 4 km gridded PRISM spatial climate datasets (PRISM Climate Group, 2015) were chosen as climate input data (including daily maximum temperature, minimum temperature, and precipitation). As solar radiation was not provided by PRISM, the DayCent model estimated it using a modified method described in Thornton and Running (1999). Reference ET was calculated using Hargreaves' equation (Hargreaves and Allen, 2003).

5.3.3. Crop parameterization

5.3.3.1 Crop groups

We divided corn varieties into six groups and soybean into seven (Table 5.1). The groups of corn varieties were created according to the variety map from Dupont Pioneer Seed Company (https://www.pioneer.com/home/site/us/agronomy/library/compare-maturity-corn-products/; accessed 05/06/2016). The grouping was based on comparative relative maturity (CRM) values (Table 5.1 and Fig. 5.1a). The crop group map of soybean was adapted from Monsanto Company (https://www.aganytime.com/asgrow/mgt/planting/Pages/Soybean-Maturity.aspx; accessed 05/06/2016) which was based on the widely recognized soybean maturity group (MG) system (Table 5.1 and Fig. 5.1b).

5.3.3.2. Corn

We created general crop parameter values to represent different crop groups (Table 5.1). The most sensitive and important crop parameters in DayCent (Chapter 4) were first calibrated using experimental sites data (Appendix Table A2). Based on the comparison between the experimental site yields and NASS reported yields at that location, we slightly adjusted the RUETB (radiation use efficiency for total biomass) parameter to reflect the lower yields obtained by farmers which are mainly due to suboptimal management (Grassini et al., 2011). Parameters from each experimental location were pooled and used to generate one set of parameters for each crop group.

As previous studies showed, RUE is a highly sensitive parameter in DayCent (Zhang et al. in prep-b) and also in other models (DeJonge et al., 2012; Wang et al., 2005). Different from some crop models which only account for aboveground biomass production, RUE in DayCent is defined as the total biomass production (aboveground and belowground) per intercepted photosynthetically active radiation. As Stockle and Kiniry (1990) reported, 50% the variation of the field measured RUE can be explained by vapor pressure deficit (VPD); thus we developed an equation similar to the one in Kiniry et al. (1997) based on calibrated parameter values from dry and wet regions.

$$RUETB = 0.22 - 0.04 * VPD \quad (5.1)$$

where RUETB is the RUE for total biomass (g m^{-2} $langley^{-1}$ PAR); VPD is the 33-year average vapor pressure deficit from May to September (growing season) in unit of kPa. For VPD less than 1.0 kPa, RUETB was set a constant of 0.18 g m^{-2} $langley^{-1}$ PAR. Since PRISM data did not include VPD or humidity variables, to estimate VPD for entire U.S., we used the equations in Stockle and Kiniry (1990) which only requires daily mean and minimum temperature as input (Fig. 5.2c).

Planting population for irrigated corn was assumed as 80,000 plants ha^{-1} at all locations (Grassini et al., 2009). For dryland corn, the planting population decreases from east of U.S. to the west along the VPD gradient (Grassini et al., 2009); so we used a linear equation to proximate the change in planting population.

$$POPULATION_{planting} = 1000 * (-5 * VPD + 13) \quad (5.2)$$

where $POPULATION_{planting}$ is in unit of plants ha^{-1}. Because there is no explicit parameter for planting population in DayCent, we adjusted the parameter of initial biomass at emergence to reflect the difference.

One major difference in parameters between crop groups was the values of phenological parameters. DayCent uses the GDD method for phenology development. As corn CRM values have been found to be linearly related to GDD (Kucharik, 2003), we assigned different GDD values for each crop group. We used values of GDD of physiological maturity ranging from 1050 ^{0}C to 1600 ^{0}C (base temperature 10 ^{0}C and ceiling temperature 30 ^{0}C) to represent the different maturity classes.

5.3.3.2 Soybean

Similar procedures were used to develop parameters for soybean. The field experimental data (Appendix A2) were mainly from the example datasets in the DSSAT crop model package (Hoogenboom et al., 2010) and GRACEnet online database (Del Grosso et al., 2013). As soybeans in U.S. are grown in relatively moist regions compared with corn and there are not enough field studies to assess whether RUE of soybean was also affected by VPD, we used one constant RUETB for all the simulations (Table 5.1). The calibrated RUETB values using field experiments were also slightly lowered to account for the lower

yields on farms (Jagtap and Jones, 2002). We did not simulate the difference of soybean planting population in irrigated and non-irrigated conditions as it is small (Chapter 2).

5.3.4 Data Post-processing

Simulations and post-processing were conducted on a mid-performance computer cluster (256 processors and 463 GB memory). Simulated corn and soybean yields were extracted and summarized for each county. In the NRI survey design, each NRI location is associated with an expansion factor which indicates the area represented by the point location. The expansion factors were used to area-weight DayCent output for the locations within each county to derive county-level yield estimates. Since cropping patterns result in varying acreages across years, area-weighted yields were calculated for each crop and irrigation type combination on an annual basis. The area-weighted DayCent yield estimates were compared to NASS reported yields from 1993 to 2007 (last year of NRI records obtained). In many counties, irrigated and non-irrigated fields both exist but in some cases only total yields were reported by NASS and therefore we computed an area-weighted average for the county assuming that the survey design of the NRI locations reflects the proportion of fields with different irrigation management. For counties where irrigated yields are explicitly reported, we were able to compare the irrigated and non-irrigated yields separately. To avoid problems with limited sample size, we filtered out the years with less than five NRI records in a county and those years for which the reported NASS crop area was less than 1214 ha (3000 acres). Grain yield values were adjusted to 15.5% moisture content for corn and 13% moisture content for soybean. Maps were generated using the R program with package ggmap (Kahle and Wickham, 2013).

5.4. RESULTS AND DISCUSSION

5.4.1. Climate and NRI data

Crop growth and production are largely affected by climate, with water and temperature as main regulators, and human management. The annual precipitation in the mainland U.S. east of the Rocky Mountains changes generally along an east to west gradient, decreasing from more than 120 cm in the east to less than 30 cm in the west (Fig. 5.2a). The average daily temperature during the growing season

(May to September) ranges from above 29 ^{0}C in southern Texas to below 20 ^{0}C in the states along the Canadian border with the exception of the Rocky Mountain area in the west (Fig. 5.2b). The estimated average VPD of the growing season shows a trend of gradual decrease from below 1.0 kPa in the north-east to above 2.0 kPa in the arid region in the south-west (Fig. 5.2c).

Climate substantially impacts the distribution of crop land. The majority of corn and soybean are grown in the wet regions (VPD less than 1.6 in Fig. 5.2c) which are east of the Rocky Mountain (Fig. 5.1). There were considerably more NRI records (combination of location and year) of corn and soybean (more than 500 records in a county) in the "Corn Belt", the major production region located in the Midwest (Fig. 5.1). Outside the Corn Belt, the planting areas were generally low, with only a few NRI records found in some counties. When the number of NRI records were low, the simulated results may not represent the actual distribution of soil type, management and weather in a county, potentially leading to biased predictions.

5.4.2. Corn yield prediction

The 15-year average of NASS reported yields of corn (irrigated and non-irrigated combined) was generally higher in the center of the Corn Belt (Fig. 5.3a), with yields of 9-11 Mg ha^{-1} in south Minnesota, Iowa, and Illinois where plentiful rainfall was received and temperature is optimal for growth. Relatively high yields were also achieved in the south Nebraska and north-east Colorado because of the application of irrigation in this semi-arid region. Low yield (less than 5 Mg ha^{-1}) were observed in North Dakota and South Texas, likely due to sub-optimal temperature conditions. High total yields were also reported in south-west Kansas, north Texas, south New Mexico and California, due to the application of irrigation and long growing seasons.

The modeled yields exhibited a very similar pattern to the NASS data (Fig. 5.3b). In most counties (91% in the major production states of Minnesota, Wisconsin, Michigan, Iowa, Illinois, Indiana, and Ohio), our predictions were within ±20% of the NASS reported 15-year average yields. And 63% of predicted yields were within ±10% of NASS reported yields. In the semi-arid region of eastern Colorado,

south west Nebraska, and north-west Kansas, the prediction was also relative accurate with majority counties' yields within ±20%.

In the states along the south-east coast (Virginia, North Carolina, and South Carolina), the no nitrogen stress scenario predicted corn yields that exceeded NASS results by more than 30% for most counties (Fig. 5.3c). However, the modeled yield prediction was much closer to NASS reported yield in the scenario using state average N fertilization rate (Fig. 5.3d). This suggests that the farmers might achieve higher yield by increasing the fertilization rate. However, in an analysis of crop yield trends in the SE US, Jagtap and Jones (2002) suggested that typical yield losses due to insects, pathogens and weeds can be severe in this region, and thus farmers may fertilize less than required to achieve climatic-potential yields.

Our model also over-predicted yields for a strip of counties in north and middle of Texas (Fig. 5.3c). This region is dominated with Houston Black-Heiden-Wilson soil series comprised of Vertisol soils which are subject to extensive, deep cracking when dry. Since the DayCent model does not simulate macro-pore flow which bypasses the root zone through cracks, the simulation of the water balance is difficult and soil available water was likely over-predicted, leading to an over-prediction of yield. In north-west Texas, yields were correctly predicted for the region of corn group 5 but over-estimated for corn group 6. The assumed boundary between group 5 and group 6 might not be correct as in reality a mixture of corn varieties of different CRM was planted in this region. In southern Kansas, irrigated corn yields were under-estimated by more than 20% (Fig. 5.4a). We found that it was likely that the RUETB was too low after the adjustment using VPD (high VPD region). We also predicted lower yield for middle and western North Dakota and higher yield in California, but the reasons are not clear.

From eastern Nebraska to northeastern Colorado, precipitation gradually decreases from around 80 cm to around 40 cm per year. Because many NRI records were available and there was minimal missing data in the NASS database for this region, we used the data from Nebraska and Colorado to examine the models capability to simulate water limitations on yield at regional scale. As shown in Fig. 5.4b, dryland yield was over-predicted in southern Nebraska with an apparent systematic bias. Looking

at the 15-year average, the modeled yields were highly correlated with observed yields but predicted yields were consistently higher (Fig. 5.5a; R^2= 0.89; RMSE= 1342.86 kg ha^{-1}), with a slope of 1.12 and 490.20 kg ha^{-1}. Since the slope of the fitted regression was close to 1.0, applying a correction factor would eliminate the positive bias of our prediction which might be due to the yield losses in some years from severe hail damage, disease, and pest that were not simulated by the model. Looking at the yield trends over time in the counties in Nebraska and Colorado, the model captured the inter-annual variability with overall R^2 of 0.58. We also calculated the statistics for each county (Appendix Table A3); there were 37 counties whose minimum dryland yield in 15 years was lower than 30% of the observed maximum dryland yield (mainly caused by drought stress). Among them, 28 counties have R^2 values of above 0.5, which suggest the inter-annual variability was well represented by the model. We also noticed that in some years, the model substantially over-predicted those in the no nitrogen stress scenario. In the scenario of using state level average nitrogen rate, yield values of those years were much lower. So it possible that in real world, dryland crops experienced some nutrient stress when there was a wet year with optimal temperature.

Several authors have demonstrated that dynamic models could accurately simulate corn yield at different locations across climate regions (Kiniry et al., 1997; Wilson et al., 1995). Because of the limitation of input data for many simulation models, only a few studies have been conducted for large regional analysis for U.S. in the past. In 1990s and before that, the resolution of input data of these studies was very low. The weather data were from meteorological stations in the study region and every station was assumed to represent a certain area in the simulations (Hodges et al., 1987; Kunkel et al., 1991; Moen et al., 1994). These studies only used one or a few dominant soil types. Therefore, most of these studies have produced more aggregate estimates and less spatial and temporal variability due to averaging over larger land areas and time spans. In more recent years, gridded weather products and intensive soil survey data have become available. Kucharik (2003) used the ecosystem model Agro-IBIS to simulate corn yield for 13 states in Corn Belt with 0.5° grid (50 km) climate and soil data (derived from STATSGO database). In comparison with our simulation, with the exponential rise in computational

power, our regional analysis can be conducted at much higher resolution with detailed input. The PRISM weather data used in our study were at 4 km grid and the soil data were at scales ranging from 1:12,000 to 1:63,360 compared to the scale of 1:250,000 of State Soil Geographic (STATSGO) data used in Kucharik (2003). In the Kucharik (2003) study, compared to 15-year average NASS data, the model predictions for rain-fed yields accounted for about 50% of the observed variability in yields ($R^2 = 0.46$).

5.4.3. Soybean yield prediction

Compared to corn, there is almost no soybean grown in the semi-arid region in west Great Plain, with the bulk of production located in the Corn Belt and southeastern US. Observed 15-year average total yields (including irrigated and non-irrigated) from NASS were highest (above 3200 kg ha^{-1}) in the middle and west of the Corn Belt (Fig. 5.6a). The soybean varieties used in these high yield regions were the MG II and III. Grain yields in the south and southeast were relative low, mainly in the range of 1200 to 2400 kg ha^{-1}. Maturity group V and above which are determinate varieties of soybeans were majorly grown in these regions (Bruns, 2009). As temperature is low and growing season is short in the north (North Dakota and northern Minnesota), soybean yields were less than 2400 kg ha^{-1}.

Our simulation captured the pattern of yield change in the main Corn Belt (Fig. 5.6b). Our predictions in 93% of the counties in the major production states (Minnesota, Wisconsin, Michigan, Iowa, Illinois, Indiana, and Ohio) were within ±20% of NASS reported yields and 64% of them were within ±10% (Fig. 5.6c). These statistics were similar to those of our corn predictions.

In Nebraska, high average total yields were found in both NASS data and our simulation. The high yields were associated with widely used irrigation systems in this region. The model correctly simulated the yields of irrigated and non-irrigated fields in this state with most counties within ±20% of NASS data (Fig. 5.7a and 5.7b). The model tended to slightly over-predict the yields of rainfed soybean (Fig. 5.8a). Looking at year-to-year data, inter-annual variability which was mainly due to drought stress in Nebraska and that trend was also captured in the model (Fig. 5.8b; $R^2 = 0.39$ and RMSE 481.42 kg ha^{-1}). For counties whose minimum annual yield was less than 40% of its maximum yields in the 15 years (14 counties), the R^2 values were all above 0.55 (Appendix Table A4).

However, in the south and southeast, model predictions were more than 30% greater than reported yields for a majority of counties (Fig. 5.6c). In another study, Irmak et al. (2005) predicted regional soybean yields for Alabama, Arkansas, Georgia, Louisiana, Mississippi, North Carolina, and South Carolina using CROPGRO-Soybean model and found the also model over-predicted yields for all locations when no adjustment was used. Jagtap and Jones (2002) reported GROPGRO-Soybean largely over-predicted soybean yields in Georgia in comparison to NASS county yield but the predictions were much closer to the measured yield at an experiment site. The major causes of the actual yield loss in those years were disease, insects, weeds and operational problems which were not simulated in the model but commonly seen in this region. The soybean simulated in this region was MG V; however, in our calibration, no experimental site data contained soybean MG V, which was one of the reasons for the biased prediction. Another reason might be the crop group boundary was not drawn properly. In northern Arkansas and Tennessee where MG IV soybean was simulated, our modeled results were accurate. However, crossing the boundary, the difference in yields suddenly increased in the region specified for MG V (Fig. 5.6c). While assuming such an abrupt geographic transition in crop variety deployment is a simplification needed to make a large regional simulation tractable, it is likely that in reality there is a gradual transition in the soybean maturity groups and in many places a mixture of maturity groups is grown. However, there is very limited data available documenting which varieties are actually grown in these transition areas. In the past two decades, soybean production systems in the Mississippi Delta have been reported to change dramatically. An early soybean production system using MG III, MG IV and MG V varieties (planted from March to early May earlier than traditional May and June) has been developed and used; the high yields for Mississippi during 2000 to 2005 were suggested to be a result of adapting the early production system (Bruns, 2009). So by simulating mixtures of MG of soybeans with difference in planting dates, our predictions should improve.

As soybean fixes nitrogen through symbiotic relationship with rhizobia bacteria, nitrogen fertilization requirement is generally very low. As a result, there was no substantial difference in yield predictions in our two nitrogen scenarios for soybean (Fig. 5.6c and 5.6d).

5.5. CONCLUSIONS

Our predictions of corn and soybean in the major production areas of U.S. were generally accurate with the model capable of representing the geographically-distributed differences in crop yields due to climate, soil, and management. In our simulations, not only the county level 15-year average yields, but also the interannual variability was well simulated for both crops. The use of NRI survey data and high resolution and quality weather product and soil property database enabled us to capture the major changes in spatial and temporal input variables. The results demonstrated that a general model parameterization, with a few broadly defined regional crop varieties, was sufficient to use the model for large regional analysis.

In this study, we demonstrated that the RUE approach used in crop production modeling could be applied across broad climate regions. Although measured RUE values from field studies were dramatically different (Kiniry et al., 1989), the variation generally can be explained by the differences in temperature, VPD and growth stages in growing season (Muchow et al., 1990; Stockle and Kiniry, 1990). In comparison with other studies which have varied the RUE parameter of same crop substantially for different regions to match measured production (Cheng et al., 2014; Stehfest et al., 2007), the approach used in our study and a few others, of specifying a constant RUE parameter of potential production for each species of crop, is more appropriate and robust (Kiniry et al., 1997; Soltani and Sinclair, 2012; Wilson et al., 1995).

We also identified several challenges in large regional simulations of crop production. First, it is difficult to draw distinct 'monolithic' crop variety boundaries; in reality, a mixture of different maturity classes of crops is used within a particular region. Second, as identified by some previous studies (Irmak et al., 2005; Jagtap and Jones, 2002), the loss of yield caused by weed, disease, pest, lodging, and hail damage is not well accounted for in models. We chose to adjust RUE parameter to partially correct the bias by comparing well managed experimental field yields to farmers', but a more accurate way of estimating these stresses is needed. Third, we found regional prediction of crop yields is associated with

uncertainty from a lot of sources. There is a big challenge to quantify the uncertainties from model inputs, parameters, and model structure.

In summary, as we demonstrated, a dynamic model is able to predict the variations of crop yields under current climate at national scale. Although more work is needed to model crop response to the rising of CO_2 and possible management changes, our result suggests the DayCent model can potentially be used to predict regional-scale yield changes under scenarios of climate change in the future.

Table 5.1. The crop groups for corn and soybean and major parameters used for each crop group (values of RUETB and BMINI of corn is conditioned for VPD under 1.0). Definitions and units of these parameters are in Appendix Table A3.

	Corn						Soybean						
Crop group	**1**	**2**	**3**	**4**	**5**	**6**	**0**	**1**	**2**	**3**	**4**	**5**	**6**
CRM or MG[I]	68 - 77	78 – 87	88 – 97	98 – 105	106 – 115	116+	00 & 0	I	II	III	IV	V	VI & VII
DDBASE	600	600	700	700	800	850	500	600	700	700	800	800	900
MXDDHRV	450	550	550	650	700	750	550	600	600	700	700	800	900
DDLAIMX	600	600	700	700	800	850	700	800	900	1000	1100	1200	1300
BMINI	0.3	0.3	0.3	0.3	0.3	0.9	1	1.5	1.5	1	1.5	2	2
SLA	0.02	0.02	0.02	0.02	0.02	0.02	0.025	0.025	0.025	0.025	0.025	0.03	0.03
LEAFCL	0.9	0.9	0.9	0.9	0.9	0.9	0.8	0.8	0.8	0.8	0.8	0.75	0.75
LEAFEMERG	0.9	0.9	0.9	0.9	0.9	0.9	0.85	0.85	0.85	0.85	0.85	0.85	0.85
LEAFMX	0.25	0.25	0.25	0.25	0.25	0.25	0.35	0.35	0.35	0.35	0.35	0.3	0.3
RUETB	0.17	0.17	0.17	0.17	0.17	0.18	0.09	0.09	0.09	0.09	0.09	0.09	0.09
PPDF(1)	27	27	27	27	27	27	25	25	25	25	25	25	25
PPDF(2)	45	45	45	45	45	45	40	40	40	40	40	40	40
KLIGHT	0.55	0.55	0.55	0.55	0.55	0.55	0.5	0.5	0.5	0.5	0.5	0.5	0.5
HIMAX	0.55	0.55	0.55	0.55	0.55	0.55	0.4	0.4	0.4	0.4	0.4	0.4	0.4
HIWSF	0.7	0.7	0.7	0.7	0.7	0.7	0.5	0.5	0.5	0.5	0.5	0.5	0.5
KCET	1.2	1.2	1.2	1.2	1.2	1.2	1.15	1.15	1.15	1.15	1.15	1.15	1.15

ł The comparative relative maturity for corn or maturity group class for soybean.

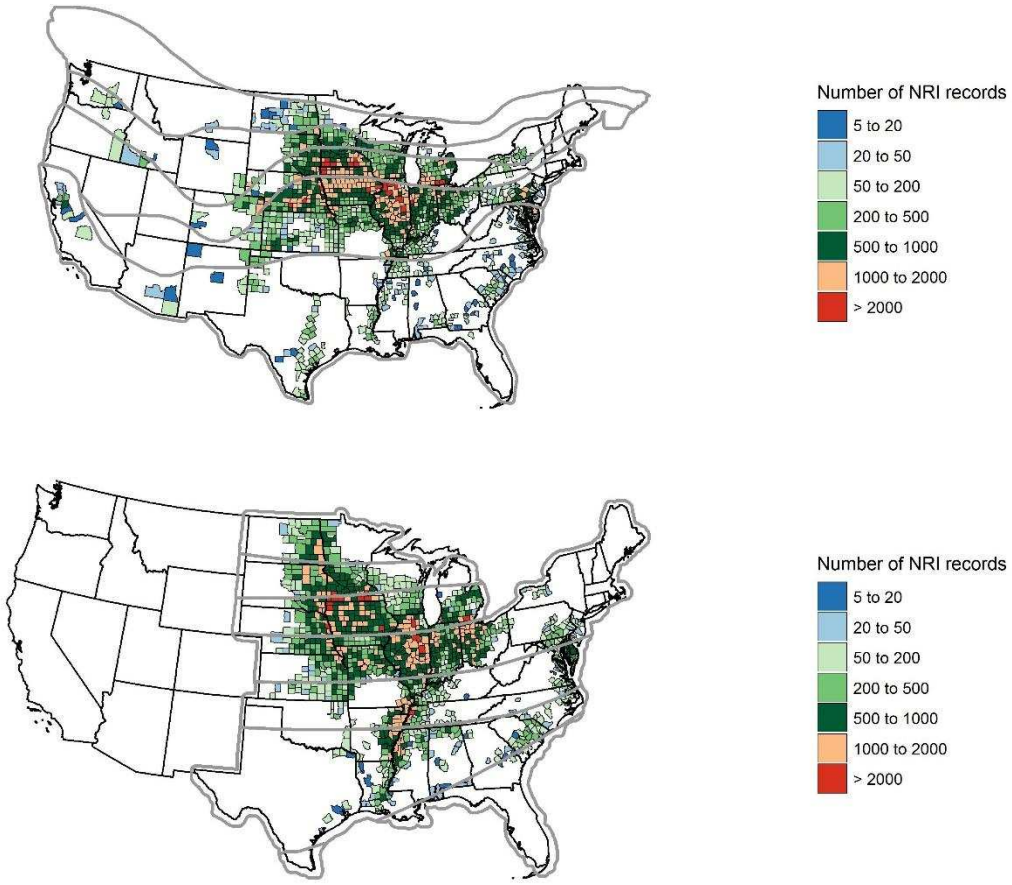

Fig. 5.1 The number of NRI records (combination of location and year) in each county used in our simulation for a) corn and b) soybean. Counties with NRI records less than 5 were filtered out. The gray lines are the boundaries of crop groups and the numeric numbers indicate the crop group.

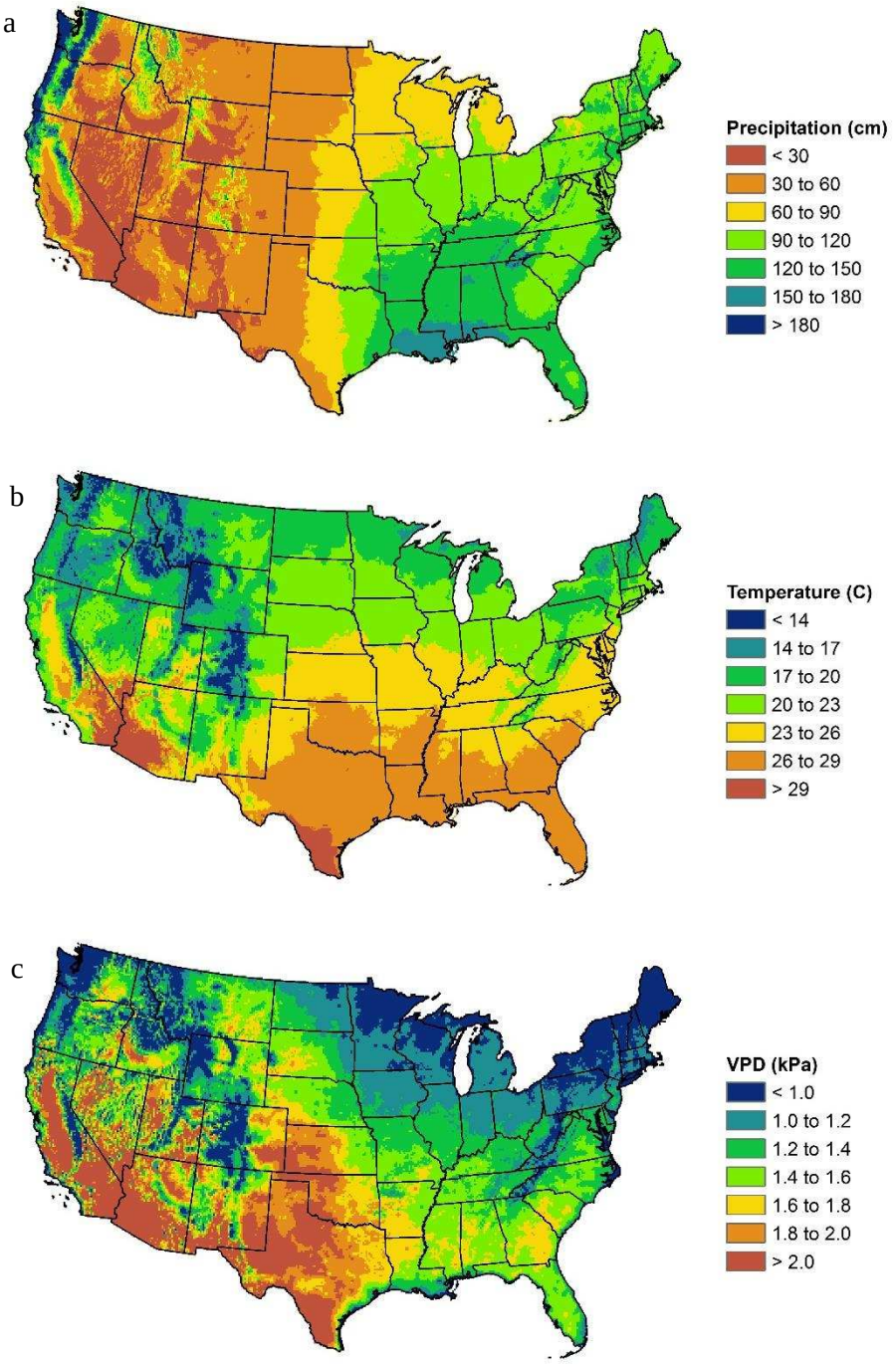

Fig. 5.2 The maps of a) annual total precipitation, b) growing season average temperature (May to September), and c) growing season average VPD. Data were derived from PRISM dataset (1981-2013).

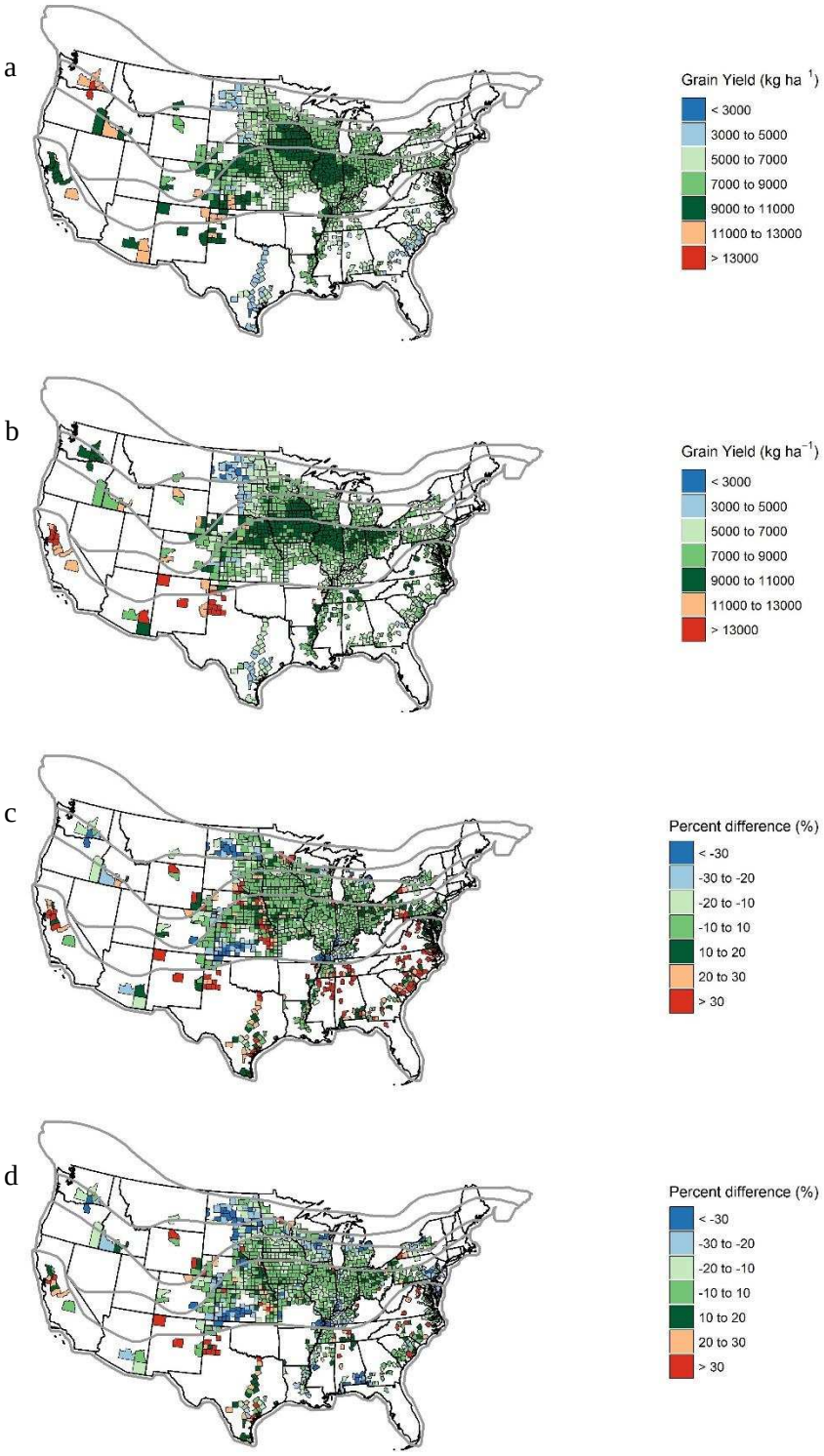

Fig. 5.3 The maps of a) 15-year average NASS yields of corn, b) simulated average yields of the same period, c) the percentage difference of simulated yields to NASS yields of the double nitrogen rates scenario, and d) the percentage difference of simulated yields to NASS yields of the average nitrogen rates scenario.

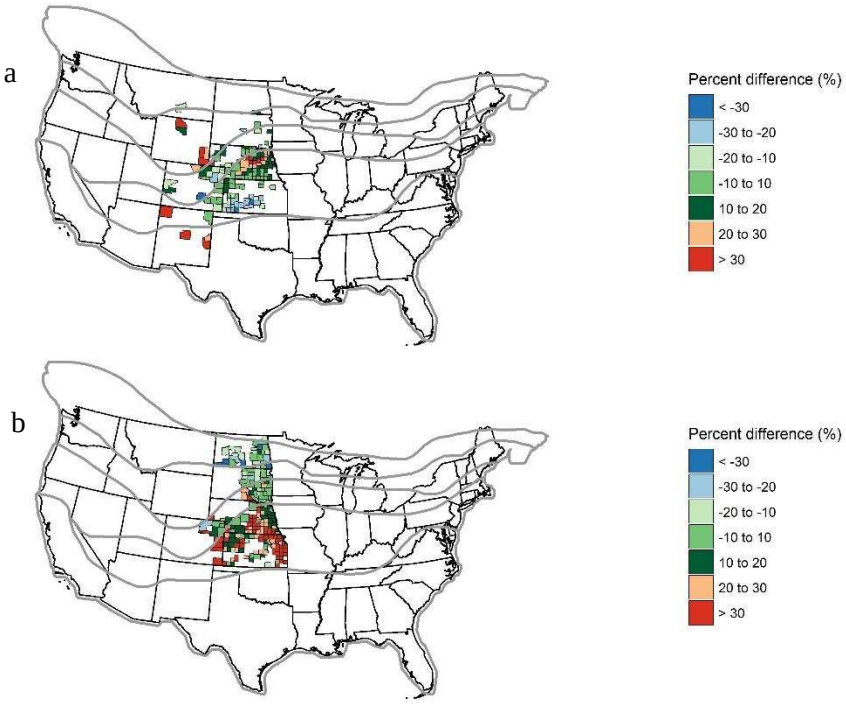

Fig. 5.4 The maps of a) the percentage difference of simulated irrigated yields to NASS irrigated corn yields of the double nitrogen rates scenario and b) the percentage difference of simulated non-irrigated yields to NASS non-irrigated yields of the double nitrogen rates scenario.

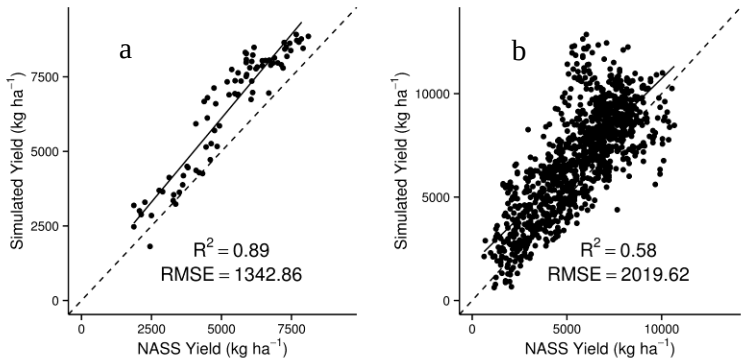

Fig. 5.5 Relationship a) between 15-year average NASS corn yields of counties in Nebraska and Colorado (across moisture gradient) and simulated yields and b) between NASS yields of individual years and simulated yields.

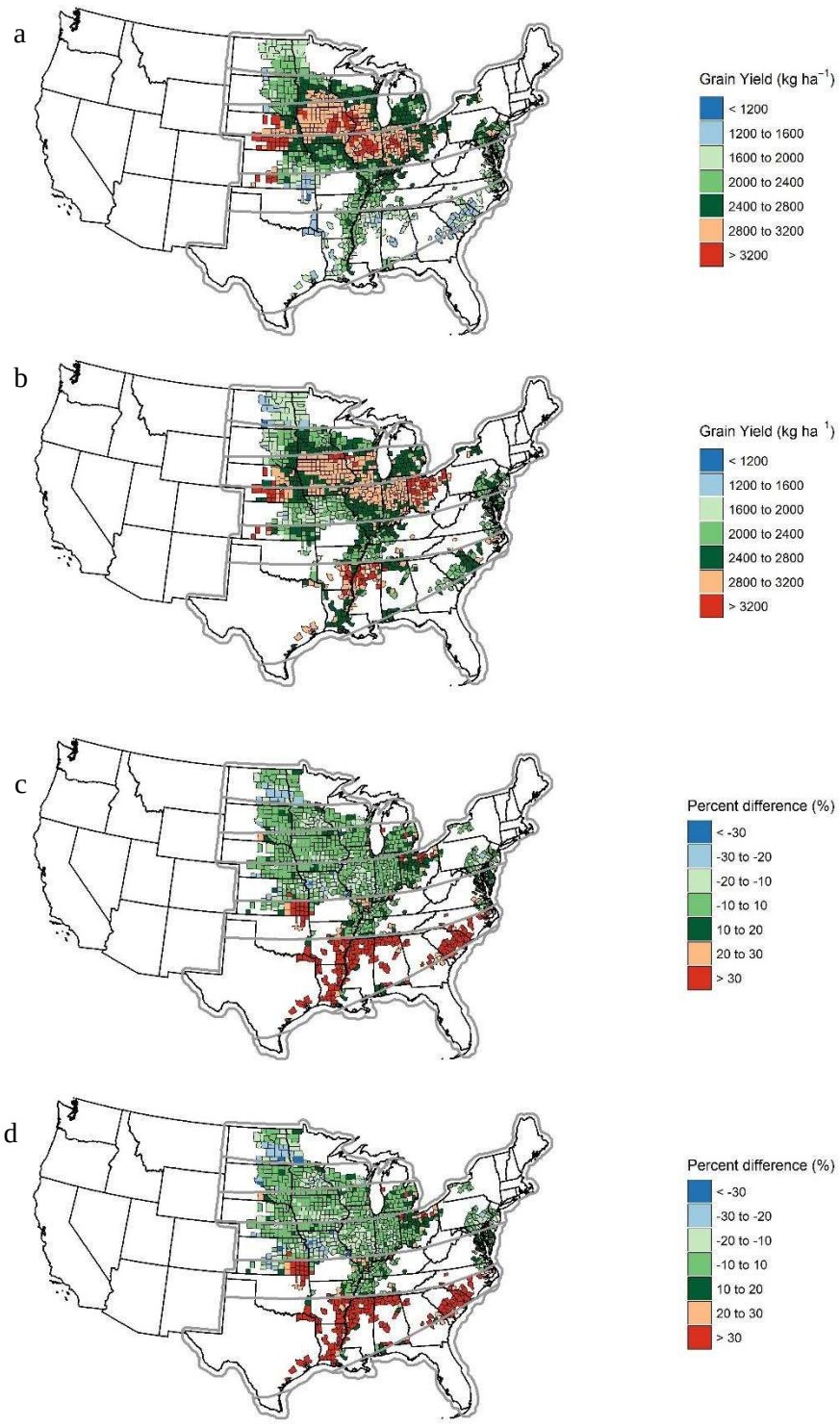

Fig. 5.6 The maps of a) 15-year average NASS yields of soybean, b) simulated average yields of the same period, c) the percentage difference of simulated yields to NASS yields of the double nitrogen rates scenario, and d) the percentage difference of simulated yields to NASS yields of the average nitrogen rates scenario.

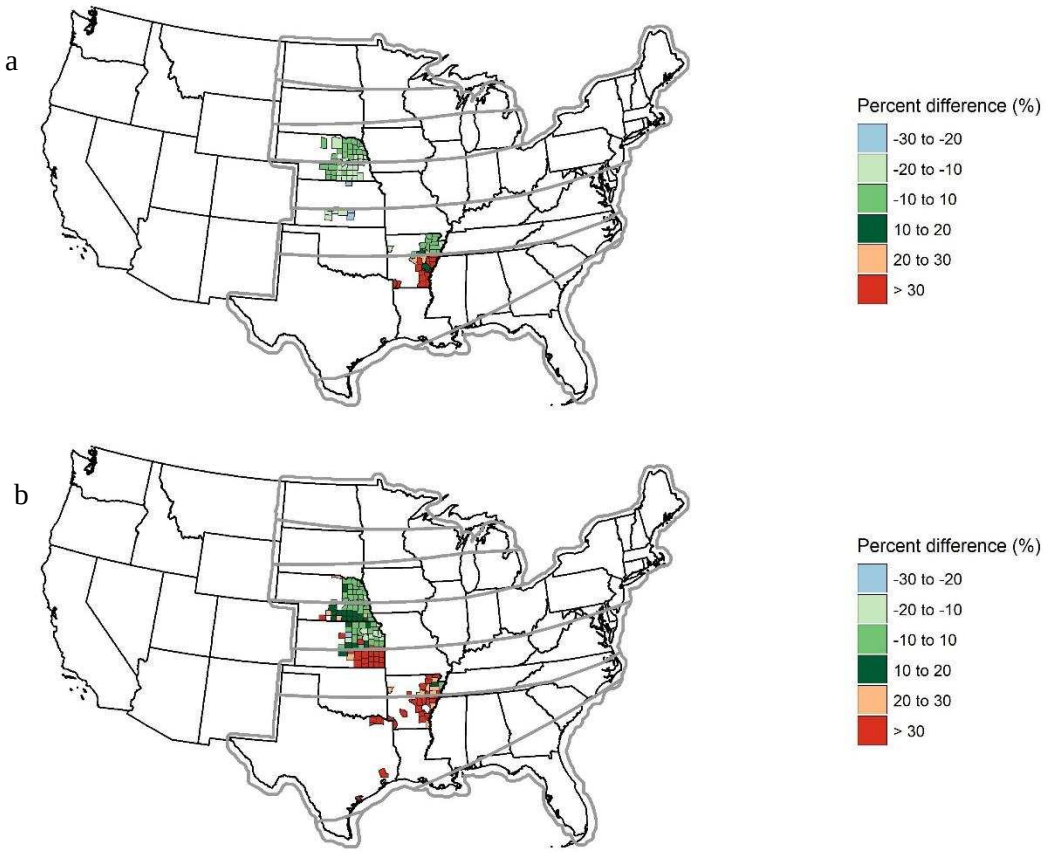

Fig. 5.7 The maps of a) the percentage difference of simulated irrigated yields to NASS irrigated soybean yields of the double nitrogen rates scenario and b) the percentage difference of simulated non-irrigated yields to NASS non-irrigated yields of the double nitrogen rates scenario.

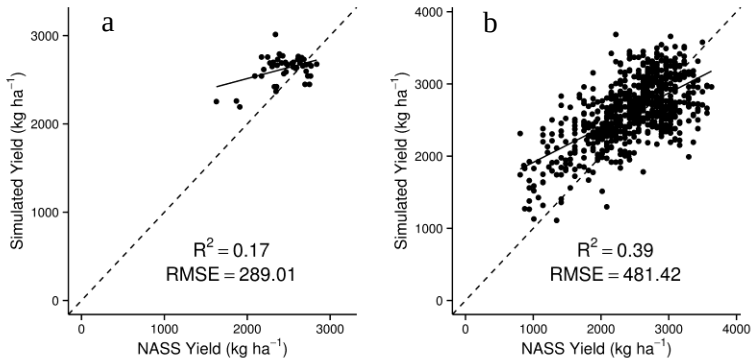

Fig. 5.8 Relationship a) between 15-year average NASS soybean yields of counties in Nebraska and simulated yields and b) between NASS yields of individual years and simulated yields.

REFERENCES

Adam M, Van Bussel LGJ, Leffelaar PA, Van Keulen H, Ewert F. (2011) Effects of modelling detail on simulated potential crop yields under a wide range of climatic conditions. Ecological Modelling 222: 131-143.

Adams RM, Rosenzweig C, Peart RM, Ritchie JT, McCarl BA, Glyer JD, Curry RB, Jones JW, Boote KJ, Allen LH. (1990) Global climate change and US agriculture. Nature 345: 219-224.

Allen RG, L.S. Pereira, D. Raes, Smith M. (1998) Crop evapotranspiration: Guidelines for computing crop requirements. FAO Irrigation and Drainage Paper No. 56. Rome, Italy.

Basso B, Gargiulo O, Paustian K, Robertson GP, Porter C, Grace PR, Jones JW. (2011) Procedures for Initializing Soil Organic Carbon Pools in the DSSAT-CENTURY Model for Agricultural Systems. Soil Science Society of America Journal 75: 69-78.

Bruns HA. (2009) A Survey of Factors Involved in Crop Maturity. Agronomy Journal 101: 60-66.

Cheng K, Ogle SM, Parton WJ, Pan G. (2014) Simulating greenhouse gas mitigation potentials for Chinese Croplands using the DAYCENT ecosystem model. Global Change Biology 20: 948-962.

DeJonge KC, Ascough JC, II, Ahmadi M, Andales AA, Arabi M. (2012) Global sensitivity and uncertainty analysis of a dynamic agroecosystem model under different irrigation treatments. Ecological Modelling 231: 113-125.

Del Grosso SJ, Parton WJ, Keough CA, Reyes-Fox M. (2011) Special Features of the DayCent Modeling Package and Additional Procedures for Parameterization, Calibration, Validation, and Applications. In: Ahuja LR, Ma L (eds) Methods of Introducing System Models into Agricultural Research. American Society of Agronomy, Crop Science Society of America, Soil Science Society of America, pp 155-176.

Del Grosso SJ, Parton WJ, Mosier AR, Ojima DS, Kulmala AE, Phongpan S. (2000) General model for N2O and N-2 gas emissions from soils due to dentrification. Global Biogeochemical Cycles 14: 1045-1060.

Del Grosso SJ, Parton WJ, Mosier AR, Walsh MK, Ojima DS, Thornton PE. (2006) DAYCENT national-scale simulations of nitrous oxide emissions from cropped soils in the United States. Journal of Environmental Quality 35: 1451-1460.

Del Grosso SJ, White JW, Wilson G, Vandenberg B, Karlen DL, Follett RF, Johnson JMF, Franzluebbers AJ, Archer DW, Gollany HT, Liebig MA, Ascough J, Reyes-Fox M, Pellack L, Starr J, Barbour N, Polumsky RW, Gutwein M, James D. (2013) Introducing the GRACEnet/REAP Data Contribution, Discovery, and Retrieval System. Journal of Environmental Quality 42: 1274-1280.

Grassini P, Thorburn J, Burr C, Cassman KG. (2011) High-yield irrigated maize in the Western U.S. Corn Belt: I. On-farm yield, yield potential, and impact of agronomic practices. Field Crops Research 120: 142-150.

Grassini P, Yang H, Cassman KG. (2009) Limits to maize productivity in Western Corn-Belt: A simulation analysis for fully irrigated and rainfed conditions. Agricultural and Forest Meteorology 149: 1254-1265.

Hargreaves GH, Allen RG. (2003) History and evaluation of Hargreaves evapotranspiration equation. Journal of Irrigation and Drainage Engineering-Asce 129: 53-63.

Hartman MD, Merchant ER, Parton WJ, Gutmann MP, Lutz SM, Williams SA. (2011) Impact of historical land-use changes on greenhouse gas exchange in the US Great Plains, 1883-2003. Ecological Applications 21: 1105-1119.

Hodges T, Botner D, Sakamoto C, Haug JH. (1987) USING THE CERES-MAIZE MODEL TO ESTIMATE PRODUCTION FOR THE UNITED-STATES CORN-BELT. Agricultural and Forest Meteorology 40: 293-303.

Hoogenboom G, Jones JW, Porter CH, Wilkens PW, Boote KJ, Hunt LA, Tsuji GY. (2010) Decision Support System for Agrotechnology Transfer Version 4.5., University of Hawaii, Honolulu, HI.

IPCC. (1990) Climate Change: The IPCC Scientific Assessment. Cambridge University Press, Cambridge, Great Britain, New York, NY, USA and Melbourne, Australia

Irmak A, Jones JW, Jagtap SS. (2005) Evaluation of the CROPGRO-soybean model for assessing climate impacts on regional soybean yields. Transactions of the Asae 48: 2343-2353.

Jagtap SS, Jones JW. (2002) Adaptation and evaluation of the CROPGRO-soybean model to predict regional yield and production. Agriculture Ecosystems & Environment 93: 73-85.

Kahle D, Wickham H. (2013) ggmap: Spatial Visualization with ggplot2. R Journal 5: 144-161.

Kiniry JR, Jones CA, Otoole JC, Blanchet R, Cabelguenne M, Spanel DA. (1989) RADIATION-USE EFFICIENCY IN BIOMASS ACCUMULATION PRIOR TO GRAIN-FILLING FOR 5 GRAIN-CROP SPECIES. Field Crops Research 20: 51-64.

Kiniry JR, Williams JR, Vanderlip RL, Atwood JD, Reicosky DC, Mulliken J, Cox WJ, Mascagni HJ, Hollinger SE, Wiebold WJ. (1997) Evaluation of two maize models for nine US locations. Agronomy Journal 89: 421-426.

Kucharik CJ. (2003) Evaluation of a Process-Based Agro-Ecosystem Model (Agro-IBIS) across the US Corn Belt: Simulations of the Interannual Variability in Maize Yield. Earth Interactions 7.

Kunkel KE, Hollinger SE, Amer Meteorol SOC. (1991) OPERATIONAL LARGE AREA CORN AND SOYBEAN YIELD ESTIMATION. 20th Conference on Agricultural and Forest Meteorology: 13-16.

Ma L, Nielsen DC, Ahuja LR, Malone RW, Saseendran SA, Rojas KW, Hanson JD, Benjamin JG. (2003) Evaluation of RZWQM under varying irrigation levels in eastern Colorado. Transactions of the Asae 46: 39-49.

Moen TN, Kaiser HM, Riha SJ. (1994) REGIONAL YIELD ESTIMATION USING A CROP SIMULATION-MODEL - CONCEPTS, METHODS, AND VALIDATION. Agricultural Systems 46: 79-92.

Muchow RC, Sinclair TR, Bennett JM. (1990) TEMPERATURE AND SOLAR-RADIATION EFFECTS ON POTENTIAL MAIZE YIELD ACROSS LOCATIONS. Agronomy Journal 82: 338-343.

NASS. (2003) Agricultural Chemical Usage: 2002 Field Crops Summary. Report AgCh1(03). National Agricultural Statistics Service. USDA.

NASS. (2010) Field Crops: Usual Planting and Harvesting Dates. USDA National Agricultural Statistics Service, Agricultural Handbook Number 628.

NRCS. (2009) Soil Survey Geographic (SSURGO) Database. USDA Natural Resources Conservation Service. .

Nusser SM, Goebel JJ. (1997) The National Resources Inventory: A long-term multi-resource monitoring programme. Environmental and Ecological Statistics 4: 181-204.

Parton WJ, Hartman M, Ojima D, Schimel D. (1998) DAYCENT and its land surface submodel: description and testing. Global and Planetary Change 19: 35-48.

PRISM Climate Group. (2015) Parameter-elevation Regressions on Independent Slopes Model. Oregon State University, http://prism.oregonstate.edu.

Saxton KE, Rawls WJ, Romberger JS, Papendick RI. (1986) ESTIMATING GENERALIZED SOIL-WATER CHARACTERISTICS FROM TEXTURE. Soil Science Society of America Journal 50: 1031-1036.

Soltani A, Sinclair TR. (2012) Modeling Physiology of crop development, growth and yield. CABI International, Wallingford, UK.

Stehfest E, Heistermann M, Priess JA, Ojima DS, Alcamo J. (2007) Simulation of global crop production with the ecosystem model DayCent. Ecological Modelling 209: 203-219.

Stockle CO, Kiniry JR. (1990) VARIABILITY IN CROP RADIATION-USE EFFICIENCY ASSOCIATED WITH VAPOR-PRESSURE DEFICIT. Field Crops Research 25: 171-181.

Tan GX, Shibasaki R. (2003) Global estimation of crop productivity and the impacts of global warming by GIS and EPIC integration. Ecological Modelling 168: 357-370.

Thornton PE, Running SW. (1999) An improved algorithm for estimating incident daily solar radiation from measurements of temperature, humidity, and precipitation. Agricultural and Forest Meteorology 93: 211-228.

USDA. (2009) Summary Report: 2007 National Resources Inventory. Natural Resources Conservation Service, Washington, DC, and Center for Survey Statistics and Methodology, Iowa State University, Ames, Iowa, p 123.

USEPA. (2015) Inventory of U.S. Greenhouse Gas Emissions and Sinks: 1990-2014.

Wang X, He X, Williams JR, Izaurralde RC, Atwood JD. (2005) Sensitivity and uncertainty analyses of crop yields and soil organic carbon simulated with EPIC. Transactions of the Asae 48: 1041-1054.

Wilson DR, Muchow RC, Murgatroyd CJ. (1995) Model analysis of temperature and solar radiation limitations to maize potential productivity in a cool climate. Field Crops Research 43: 1-18.

Zhang Y, Qian YL, Bremer DJ, Kaye JP. (2013a) Simulation of Nitrous Oxide Emissions and Estimation of Global Warming Potential in Turfgrass Systems Using the DAYCENT Model. Journal of Environmental Quality 42: 1100-1108.

Zhang Y, Qian YL, Mecham B, Parton WJ. (2013b) Development of Best Turfgrass Management Practices Using the DAYCENT Model. Agronomy Journal 105: 1151-1159.

APPENDIX

Table A1. Management practices of corn and soybean used in simulations for each state.

State	Corn				Soybean			
	Planting date	Harvest date[ł]	Fertilization rate of irrigated fields (kg N ha-1)	Fertilization rate of non-irrigated fields (kg N ha-1)	Planting date	Harvest date	Fertilization rate of irrigated fields (kg N ha-1)	Fertilization rate of non-irrigated fields (kg N ha-1)
AL	4/9	8/31	20.4	13.8	6/9	11/12	2	2
AZ	4/23	10/16	18.3	7.8				
AR	4/13	9/7	20.4	13.8	5/29	10/21	4.8	3.2
CA	5/16	10/16	18.9	14.7				
CO	5/9	10/26	18.3	7.8				
DE	5/8	10/2	18.9	8.7	6/13	11/2	2.1	2.1
FL	4/4	8/21	20.4	13.8	5/23	11/4	2	2
GA	4/6	9/3	20.4	13.8	6/6	11/16	2	2
ID	5/15	10/30	18.3	7.8				
IL	5/7	10/14	20.2	17.7	5/25	10/11	1.8	1.9
IN	5/16	10/21	20.2	17.1	5/23	10/16	2	2
IA	5/6	10/22	20.2	15	5/20	10/9	1.2	1.2
KS	4/30	10/2	21.1	12	6/2	10/16	2.5	1.8
KY	5/4	10/1	18.9	17.9	6/6	10/27	3.7	3.7
LA	3/29	8/22	20.4	13.8	5/14	9/29	2.9	1
MD	5/10	10/7	18.9	8.7	6/11	11/1	2.1	2.1
MI	5/14	11/2	15.9	13.7	5/25	10/18	1.8	1.8
MN	5/7	10/23	15.9	13.6	5/20	10/8	1.9	1.9
MS	4/10	9/7	20.4	13.8	5/13	10/7	1.8	1.5
MO	5/4	10/6	20.5	15.5	6/3	10/21	2.2	2.1
MT	5/16	11/13	18.3	7.8				
NE	5/6	10/22	18	11.3	5/21	10/11	1.4	1.5
NJ	5/10	10/21	18.9	8.7	6/10	10/30	2.1	2.1
NM	4/30	10/15	18.3	7.8			2.1	2.1
NY	5/24	10/29	18.9	7.4	6/5	10/26	2.5	2.5
NC	4/17	9/25	18.9	14.4	6/9	11/22	1.9	2.1
ND	5/15	10/29	18.7	13.3	5/24	10/7	1.3	1.3
OH	5/9	10/31	20.2	18	5/16	10/15	2	2
OK	4/20	9/18	20.6	12.6	5/27	10/21	2.1	2.1
OR	5/15	11/4	18.9	14.7				
PA	5/17	11/2	18.9	9.7	5/30	10/30	2	2
SC	4/4	9/7	20.4	13.8	6/11	11/25	1.6	1.8
SD	5/14	10/26	18.7	12.5	5/28	10/11	2.3	2.3
TN	4/22	9/20	18.9	16.7	6/4	10/28	2	2
TX	4/7	9/5	20.6	12.6	4/29	9/19	1.8	1.8
UT	5/10	10/20	18.3	7.8				
VA	4/30	10/2	18.9	16.7				
WA	5/5	10/25	18.9	14.7	6/8	11/6	3.2	3.2
WV	5/18	10/25	18.9	16.7	6/4	11/2	1.7	1.7
WI	5/14	10/31	15.9	10.8	5/24	10/16		
WY	5/12	11/5	18.3	7.8				

ł In our simulations, if the harvest date is before crop maturity (based on GDD), harvest will be postponed until maturity.

Table A2. Experimental sites used for initial calibration of the model.

State	City	Latitude	Longitude	Records (Yr * location) of corn	Records (Yr * location) of soybean	In-season measurement	Source
CO	Fort Collins	40.7	-105.0	15	0	No	GRACEnet database[ł]
IA	Ames	42.0	-93.8	4	0	No	GRACEnet database
KY	Bowling Green	36.9	-86.5	6	0	No	GRACEnet database
MN	Morris	45.7	-95.8	8	8	No	GRACEnet database
NE	Mead	41.2	-96.4	17	0	No	GRACEnet database
SD	Brookings	44.4	-96.8	5	5	No	GRACEnet database
AL	Shorter	32.4	-85.9	3	0	No	Causarano et al.(2007)
IL	Bondville	40.0	-88.3	3	2	Yes	Chapter 1
NE	Mead	41.2	-96.5	26	10	Yes	Chapter 1
CO	Akron	40.2	-103.1	3	0	Yes	Chapter 2
CO	Fort Collins	40.7	-105.0	5	0	Yes	Chapter 2
CO	Greeley	40.5	-104.6	4	0	Yes	Chapter 2
FL	Gainesville	29.6	-82.4	0	12	Yes	DSSAT database[ǂ]
IW	Ames	42.0	-93.5	0	4	Yes	DSSAT database
MN	Morris	45.6	-95.7	0	1	Yes	DSSAT database
OH	Wooster	40.8	-81.9	0	2	Yes	DSSAT database
MO	Centralia	39.2	-92.2	0	3	Yes	Wang et al. (2003)

ł GRACEnet (Greenhouse gas Reduction through Agricultural Carbon Enhancement network) is a USDA-ARS research program (Del Grosso et al., 2013).

ǂ DSSAT database is within DSSAT crop model package (Hoogenboom et al., 2010).

Table A3. The definitions and units of parameters in Table 5.1.

Name	Definition	Unit
DDBASE	GDD from planting to anthesis	^{0}C
MXDDHRV	GDD from anthesis to harvest without water stress	^{0}C
DDLAIMX	GDD from planting to maximum GLAI	^{0}C
BMINI	Initial biomass at emergence	g m^{-2}
SLA	Specific leaf area	m^2 g^{-1}
LEAFEMERG	Intercept of the second stage linear equation at emergence	g g^{-1}
LEAFMX	Green leaf weight ratio at maximum GLAI	g g^{-1}
RUETB	Radiation use efficiency for total biomass production	g m^{-2} $langley^{-1}$ PAR
PPDF(1)	Optimum temperature for production for parameterization of a Poisson Density Function curve to simulate temperature effect on growth	^{0}C
PPDF(2)	Maximum temperature for production for parameterization of a Poisson Density Function curve to simulate temperature effect on growth	^{0}C
KLIGHT	Extinction coefficient of Beer's Law	-
HIMAX	The maximum harvest index	g g^{-1}
HIWSF	Water stress factor on harvest index	-
KCET	Crop coefficient for evapotranspiration	-

Table A4. The statistics of predicted annual dryland yields (from 1993 to 2007) for counties in Nebraska. Observed yields were from NASS.

County	Corn			Soybean		
	R^2	RMSE (kg ha^{-1})	ratio of minimum observed yield to maximum	R^2	RMSE (kg ha^{-1})	ratio of minimum observed yield to maximum
Adams	0.56	2433	0.22	0.65	529	0.35
Antelope	0.17	2191	0.45	0.76	432	0.48
Boone	0.16	2428	0.47	0.64	322	0.47
Boyd	0.61	2132	0.21	0.55	634	0.36
Buffalo	0.79	2043	0.16	0.90	503	0.35
Burt	0.03	2101	0.60	0.06	416	0.63
Butler	0.31	2278	0.34	0.51	396	0.48
Cass	0.21	1970	0.30	0.26	424	0.53
Cedar	0.02	1694	0.51	0.31	385	0.64
Chase	0.78	807	0.29			
Clay	0.58	2497	0.26	0.55	580	0.36
Colfax	0.21	2184	0.43	0.19	421	0.57
Cuming	0.15	2223	0.47	0.25	443	0.57
Custer	0.60	1266	0.23			
Dakota	0.07	2608	0.60	0.04	478	0.62
Deuel	0.82	1236	0.25			
Dixon	0.00	2685	0.43	0.27	402	0.62
Dodge	0.15	1923	0.51	0.07	466	0.60
Douglas	0.25	1917	0.49	0.33	454	0.51
Dundy	0.54	1440	0.11			
Fillmore	0.63	2189	0.24	0.79	474	0.42
Franklin	0.70	1608	0.21	0.87	486	0.28
Frontier	0.46	2142	0.44			
Furnas	0.60	1331	0.18	0.76	760	0.30
Gage	0.12	2769	0.37	0.26	569	0.46
Gosper	0.83	1603	0.23			
Greeley	0.58	2561	0.25			
Hall	0.67	2406	0.22			
Hamilton	0.59	2475	0.26	0.85	445	0.34
Harlan	0.61	1842	0.19			
Hayes	0.48	1596	0.29			
Hitchcock	0.76	852	0.24			
Holt	0.15	1220	0.40	0.01	394	0.50
Howard	0.73	1814	0.29			
Jefferson	0.54	2236	0.24	0.33	492	0.47
Johnson	0.35	2579	0.18	0.39	644	0.44
Kearney	0.54	2414	0.25	0.76	497	0.32
Keith	0.44	1261	0.26			
Kimball	0.00	1433	0.78			
Knox	0.10	1718	0.42	0.42	381	0.67
Lancaster	0.35	1686	0.39	0.27	408	0.49
Lincoln	0.54	824	0.41			
Madison	0.13	2257	0.53	0.14	512	0.61
Merrick	0.50	1245	0.33			
Nance	0.50	2046	0.20	0.60	542	0.28
Nemaha	0.46	1679	0.27	0.43	404	0.43
Nuckolls	0.74	1790	0.24	0.76	558	0.26
Otoe	0.39	2062	0.19	0.35	453	0.45
Pawnee	0.27	2606	0.25	0.34	535	0.47
Perkins	0.60	1097	0.33			
Phelps	0.68	2667	0.20	0.85	639	0.42
Pierce	0.11	2151	0.47	0.51	346	0.53
Platte	0.24	2333	0.43	0.42	410	0.49

Polk	0.55	2154	0.20	0.75	415	0.33
Red Willow	0.58	1496	0.20			
Richardson	0.38	1414	0.40	0.31	433	0.51
Saline	0.44	2598	0.31	0.49	547	0.41
Sarpy	0.33	1863	0.29	0.44	435	0.47
Saunders	0.23	1834	0.44	0.25	387	0.47
Seward	0.30	2170	0.26	0.59	395	0.46
Sherman	0.56	2830	0.30	0.54	787	0.48
Stanton	0.06	2499	0.44	0.16	485	0.52
Thayer	0.64	1892	0.29	0.59	501	0.40
Thurston	0.00	2461	0.54	0.09	453	0.59
Valley	0.53	2985	0.33			
Washington	0.15	1821	0.51	0.05	530	0.58
Wayne	0.08	2649	0.44	0.39	420	0.51
Webster	0.74	2009	0.19	0.78	546	0.30
York	0.33	2384	0.22	0.60	431	0.32

REFERENCES

Causarano, H.J. et al., 2007. Simulating field-scale soil organic carbon dynamics using EPIC. Soil Science Society of America Journal, 71(4): 1174-1185.

Del Grosso, S.J. et al., 2013. Introducing the GRACEnet/REAP Data Contribution, Discovery, and Retrieval System. Journal of Environmental Quality, 42(4): 1274-1280.

Hoogenboom, G. et al., 2010. Decision Support System for Agrotechnology Transfer Version 4.5., University of Hawaii, Honolulu, HI.

Wang, F., Fraisse, C.W., Kitchen, N.R. and Sudduth, K.A., 2003. Site-specific evaluation of the CROPGRO-soybean model on Missouri claypan soils. Agricultural Systems, 76(3): 985-1005.